KIEL INSTITUTE FOR THE WORLD ECONOMY

KIEL WORKING PAPER

Spatial distribution of housing liquidity

No. 2284 March 2025

Francisco Amaral, Mark Toth and Jonas Zdrzalek

Kiel Institute for the World Economy
ISSN 1862–1155

Leibniz Association

KIEL WORKING PAPER NO. 2284 | MARCH 2025

ABSTRACT

SPATIAL DISTRIBUTION OF HOUSING LIQUIDITY*

Francisco Amaral, Mark Toth and Jonas Zdrzalek

This paper examines the relationship between location, liquidity, and prices in housing markets. We construct spatial datasets for German and U.S. cities and show that liquidity and prices decline with distance to the city center. To rationalize these results, we build and estimate a spatial housing search model. Our model demonstrates that travel costs determine the spatial distribution of liquidity and prices. In a counterfactual analysis, we suppress search frictions and find that frictional illiquidity reduces prices and welfare, particularly in the outskirts. Our findings underpin the importance of demand-side preferences for asset pricing.

Keywords: housing liquidity, housing prices, cities, spatial equilibrium, housing demand, asset pricing

JEL Classification: G12, G51, R21, R30

Francisco Amaral (corresponding author)
University of Zurich; Swiss Finance Institute
Rämistrasse 71, CH-8006 Zürich
Email: francisco.amaral@df.uzh.ch
www.uzh.ch

Mark Toth
University of Bonn
Regina-Pacis-Weg 3, D-53113 Bonn
Email: mark-toth@uni-bonn.de
www.uni-bonn.de

Jonas Zdrzalek
Kiel Institute for the World Economy,
University of Cologne
Kiellinie 66, D-24105 Kiel
Email: jonas.zdrzalek@ifw-kiel.de
www.ifw-kiel.de

*Amaral and Zdrzalek were part of the Young ECONtribute Program by the Cluster of Excellence ECONtribute, a joint initiative of the Universities Bonn and Cologne and therefore wish to acknowledge support from the Deutsche Forschungsgemeinschaft (DFG) under Germany's Excellence Strategy – EXC 2126/1 – 390838866. Toth acknowledges support from the Bonn Graduate School of Economics and the Deutsche Forschungsgemeinschaft (DFG) under the Research Training Group 2281 – The Macroeconomics of Inequality. For helpful feedback, we thank Gabriel Ahlfeldt, Christian Bayer, Pierre Collin-Dufresne, Gilles Duranton, Rüdiger Fahlenbrach, Andreas Fuster, James Graham, Janko Heineken, Christian Hilber, Thomas Hintermaier, Matthijs Korevaar, Martin Kornejew, Lorenz Kueng, Keith Kuester, Antoine Levy, Per Östberg, Andrii Parkhomenko, Kathleen Rauck, Farzad Saidi, Zacharias Sautner, Moritz Schularick, Maxence Valentin, Anthony Lee Zhang, and Tom Zimmermann. We also thank seminar and workshop participants at the 13th European Meeting of the Urban Economics Association at Aalborg University Copenhagen; the 3rd Workshop on Residential Housing Markets at WU Vienna; the University of Bonn Institute of Finance and Statistics Seminar; the University of Bonn Macro Internal Seminar; the 1st and 2nd Bonn-Frankfurt-Mannheim PhD Conference; the UNSW Macro Lunch, UNSW Sydney; the 2024 ECHOPPE Housing Conference in Toulouse; the 2024 Wisconsin Real Estate Conference at UW-Madison; the 17th Annual Meeting of The Portuguese Economic Journal in Faro; the CERF Seminar at the Judge Business School, Cambridge; the Financial EconomicsWorkshop 2024 in St. Gallen; the CREDWorkshop on Regional and Urban Economics 2025 in Bern; the Swiss Finance Institute Brown Bag Seminar; the CEPR Publishing in Top Macro and Finance Journals Workshop; the Oxford Real Estate Research Conference, Saïd Business School; and the CMR Macro & Public Economics Seminar, University of Cologne.

1 Introduction

Transactions in real estate markets are impeded by search frictions and typically take months to complete. This makes real estate a particularly illiquid asset class (see, for example, Ngai and Tenreyro, 2014; Piazzesi, Schneider, and Stroebel, 2020). Given the large relative size of housing in household balance sheets, variation in housing liquidity has substantial aggregate economic consequences (see, for example, Head, Lloyd-Ellis, and Sun, 2014; Garriga and Hedlund, 2020). Moreover, houses are tied to their locations. Although housing market liquidity varies across space as much as it varies across the business cycle (Jiang, Kotova, and A. L. Zhang, 2024), we know little about the determinants of this spatial variation. In this paper, we show that location preferences determine spatial differences in housing liquidity in conjunction with prices.

Scarcity of data has so far limited our knowledge about the spatial variation in housing liquidity. We fill this gap by building spatial datasets on housing prices and liquidity for cities in two of the world's largest housing markets. We empirically show that housing prices and various measures of housing liquidity decrease with distance to the city center in both German and U.S. cities, even when taking into account spatial differences in property characteristics, income, and demographics. These spatial differences are comparable in magnitude to cyclical fluctuations in housing prices and liquidity. While the result that prices decrease with distance to the city center is established in the literature (see Duranton and Puga, 2015), we are the first to establish that liquidity also decreases with distance to the city center. To rationalize our results, we build a quantitative urban housing model with search frictions. In our model, travel costs increase with distance to the city center, which reflects a fundamental locational preference of buyers. This leads to fewer potential buyers in the outskirts, decreasing market tightness and therefore liquidity. Sellers, facing less tight markets, reduce their offered prices with increasing distance to the city center. We estimate the structural parameters of our model and reproduce the spatial distribution of liquidity and prices with high precision for both Germany and the United States without targeting spatial variation in our estimation. We then quantify and decompose the impact of search frictions on welfare and prices using a counterfactual model analysis. We find that, on average, welfare decreases by 3% due to search frictions, which is equivalent to 1.5% of housing prices. This effect is mostly driven by lower matching probabilities and correspondingly higher vacancy rates, especially in the outskirts. We also show that search frictions widen the gap in housing prices between city center and outskirts. Quantitatively, the steepness of the spatial price gradient triples. Overall, we show how buyers' location preferences simultaneously determine liquidity and prices in housing markets. Our results provide new insights on the role of frictions in decentralized markets, which is particularly important in light of the recent "great rotation" (Koijen, Shah, and Van Nieuwerburgh, 2025) toward illiquid, private assets.

In our empirical analysis, we combine the universe of real estate transactions from German cities (introduced in Amaral et al., 2023) with an extensive set of real estate advertisements assembled by a private company[1] using a nearest-neighbor algorithm. We end up with geocoded datasets on housing liquidity and prices from 2012 to 2024 for Hamburg, Munich, Cologne, Frankfurt, and Duesseldorf. For the United States, we use ZIP-Code-level data from Redfin on housing liquidity and prices from 2012 to 2023, combined with data on local housing characteristics and demographics from the American Community Survey and data on neighborhood quality from Chetty et al. (2025). With these datasets, we cover two large and fundamentally distinct housing markets: the German housing market has a low homeownership rate and low turnover, while the U.S. housing market has a high homeownership rate and high turnover.

Our primary measure of liquidity is the time that properties stay on the market as online listings, the standard measure in the housing literature (see Han and Strange, 2015). We find that within-city spatial differences in the time on the market are substantial and systematic. Conditional on property characteristics and neighborhood characteristics, housing units stay on the market for 20% longer in the outskirts compared to the city center in both German and U.S. cities. This constitutes a negative liquidity gradient in urban housing markets, a novel finding which adds to the well-documented negative price gradient. We also show that the spread between asking and sales price, a measure that we construct analogously to the bid-ask spread in stock or bond markets, becomes more negative with distance to the city center. Furthermore, we use buyers' contact clicks for listings as a proxy measure for market tightness and show that they decline with distance to the city center. All of our empirical results hold in an extensive series of robustness checks. Among these, a time series analysis shows that the liquidity gradient flattens

[1]We are very grateful to Sebastian Hein from *VALUE Marktdaten* for giving us access to the data and support throughout the process of writing the paper.

during the COVID-19 pandemic, but starts to recover thereafter. This finding is in line with the flattening of the price gradient during the COVID-19 pandemic as a consequence of the shift to working from home (see Gupta et al., 2022). Lastly, using data on job accessibility across U.S. ZIP Codes from Delventhal and Parkhomenko (2024), we show that our findings can be extended to locations beyond city centers which attract a large enough number of commuters.[2]

In our theoretical analysis, we model a housing market with search frictions, building on an established model structure from Krainer (2001). With this setup, we take a similar approach as prominent recent papers on housing market search, such as Piazzesi, Schneider, and Stroebel (2020) and Guren and McQuade (2020). We assume that households want to minimize their distance to a central location, which gives rise to a spatial distribution of travel costs.[3] Our model thus allows us to examine the interaction of search frictions and location preferences. We show that as the cost of travel increases with distance to the city center, market tightness, defined as the number of potential buyers per seller, decreases. This is reflected in a lower probability of sale and therefore a longer time on the market outside of the city center. Sellers act as price setters for spatially differentiated goods and, consistently with the lower probability of sale, decrease their listing prices. Importantly, they trade off the listing price and the time to sell a housing unit (as emphasized in, for example, Guren, 2018). It is therefore not optimal for sellers to adjust prices downward so far that spatial liquidity differences disappear. Hence, liquidity and prices are endogenously co-determined by travel costs which reflect fundamental demand-side location preferences. Analogously to our additional empirical findings, this mechanism can be generalized to other locations beyond the city center for which homebuyers share a common preference to live nearby.

We estimate the structural parameters of our model for German and U.S. cities via the method of simulated moments. The only spatial input required for our model to generate quantitatively accurate spatial liquidity and price distributions is the spatial distribution of travel time to the city center. Then, we conduct a counterfactual analysis to quantify the effects of search frictions on welfare and housing prices. We compare our frictional market equilibrium model with an efficient model in which we abstract from search

[2]We are very grateful to Andrii Parkhomenko for providing us access to the data.

[3]This is in line with the canonical monocentric city model (Alonso, 1964; Mills, 1967; Muth, 1969) in which housing prices depend on the cost of travel to the city center. As an alternative interpretation of this travel cost, we also consider an opportunity cost of travel to the city center in terms of foregone wages.

frictions. We find that search frictions decrease welfare by 3% on average. Welfare losses are mostly driven by high vacancies due to excess search in the market equilibrium. In addition, we show that welfare losses are higher in the outskirts than in the city center, as frictional vacancies increase with distance to the city center. The spatial difference in welfare losses between city center and outskirts amounts to one-third of the average welfare loss. Regarding prices, we find that search frictions amplify spatial differences, as search frictions are particularly strong in the outskirts. The spatial price gradient is 3 times as steep in the market equilibrium as in the frictionless model.

In an extension of the model, we introduce a bargaining process which creates spreads between asking and sales prices that we can compare to our additional empirical measure. We show that the time on the market and this spread are interchangeable measures of liquidity in the model and reflect the same structural relationships, as do the time on the market and market tightness. Lastly, in an additional model experiment, we replicate the empirical flattening of the liquidity gradient due to the shift to working from home induced by the COVID-19 pandemic. Overall, our results show how accounting for the interaction between location preferences and search frictions significantly enhances our understanding of the cross-sectional variation in housing liquidity and prices.

Related literature. We are the first to establish that housing liquidity decreases with distance to the city center. This adds to the well-known fact that housing prices also decrease with distance to the city center (for recent research on the spatial price gradient, see Gupta et al., 2022; Albouy, Ehrlich, and Shin, 2018).

Our paper contributes to the growing literature on the spatial variation in housing liquidity. Gerardi, Qian, and D. Zhang (2025), Jiang, Kotova, and A. L. Zhang (2024), and Vanhapelto and Magnac (2024) examine differences in housing liquidity across regions. Piazzesi, Schneider, and Stroebel (2020) show how segmented search behavior is important to understand within-city spatial differences in housing liquidity and prices. We complement their work by quantifying the effects of search frictions on the spatial distribution of prices and the associated welfare effects. This approach is related to the literature on search frictions in OTC markets (for prominent early work, see Duffie, Gârleanu, and Pedersen, 2005; Lagos and Rocheteau, 2009).

We also contribute to the literature on urban housing market models[4] by showing

[4]See Duranton and Puga (2015) for an overview.

that taking into account search frictions significantly improves our understanding of the urban spatial price gradient. Moreover, introducing search frictions allows us to formulate a more realistic equilibrium condition than in standard urban models. In our model, buyers have the same net utility across space in expectation, which contrasts with standard spatial equilibrium conditions which let the realized net utility of buyers equalize across space.

Lastly, by integrating space into a framework with trading frictions, we contribute to, first, the well-established literature on housing market search,[5] and second, the emerging literature on urban finance which combines elements of structural urban models with elements of structural macro-finance models (see, for example, Koijen, Shah, and Van Nieuwerburgh, 2025; Favilukis, Mabille, and Van Nieuwerburgh, 2023).

The rest of this paper is organized as follows. Section 2 describes our data and our measurement of spatial variables and liquidity. Section 3 presents our empirical analysis. Section 4 describes our model framework and presents analytical and quantitative results. Section 5 presents our counterfactual analysis. Section 6 concludes.

2 Data and measurement

To study the spatial distribution of housing liquidity and prices, we construct two new spatial datasets for large cities in Germany and the United States. For Germany, we use property-level data covering Hamburg, Munich, Cologne, Frankfurt, and Duesseldorf. Berlin is excluded from our sample due to missing information on addresses. For the United States, we use ZIP-Code-level data covering the 30 largest MSAs.

2.1 Data for German cities

We combine administrative records on the universe of housing transactions in our sampled cities with a comprehensive dataset on housing advertisements. We focus our analysis on apartments, which allows us to examine the role of location consistently within a city, since other types of housing are typically scarce in German city centers.

Our transaction dataset covers the universe of residential housing transactions in large German cities over several decades. This dataset, introduced in Amaral et al. (2023), is based on data from local real estate committees (*Gutachterausschuesse*). Collecting

[5] See Han and Strange (2015) for an overview.

information on all real estate transactions from notaries, these committees register information on sales prices, contract dates, addresses, and an extensive list of property characteristics which we document in Supplemental Appendix A.1.

We obtain data on apartment advertisements via *VALUE Marktdaten* who scrape and process real estate advertisements from online platforms and real estate agencies. The company's algorithm ensures that ads with both shorter and longer durations are scraped, preventing potential bias from user-influenced advertisement ordering.[6] We observe the dates on which ads were posted and removed, addresses (if available), further information on location such as ZIP Code or neighborhood, asking prices, and property characteristics. The dataset covers the period between 2012 and 2024, which, in combination with the longer time span covered by the transaction data, limits our sample to this period.

We match the two datasets using a nearest-neighbor algorithm based on location, contract and listing dates, asking and sales prices, apartment sizes, and building year of properties. As we do not observe the addresses of all listings, we match only about one-third of the transactions with corresponding listings. Our final dataset consists of more than 80 thousand observations. In Supplemental Appendix A.1, we provide further details on the matching process and show that the matched sample is representative of the universe of transactions.

2.2 Data for U.S. cities

For the United States, we gather ZIP-Code-level data on median time on the market and median sales prices from Redfin.[7] To obtain control variables for our empirical analysis, we gather ZIP-Code-level data on average housing size, average building year, income composition, and racial composition from the American Community Survey (U.S. Census Bureau, 2012–2023a; U.S. Census Bureau, 2012–2023b; U.S. Census Bureau, 2012–2023c) as well as ZIP-Code-level data on neighborhood quality from Chetty

[6]Note that if an advertisement is posted multiple times across different platforms or within the same platform, this is taken into account when assigning identifiers to advertisements.

[7]Redfin is a real estate brokerage company that obtains its data directly from local listing services, especially those based in the largest MSAs (see: `https://www.redfin.com/news/data-center/`). We do not use data from Zillow, the most popular provider of U.S. real estate data, as Zillow does not provide access to data on time on the market at a more granular level than MSA. However, as we show in Supplemental Appendix A.2, the differences in coverage between Zillow and Redfin for the 30 largest MSAs are very small and should not affect our results. Moreover, we show that our results are robust to using data from Realtor.com, another online listing platform (`https://www.realtor.com/research/data/`).

et al. (2025).

We focus our analysis on single-family homes, the most common housing type in U.S. cities. In Supplemental Appendix D.3, we show that our results also hold for condominiums, multi-family houses, and townhouses. Our dataset covers the 30 largest MSAs from 2012 to 2023 at a monthly frequency. Supplemental Appendix A.2 describes our data preparation procedure in further detail.

2.3 Measurement of spatial variables

We measure spatial variation in our data using the distance to the city center, an established measure in the urban economics literature (see Duranton and Puga, 2015). For Germany, we choose historic city centers for our baseline analysis.[8] In a robustness check, we show that selecting the centroid of the business district with the highest land value (via the *Bodenrichtwerte* land value measurements from the *Gutachterausschuesse* real estate committees[9]) yields nearly identical city centers as the ones we choose by hand. We calculate kilometer distances between city centers and locations of apartments transacted within the corresponding city boundaries. For the United States, we define the center of an MSA as the location of its city hall (as done in, for example, Gupta et al., 2022). We calculate kilometer distances between MSA centers and ZIP Code centroids located within the corresponding MSA boundaries.[10] In a robustness analysis, we find alternative city centers by selecting locations with the highest volumes of residential construction from the Global Human Settlement Layer database by the European Commission Joint Research Centre. Moreover, we create a job access index using data from Delventhal and Parkhomenko (2024) which we use to find locations with high job access as alternative focal points beyond city centers.

As an alternative spatial measure, we use travel time estimates. The spatial structure of cities can feature rivers or other factors that influence local transportation. Such features could be more accurately represented via the travel time rather than the kilometer distance to the city center. Via openrouteservice,[11] we request the typical travel time

[8]We choose the following historic city centers: Hamburg: *Alsterhaus*, Munich: *Marienplatz*, Cologne: *Koelner Dom*, Frankfurt: *Konstablerwache*, Duesseldorf: *Marktplatz*.

[9]Retrieved from the *BORIS-D* database (https://www.bodenrichtwerte-boris.de/).

[10]Population-weighted ZIP Code centroids retrieved from https://catalog.data.gov/dataset/zip-code-population-weighted-centroids. MSA boundaries retrieved from https://www2.census.gov/geo/tiger/TIGER2021/CBSA/.

[11]https://openrouteservice.org/.

to the city center by car. For robustness, we also request car and public transport travel times via the Google Maps Directions API.[12]

2.4 Measurement of liquidity

Our main measure of housing liquidity is the time on the market. For the German dataset, we define this time as the period between the start and the end of an advertisement and report the number of weeks an apartment has been advertised if it sells on day T of being advertised, that is, $T/7$ weeks. For the U.S. dataset, we directly obtain the time on the market via Redfin. This time refers to the median number of advertised days for housing units sold within a ZIP Code area in a calendar month. Table 1 presents summary statistics for the German and U.S. datasets. In Supplemental Appendix B, we present summary statistics by city. Overall, we observe that the German market is generally less liquid than the U.S. market, with properties typically taking almost twice as long to sell.

Table 1: *Summary statistics for both datasets*

	Time on the market in weeks				Sales price in 1,000 € or $				
Dataset	Mean	SD	P25	P75	Mean	SD	P25	P75	N
Germany	13.51	16.71	2.40	17.80	374	274	189	478	84,292
U.S.	7.60	7.87	3.50	9.64	446	502	205	530	682,100

Notes: N is the number of transactions for the German dataset. For the U.S. dataset, it represents the number of ZIP-Code-year-month pairs.

We also construct additional liquidity measures using the richer German dataset. First, we calculate the spread between the asking price and the sales price, akin to the bid-ask spread in stock or bond markets. We call this measure the *asking price discount*. We also construct this measure at the ZIP-Code level for the United States with the Redfin data. Second, we use the number of contact clicks per ad as a proxy variable for market tightness. This measure refers to the number of times that potential buyers directly contacted a seller who placed an advertisement.

[12] https://developers.google.com/maps/documentation/directions.

3 Empirical analysis

In this section, we document new stylized facts on the spatial variation in housing liquidity within German and U.S. cities and replicate established stylized facts on the spatial variation in housing prices.

3.1 Spatial variation in liquidity and prices

Regression framework. In our baseline analysis, we use hedonic regressions. This approach allows us to rule out that spatial liquidity or price differences are driven by systematic spatial variation in housing characteristics or demographics. We estimate

$$y_I = \alpha \times distance_I + \beta \times X_I + f_{ct} + \varepsilon_I, \tag{1}$$

where for the German dataset, I indexes transactions, with every transaction I being assigned to a a city c and a calendar quarter t, while for the U.S. dataset, $I = it$ includes an index i for ZIP Codes, with every ZIP Code i being assigned to an MSA c, and an index t for time measured in months. The dependent variable y_I refers to the time on the market or sales prices. The explanatory variable $distance_I$ is the (time-invariant) distance to the city center, measured as a kilometer distance in the baseline specification and as a travel time in the alternative specification.

For regressions using the German dataset, the control vector X_I includes an extensive set of property characteristics, such as size, building year, number of bathrooms, or type of heating. For regressions using the U.S. dataset, X_I includes the share of 1-room, 2–3-room, 4–5-room, 6–7-room, and 8-or-more-room dwellings; the share of housing units built after 2010, in 2000–2009, 1980–1999, 1960–1979, 1940–1959, and in 1939 or earlier; median household income; the share of households with annual income above \$150,000; the homeownership rate; and the share of Black households. The observations of these control variables are at the yearly level. A yearly observation is assigned to all months within that year. In addition, we control for state fixed effects and for spatial differences in neighborhood quality from Chetty et al. (2025), measured by the fraction of children born born between 1978 and 1983 in a given ZIP Code area who were incarcerated by April 1, 2010. For U.S. regressions with the time on the market, we also control for the price level in 2011 to capture unobserved housing characteristics. Note that by considering within-city variation, we furthermore rule out bias due to confounding across-city variation in unobserved variables. Lastly, f_{ct} captures city-time fixed effects to account for common time trends in liquidity or prices within a city, and ε_I denotes the error term. To address spatial correlation in the error terms, we cluster standard errors at the city-year level.

Figure 1: *Liquidity and price gradients for Germany (2012–2024) and the U.S. (2012–2023)*

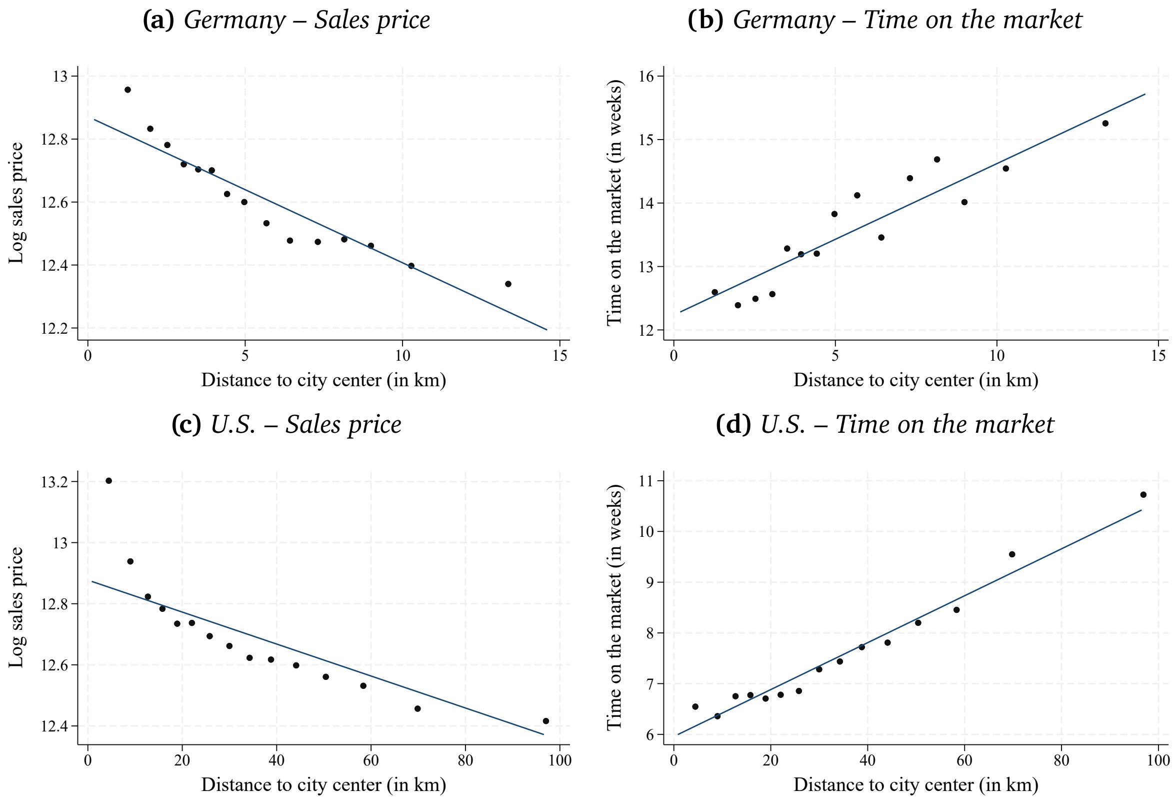

Notes: These binned scatter plots display the results of Regression (1) *with log sales price and time on the market as the outcome variables, using 15 equally-sized distance bins. The binned scatter plots are based on the complete regression specification, as shown in columns three and six of Tables 2 and 3. The binned scatter plots are produced following Cattaneo et al. (2024).*

Results. In Figure 1, we present binned scatter plots based on Regression (1). The left-hand panels display a clear negative relationship between sales prices and distance to the city center. This negative price gradient has been documented in the literature for cities in the United States (Harris, 2024) and across the globe (Liotta, Viguié, and Lepetit, 2022). The right-hand panels display a clear positive relationship between time on the market and distance to the city center, which constitutes our novel finding of a *negative liquidity gradient*. By showing the results for both German and U.S. cities, we demonstrate that these stylized facts hold for very different housing markets as well as different city structures – U.S. cities are typically larger and more sprawled than European cities (see, for example, Nechyba and Walsh, 2004).

Table 2: *Time on the market and distance to the city center, Germany (2012–2024)*

	(1) TOM	(2) TOM	(3) TOM	(4) TOM	(5) TOM	(6) TOM
Distance to center (in km)	0.34***	0.24***	0.20***			
	(0.04)	(0.03)	(0.03)			
Travel time to center (in min)				0.15***	0.10***	0.08***
				(0.02)	(0.01)	(0.01)
City × Year-quarter FE	✓	✓	✓	✓	✓	✓
Property characteristics		✓	✓		✓	✓
Borough FE			✓			✓
N	84,292	84,292	84,292	84,292	84,292	84,292
Adj. R^2	0.04	0.13	0.13	0.04	0.13	0.13
Mean(TOM)	13.51	13.51	13.51	13.51	13.51	13.51

Notes: This table displays the output of Regression (1) *on time on the market (TOM), measured in weeks. The first three columns show the results for distance to the city center measured in kilometers, while the last three columns show the results for car travel time to the city center measured in minutes. The list of property characteristics is available in Supplemental Appendix A.1. Regressions are based on the matched sample for all cities covering the period between 2012 and 2024. Standard errors (in parentheses) are clustered at the city-year level.* $*: p < 0.1; **: p < 0.05; ***: p < 0.01$.

Next, we quantify the relation between time on the market and distance to the city center using several alternative specifications of Regression (1). Tables 2 and 3 present the results for Germany and the U.S. across model specifications, ranging from the most parsimonious model, which only includes city-time fixed effects, to the most comprehensive model, which features the full set of control variables. The coefficient on kilometer distance or travel time is consistently significant at the 1% level for both German and U.S. cities across all specifications.[13] The coefficients remain highly significant but become slightly smaller when property characteristics are included as controls – the housing stock in city centers often exhibits features that enhance its liquidity, such as apartments being smaller and newer.[14] The results remain robust when focusing solely on within-borough

[13]Note that differences in average travel times between Germany and the U.S. lead to different relative magnitudes of the kilometer distance and travel time coefficients.

[14]In Supplemental Appendix C.4, we document that the most relevant of these characteristics are still substantially less relevant determinants of housing liquidity than the distance to the city center.

(*Stadtbezirk*) variation in German cities and when controlling for local median household income, neighborhood quality, and demographic characteristics in U.S. cities.[15]

Table 3: *Time on the market and distance to the city center, U.S. (2012–2023)*

	(1) TOM	(2) TOM	(3) TOM	(4) TOM	(5) TOM	(6) TOM
Distance to center (in km)	0.04***	0.03***	0.05***			
	(0.005)	(0.005)	(0.004)			
Travel time to center (in min)				0.04***	0.03***	0.06***
				(0.007)	(0.006)	(0.005)
Median income		-0.09	-0.14		-0.08	-0.09
		(0.110)	(0.088)		(0.105)	(0.085)
MSA × Year-month FE	✓	✓	✓	✓	✓	✓
State FE	✓	✓	✓	✓	✓	✓
Property characteristics			✓			✓
Demographic controls			✓			✓
N	682,100	682,100	682,100	682,100	682,100	682,100
ZIP Codes	4,943	4,943	4,943	4,943	4,943	4,943
Adj. R^2	0.29	0.29	0.32	0.29	0.29	0.32
Mean(TOM)	7.60	7.60	7.60	7.60	7.60	7.60

Notes: This table displays the output of Regression (1) *on time on the market (TOM), measured in weeks. The first three columns show the results for distance to the city center measured in kilometers, while the last three columns show the results for car travel time to the city center measured in minutes. Regressions are based on data for single-family houses for the 30 largest MSAs covering the period between 2012 and 2023. Standard errors (in parentheses) are clustered at the MSA-year level.* $*: p < 0.1; **: p < 0.05; ***: p < 0.01$.

In terms of magnitude, properties in the outskirts take approximately 20% longer to sell compared to those in the city center after taking into account spatial variation in property characteristics, income, and demographics. In German cities, this amounts to approximately two and a half weeks, while in U.S. cities, it corresponds to about two weeks. [16] As we show later in our model, these differences reflect large spatial differences in market tightness with substantial effects on welfare and prices. Moreover, as we illustrate in Supplemental Appendix C.1, the spatial variation in U.S. housing market

[15]In Supplemental Appendix J.1, we show that the variance of time on the market also increases with distance to the city center. This result confirms a prediction of our structural model in the second part of the paper.

[16]These results are based on a specification of Regression (1) in which the "city center" is defined as all observations within a 3 km radius of the city center in Germany and a 10 km radius in the U.S., while the "outskirts" are defined as areas beyond 13 km for German cities and beyond 40 km for U.S. cities.

liquidity is as large as the variation over time. The cyclical variation in time on the market amounts to up to three weeks, which has been shown to have important implications for business cycle dynamics (Garriga and Hedlund, 2020). Lastly, despite large differences in terms of city structure between German and U.S. cities, when considering the actual travel time to the city center with all controls (Column 6 in both tables), time on the market changes at almost the same rate across space in both countries.[17]

3.2 Spatial variation in other liquidity measures

Figure 2: *Alternative liquidity measures for Germany (2012–2024) and the U.S. (2012–2023)*

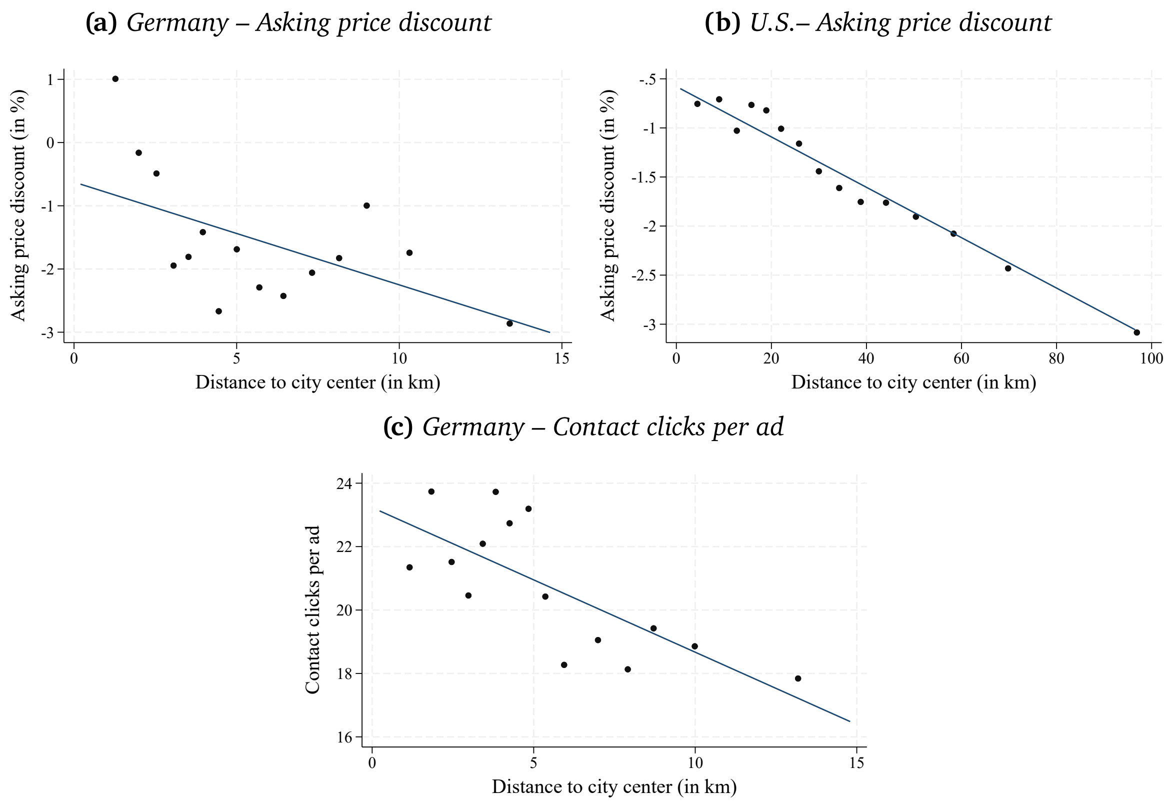

Notes: These binned scatter plots visualize the results of Regression (1) *with asking price discount and contact clicks per ad as the outcome variables, using 15 equally-sized distance bins. The binned scatter plots are produced following Cattaneo et al. (2024).*

We now show that other dimensions of liquidity in housing markets – beyond the time on the market – also decline with distance to the city center. Figure 2 presents binned scatter plots based on Regression (1). First, the spread between the asking price and the sales price decreases with distance to the city center in both German and U.S. cities. In

[17] In Supplemental Appendix C.5, we show that our results also hold when using the travel times retrieved from the Google Maps Directions API.

both countries, this spread is on average negative, indicating that final transaction prices tend to fall below initial asking prices. This finding suggests that sellers in the outskirts have a harder time selling at their asking prices. Second, market tightness, proxied by contact clicks per ad, decreases with distance to the city center in German cities.[18] Both of these effects are statistically significant, as shown in Supplemental Appendices C.6 and C.7 with detailed regression results.

3.3 Robustness analysis

Results for individual cities. In the previous section, we have presented results for pooled samples of German and U.S. cities. Given that cities vary in size and other spatial characteristics, it is possible that our results are driven by a subsample of cities. As we show in Supplemental Appendix D.1, this is not the case. We find negative liquidity and price gradients for all cities in the German dataset and negative liquidity gradients for all cities in the U.S. dataset as well as negative price gradients for most cities in the U.S. dataset. We do not explicitly analyze heterogeneity in coefficients across cities, but as our model in the second part of the paper suggests, this heterogeneity is likely driven by differences in the cost of travel to the city center.

COVID. The COVID-19 pandemic and the subsequent shift to remote work significantly flattened the price gradient in the United States (Gupta et al., 2022). In contrast, the impact on the price gradient in Europe has been comparably muted (Biljanovska and Dell'Ariccia, 2023). We test whether remote work influenced liquidity gradients by splitting our samples into pre- and post-2020 periods. For both Germany and the U.S., the liquidity gradient flattened during the COVID-19 pandemic but started to recover thereafter, as documented in Supplemental Appendix D.2. Our structural model presented in the second part of the paper is able to replicate this development, which we show in Supplemental Appendix J.6. The extent to which the flattening is persistent depends on the future evolution of remote work levels and preferences to live near city centers.

[18] Data retrieved from RWI - Leibniz-Institut für Wirtschaftsforschung and ImmobilienScout24 (2024). Recall from Section 2.4 that we can construct this measure only for German cities. Moreover, note that while lower market tightness in the outskirts could also result from a larger housing supply, we show in Supplemental Appendix C.7 that this is not the case: the residential housing stock actually decreases with distance to the city center in large German and U.S. cities.

Different housing types. In our baseline analysis, we focus on the most common housing types in German and U.S. cities: apartments and single-family houses, respectively. In this robustness check, documented in Supplemental Appendix D.3, we show that our results for German cities remain robust across apartment size categories and our results for the United States remain robust when considering different housing types (condominiums, multi-family homes, and townhouses).

Alternative city definitions. For U.S. cities, we test whether our results hold when using functional urban area boundaries from Moreno-Monroy, Schiavina, and Veneri (2021) which define cities based on commuting flows, following the EU-OECD definition from Dijkstra, Poelman, and Veneri (2019). This robustness analysis is not possible for German cities, as we only have data available that refers to apartments transacted within the administrative city boundaries. In Supplemental Appendix D.4, we show that our results hold when using functional urban area boundaries for U.S. cities.

Alternative city center definitions. In our baseline analysis, our definition of city center is based on historic locations for German cities and city halls for U.S. cities. We conduct a robustness analysis with alternative city centers. For Germany, we use the centroid of the business district with the highest land value in 2023, as given by the *Bodenrichtwerte* land values produced by the *Gutachterausschuesse* real estate committees.[19] This definition follows the concept of a central business district in the canonical monocentric city model. For the United States, we do not have appraisal data available and therefore use the locations with the highest job access index as alternative city centers. The results, documented in Supplemental Appendix D.5, show practically unchanged spatial gradients.

Non-parametric estimation. Although our main results are highly significant and robust to a multitude of controls and fixed effects, we still rely on the functional form of the OLS regression specified in Equation (1). To ensure that our results are not compromised by misspecification, we employ nonparametric methods. When applying these methods, we test whether liquidity and prices are on average lower in the outskirts than in the city center, where we match at the level of housing units based on observable characteristics. Accordingly, we can only produce these results for German cities.

[19]For this analysis, we have to exclude Munich, as we do not have access to its local *Bodenrichtwerte* appraisals. The land values for the other cities are available via the *BORIS-D* database.

First, we use augmented inverse probability weighting to estimate the average difference in outcome variables between city center and outskirts, while using LASSO regression in the first stage to estimate the probability of treatment. Second, we use propensity score matching based on our full set of apartment characteristics. Third, we use inverse probability weights from a logistic regression to estimate average differences. The results are documented in Table 4, comparing the first 3 bins of the distance to the city center with the 13th, 14th, and 15th (out of 15) bins. All non-parametric methods confirm our baseline OLS results both in terms of direction as well as in terms of magnitude. The relatively high number of observations and detailed information on properties explain the similar effect magnitudes across methods.

Table 4: *Average differences between city center and outskirts, Germany (2012–2024)*

Method	Difference in TOM	Difference in log prices	N
OLS	1.89*** (0.227)	-0.40*** (0.004)	33,717
LASSO	2.11*** (0.378)	-0.43*** (0.006)	33,717
Propensity score	1.99*** (0.446)	-0.43*** (0.013)	33,717
Inverse probability	2.20*** (0.328)	-0.43*** (0.005)	33,717

Notes: This table shows the estimated average difference between city center and outskirts for time on the market (TOM), measured in weeks, and log sales prices for different non-parametric methods. The different methods are described in the main text. $*: p < 0.1; **: p < 0.05; ***: p < 0.01$.

Properties that do not get sold. Our baseline results could be biased if the number of advertisements that did not result in a sale varies systematically across space. To assess this, we run an algorithm to identify such advertisements in the German data. Supplemental Appendix D.6 shows that the percentage of ads that do not result in a sale is small and increases slightly with distance to the city center. In addition, we conduct a survival analysis that also includes ads that do not result in a sale, and find that the probability of sale decreases with distance to the city center. By excluding these unsold ads from our main analysis, we may, if anything, be underestimating the steepness of the spatial liquidity gradient.

Information frictions. One potential explanation for lower liquidity in the outskirts is the presence of less-informed sellers, possibly due to an older population that is less engaged with housing markets. Specifically, if sellers in peripheral areas systematically overvalue their properties by setting unrealistically high asking prices, this may lead to longer marketing durations. A further implication is a wider gap between asking and transaction prices in these areas – an empirical pattern that we indeed observe. However, as demonstrated in Supplemental Appendix D.7, this overvaluation mechanism cannot explain the observed differences in housing market liquidity. We show that the spatial gradient in the time on the market remains robust when controlling for the asking price discount, and vice versa. That is, when comparing otherwise similar transactions – one in the city center and one in the outskirts – with comparable asking price discounts (or time on the market), the other respective spatial gradient persists. In fact, both liquidity gradients remain practically unchanged in magnitude when accounting for the overvaluation channel. This result is not surprising, given that real estate listing platforms are widely accessible, which implies that market participants in the outskirts are, on average, probably as informed as those in the city center.

3.4 Discussion of external validity

Our empirical analysis shows that liquidity and prices decrease with distance to the city center. In this section, we discuss to which extent these results can be generalized to other settings, considering alternative focal points beyond the city center and other markets.

In our empirical analysis, we implicitly assume that the cities in our sample exhibit a monocentric structure. However, the mechanism we propose in the theoretical part of the paper extends beyond the monocentric structure. In particular, our theoretical mechanism only requires the existence of focal points that attract sufficiently large numbers of commuters. We test whether our empirical results hold when considering alternative focal points. Using data on commuting distances and the number of employees across ZIP Codes from Delventhal and Parkhomenko (2024), we construct an index of job accessibility at the ZIP-Code level as an inverse-distance-weighted average of accessible jobs. We identify the ZIP Codes with the highest job accessibility within a given MSA, which we refer to as *focal ZIP Codes*, and calculate the distance from each ZIP Code to the nearest focal ZIP Code. We then test whether we also find liquidity and price gradients in this alternative setting. The results, presented in Supplemental Appendix D.8, confirm that both gradients are also present when measuring distances to the nearest focal ZIP Codes. This finding is robust to varying the number of focal ZIP Codes per MSA.

Second, we test whether our results also hold beyond the owner-occupied residential market. If the observed liquidity and price gradients are driven by differences in local market tightness, as suggested by our results in Section 3.2, we should expect to observe similar patterns in the rental market. To test this, we use German rental listings data from ValueAG for the same cities and time period as in our baseline analysis, applying the same cleaning procedures as for the sales listings. The results, calculated using the baseline specification of Regression (1), are presented in Table 5.[20] We find that the time on the market for rental housing units increases with distance to the city center, while net rents (defined as monthly rental prices excluding utilities) decrease. In Columns 3 and 6, we show that these results also hold when relying solely on within-ZIP-Code variation, which partially isolates confounding variation due to spatial differences in income and demographics.

Table 5: *Liquidity and price gradients in the rental market, Germany (2012–2024)*

	(1) TOM	(2) TOM	(3) TOM	(4) Net rent	(5) Net rent	(6) Net rent
Distance to center (in km)	0.17***	0.17***	0.21***	-0.02***	-0.03***	-0.02***
	(0.02)	(0.02)	(0.08)	(0.00)	(0.00)	(0.00)
City × Year-quarter FE	✓	✓	✓	✓	✓	✓
Property characteristics		✓	✓		✓	✓
ZIP Code FE			✓			✓
N	957,249	957,249	957,249	957,249	957,249	957,249
Adj. R^2	0.23	0.26	0.27	0.40	0.90	0.91
Mean(dependent variable)	6.72	6.72	6.72	6.52	6.52	6.52

Notes: This table displays the output of Regression (1) *on time on the market (TOM) and log net rental value (net rent). All columns show the results for distance to the city center measured in kilometers. The list of property characteristics is available in Supplemental Appendix A.1. Regressions are based on the cleaned sample of rental listings from ValueAG for all cities covering the period between 2012 and 2024. Standard errors (in parentheses) are clustered at the city-year level.* $*: p < 0.1; **: p < 0.05; ***: p < 0.01$.

4 Theoretical analysis

We give structure to the stylized empirical facts documented in the previous sections by building a spatial search model of a city's housing market. We start from a frictional search market for housing (see, for example, Ngai and Tenreyro, 2014; Piazzesi, Schnei-

[20] Note that due to the very high number of observations for rentals, we can use more granular location fixed effects than in our baseline analysis.

der, and Stroebel, 2020; Guren and McQuade, 2020), using the established basic setup from Krainer (2001). We introduce space following the monocentric city model going back to Alonso (1964), Mills (1967), and Muth (1969). The spatial distribution of housing in the static monocentric city model is endogenous. Here, we take the spatial distribution of housing as exogenously given to focus on liquidity, an inherently dynamic object.

4.1 Structural framework

Model environment. Time is discrete and measured in days. A large number N of infinitely-lived agents live in a monocentric city. The agents are risk neutral, financially unconstrained, and discount with factor $\beta \in (0,1)$. All agents travel to the city center for work and leisure activities. The daily travel cost $\tau(d)$ is associated with a distance to the city center $d \in \mathscr{D} = [\underline{d}, \overline{d}]$, where $\partial\tau/\partial d > 0$. There are two goods in the economy, housing and a composite consumption good which is not modeled explicitly. All costs and benefits in the model are expressed in terms of the composite consumption good.

Housing. The housing stock is exogenously given and consists of N housing units with given distances to the city center.[21] Housing units are equally distributed across distances, meaning that there is the same number of housing units at each distance.[22] Before deciding whether to purchase a housing unit, an agent draws an idiosyncratic valuation ε, referred to as *housing dividend* in the following. The housing dividend is a random variable with cumulative distribution function F and probability density function f. Having decided to purchase a property, the agent receives the corresponding dividend in every period until they are unmatched. The dividend is independently and identically distributed across agents, space, and time. An agent can only occupy one housing unit at a time, can only search for new housing units after they have been unmatched, and cannot rent out their property.

Search process. We focus on a stationary search equilibrium and omit time indices. In the first model period, every agent is endowed with a housing unit. In every following period, a match between an agent and a housing unit persists with probability π. With

[21] Due to limitations in data availability required for estimating the model, we abstract from spatial differences in housing supply elasticity which could be a complementary mechanism to explain price differences across the city.

[22] This holds true in the data by definition if we use the distance bins from the binscatters in the empirical analysis as the input for our model city.

probability $1-\pi$, an agent is unmatched, which can be interpreted as a moving shock. In this case, the agent puts their property up for sale and searches for a new one.[23] Agents are therefore sellers and buyers simultaneously.[24] In a given model period, first, sellers post prices, and second, buyers randomly visit housing units that are on the market. When visiting a housing unit, a buyer observes their dividend draw, the property's distance to the city center, and the posted price. The buyer either agrees on the price and moves into the property in the next period or does not agree on the price and continues to search. In Supplemental Appendix G, we extend the search process with a bargaining process, following Carrillo (2012).

Seller's problem. Risk neutrality, a standard assumption in search models, allows us to analyze buyer and seller decisions separately due to linear additivity of agents' value functions. A seller chooses a posted price $p(d)$ to maximize their present value

$$\Pi(d) = \gamma(d)p(d) + \big(1-\gamma(d)\big)\beta\Pi(d). \tag{2}$$

With probability of sale $\gamma(d)$, the seller receives $p(d)$. With probability $1-\gamma(d)$, they try to sell the housing unit again in the next period, obtaining a discounted continuation value $\beta\Pi(d)$. The probability of sale $\gamma(d)$ reflects expected demand, or market tightness, given $p(d)$. Sellers take into account the effect of posted prices on local market tightness. They act as local price setters.[25]

[23]While searching, agents do not necessarily own and live in properties defined formally within the model framework, as they can sell their unmatched property before having found a new property to live in. For this case, we assume that they live in rental units owned by absentee landlords. These properties are rented out at a fixed rental rate normalized to zero, such that this rental rate fully operates in the background of the model and all other costs and benefits in the model are to be understood as deviations from this rental rate. Since this rental rate is small compared to housing prices and expected travel costs for the time of living in a property, we do not explicitly take it into account in our quantitative exercises in Sections 4.5 to 5. Another interpretation of this assumption is that agents live in relatives' or friends' houses while searching if they have already sold their previously unmatched property. The travel cost incurred during the period of living in rental units or being "unhoused" is negligible, as is the rental cost in the first interpretation of this assumption.

[24]An agent can only occupy one housing unit at a time, but can have multiple housing units on the market as a seller. Such a scenario occurs if an agent is unmatched, finds a new property, is unmatched again, but has not yet sold their old property/properties. Due to the large number of agents, the probability of a single agent accumulating all housing units is approximately zero.

[25]This assumption, which we take over from the original Krainer (2001) model, serves as the basis for our spatial asset pricing exercise in Section 5 in which we compare the baseline model to more efficient model versions.

Buyer's problem. A matched buyer, that is, a buyer who has purchased a property and is either living in the housing unit or will move in next period, obtains value

$$V(d,\varepsilon) = \beta\Big(\varepsilon - \tau(d) + \pi V(d,\varepsilon) + (1-\pi)\big(\Pi(d) + W\big)\Big), \tag{3}$$

where W denotes the value of search.[26] With a delay of one period, the buyer receives the dividend ε and incurs the travel cost $\tau(d)$. With probability π, the buyer keeps on living in the housing unit for another period and receives the discounted continuation value $\beta V(d,\varepsilon)$. With probability $1-\pi$, the buyer becomes unmatched and receives the discounted resale value $\beta\Pi(d)$ and the discounted value of search

$$\beta W = \beta \mathbb{E}_{d,\varepsilon}\big[\max\big[V(d,\varepsilon) - p(d), \beta W\big]\big], \tag{4}$$

where a buyer either accepts a posted price and receives a discounted net value of $\beta(V(d,\varepsilon) - p(d))$, or continues to search and receives $\beta^2 W$.[27]

4.2 Equilibrium

Seller's optimization. Rearranging the seller profit expression (2), we have that

$$\Pi(d) = \tilde{\gamma}(d)p(d), \tag{5}$$

where $\tilde{\gamma}(d) = \gamma(d)/(1-\beta(1-\gamma(d)))$ is the discount-factor-adjusted probability that a seller can sell their property in the current period or in any future period. It reflects the expected demand that is relevant for the seller from the perspective of the current period. The first-order condition for profit maximization is then similar to that of a typical price setter, but with a probabilistic sale of a single good and without production costs:

$$\tilde{\gamma}(d) + p(d)\frac{\partial \tilde{\gamma}}{\partial p(d)|_d} = 0, \tag{6}$$

[26] The linear specification for buyer values is standard in housing search models, analogously to linear specifications of worker values in labor market search models (see Rogerson, Shimer, and Wright, 2005).

[27] To calculate the expectation over distances, we assume that it is formed using the whole set of distances $\mathscr{D}$, even if only a subset of distances is covered by the market in a given period. In other words, we assume that buyers act as if housing units at all distances to the city center will be available on the market in the next period. This modeling choice is a consequence of focusing on a stationary equilibrium. With a large number of properties, this holds approximately true in every period.

where the derivative $\partial\tilde{\gamma}(d)/\partial p(d)|_d$ is a reformulation of the derivative $\partial\gamma(d)/\partial p(d)|_d$.[28] It captures the tradeoff between price and probability of sale that the seller faces: if the seller changes their price, the probability of sale also changes. We show in Supplemental Appendix E that a seller's first-order condition provides a local maximum for their profit.

Buyer's optimization. Via the definition of the value of search (4), a buyer has to be indifferent between buying a property and continuing to search at some reservation dividend $\varepsilon^*(d)$:

$$V(d,\varepsilon^*(d)) - p(d) = \beta W. \tag{7}$$

The solution of this equation for a given distance to the city center characterizes the corresponding reservation dividend. The optimality condition (7) defines a cutoff rule for a stochastic event. Individual buyers can draw higher housing dividends than $\varepsilon^*(d)$, in which case they accept the equilibrium price $p(d)$ and obtain a net utility above βW.

Notion of spatial equilibrium. The buyers' optimality condition (7) implies reservation dividends with which buyers are indifferent between purchases at all distances to the city center, as the discounted value of search βW does not vary across space. The buyer indifference condition is hence also a spatial equilibrium condition. Note that precisely because equilibrium expected net buyer utility is constant, required dividend draws have to offset travel costs. Hence, this spatial equilibrium condition is also to be interpreted as a spatial no-arbitrage condition for housing (see, for example, Glaeser and Gyourko, 2008), such that there is no arbitrage opportunity for buyers across space.

Probability of sale. The equilibrium probability of sale at some distance to the city center is equal to the probability that a buyer's idiosyncratic dividend draw is above the

[28]Intuitively, this derivative reads

$$\frac{\partial\tilde{\gamma}}{\partial p(d)|_d} = \frac{\partial\gamma}{\partial p(d)|_d}\left(\frac{1-\frac{\beta\gamma(d)}{1-\beta(1-\gamma(d))}}{1-\beta\big(1-\gamma(d)\big)}\right),$$

where the denominator reflects that if the seller marginally changes their posting price, the probability of sale changes in the current period, but also in the next period with probability $1-\gamma(d)$ which is discounted with factor β, and so forth, ad infinitum. The numerator adjusts for the fact that the probability $1-\gamma(d)$ with which the probability of sale changes in the next period, changes as well.

reservation dividend at this distance:

$$\gamma(d) = Prob\left(\varepsilon \geq \varepsilon^*(d)\right) = 1 - F(\varepsilon^*(d)). \tag{8}$$

Thus, for the derivative in the seller's optimality condition (6) we have that

$$\frac{\partial \gamma}{\partial p(d)|_d} = -f(\varepsilon^*(d))\,\frac{\partial \varepsilon^*}{\partial p(d)|_d}. \tag{9}$$

To characterize this derivative, we rearrange the buyer's value (3) and obtain the linear expression

$$V(d,\varepsilon) = \frac{\beta}{1-\pi\beta}\Big(\varepsilon - \tau(d) + \big(1-\pi\big)\big(\Pi(d) + W\big)\Big). \tag{10}$$

Using the indifference condition (7), we isolate the reservation dividend:

$$\varepsilon^*(d) = \frac{1-\pi\beta}{\beta}p(d) + \tau(d) - \big(1-\pi\big)\Pi(d) + \big(\pi - \pi\beta\big)W. \tag{11}$$

Hence, the derivative in the first-order condition of the seller is

$$\frac{\partial \gamma}{\partial p(d)|_d} = -f(\varepsilon^*(d))\,\frac{1-\pi\beta}{\beta}, \tag{12}$$

where $\partial\Pi/\partial p(d)|_d = 0$ due to the envelope theorem. Now, we have all required information to define an equilibrium of the model.

Equilibrium definition. A *stationary spatial search equilibrium* consists of value functions $\{V,\Pi\}$, a value of search W, a posting price function p, a reservation dividend function ε^*, and a sale probability function γ that satisfy equations (2), (4), (6), (7), (8) for all distances to the city center $d \in \mathscr{D}$, given parameters $\{\beta,\pi,\underline{d},\overline{d}\}$, a cumulative distribution function for idiosyncratic dividends F with probability density function f, and a travel cost function τ.

4.3 Analytical results

Before calibrating and estimating the model's structural parameters, we first derive analytical results that rationalize our findings from the empirical part of the paper as general properties of our model. We show that the equilibrium expected time on the market increases with distance to the city center, while the equilibrium sales price decreases. We derive these results here for uniformly distributed dividends $\varepsilon \sim U[\underline{\varepsilon}, \overline{\varepsilon}]$ which we later employ in our quantitative exercise. In Supplemental Appendix F, we show that these results hold with more general assumptions about the dividend distribution, and with the exponential distribution as a specific example of an alternative dividend distribution. In Supplemental Appendix G, we show that the expected time on the market is interchangeable with the asking price discount as an alternative concept of liquidity within the extended version of our model with bargaining. In Supplemental Appendix H, we provide proofs of the equilibrium's existence and uniqueness for our extended model with bargaining and our baseline model as a nested case of the extended model.

4.3.1 Reservation dividends across space

First, as an auxiliary result, we derive that buyer reservation dividends $\varepsilon^*(d)$ increase with distance to the city center. This result is auxiliary in the sense that it is essential to understand the spatial patterns in liquidity and prices, our main results. We show that buyers need higher draws of the dividend to make a purchase the farther a housing unit they visit is away from the city center, due to a higher travel cost $\tau(d)$. To obtain that $\partial\varepsilon^*/\partial d > 0$, we reformulate $p(d)$ and $\Pi(d)$ in terms of $\varepsilon^*(d)$. We plug the resulting terms into the isolated reservation dividend expression (11) which then only depends on the travel cost and the value of search which does not vary across space. If we differentiate this expression with respect to the distance to the city center, we can express the spatial variation in buyer preferences solely as a function of the spatial variation in travel costs. This allows us to obtain features of our model which hold irrespective of parameter values.

To start our derivations, we use the seller optimality condition characterized by (6) to express the equilibrium price as a function of the probability of sale:

$$p(d) = \frac{-1}{\partial\gamma(d)/\partial p(d)|_d} \left(\gamma(d) + \frac{\beta}{1-\beta}\left(\gamma(d)\right)^2\right), \tag{13}$$

where

$$\gamma(d) = 1 - \frac{\varepsilon^*(d) - \underline{\varepsilon}}{\overline{\varepsilon} - \underline{\varepsilon}} = \frac{\overline{\varepsilon} - \varepsilon^*(d)}{\overline{\varepsilon} - \underline{\varepsilon}} \tag{14}$$

due to equilibrium relation (8) between probabilities of sale and reservation dividends. Then, together with the closed-form relation (12) for the derivative $\partial\gamma(d)/\partial p(d)|_d$,

$$p(d) = \frac{\beta\left(\overline{\varepsilon} - \varepsilon^*(d)\right)}{1 - \pi\beta} + \frac{\beta^2\left(\overline{\varepsilon} - \varepsilon^*(d)\right)^2}{(1-\beta)(1-\pi\beta)\left(\overline{\varepsilon} - \underline{\varepsilon}\right)} \tag{15}$$

and, via the definition of the seller profit (2),

$$\Pi(d) = \frac{\beta\left(\overline{\varepsilon} - \varepsilon^*(d)\right)^2}{(1-\beta)(1-\pi\beta)\left(\overline{\varepsilon} - \underline{\varepsilon}\right)}. \tag{16}$$

Plugging these results into the expression for the reservation dividend (11) and differentiating with respect to the distance to the city center, we get:

$$\frac{\partial\varepsilon^*}{\partial d}\underbrace{\left(2 + 2\frac{\pi\beta}{1-\pi\beta}\frac{\overline{\varepsilon} - \varepsilon^*(d)}{\overline{\varepsilon} - \underline{\varepsilon}}\right)}_{>0} = \frac{\partial\tau}{\partial d} > 0, \tag{17}$$

and hence, $\partial\varepsilon^*/\partial d > 0$. This provides a starting point for our following description of the spatial distribution of liquidity and prices.

4.3.2 Liquidity and prices across space

Liquidity. In line with the measurement of time on the market in the empirical part of the paper, we define that a property has been on the market for T days if it sells on day number T of being advertised. Via the expected value of the geometric distribution that results from the multiplication of sale probabilities over time, the expected time on the market in days at a given distance to the city center is

$$\mathbb{E}\left[TOM(d)\right] = \frac{1}{\gamma(d)} = \frac{\overline{\varepsilon} - \underline{\varepsilon}}{\overline{\varepsilon} - \varepsilon^*(d)}. \tag{18}$$

Therefore,

$$\frac{\partial \mathbb{E}[TOM]}{\partial d} = \underbrace{(\overline{\varepsilon} - \underline{\varepsilon})(\overline{\varepsilon} - \varepsilon^*(d))^{-2}}_{>0} \frac{\partial \varepsilon^*}{\partial d} > 0. \tag{19}$$

Intuition. Reservation dividends increase with distance to the city center, which reflects compensation for a higher cost of travel to the city center. With a higher cutoff value for dividend draws, the probability of sale decreases with distance to the city center, that is, the market thins out. A lower probability of sale implies a higher expected time on the market.[29]

Prices. Via auxiliary expression (15),

$$\frac{\partial p}{\partial d} = \underbrace{\left(\frac{\beta}{1-\pi\beta} + \frac{2\beta^2(\overline{\varepsilon} - \varepsilon^*(d))}{(1-\beta)(1-\pi\beta)(\overline{\varepsilon} - \underline{\varepsilon})}\right)}_{>0} \left(-\frac{\partial \varepsilon^*}{\partial d}\right) < 0. \tag{20}$$

Intuition. Sellers expect to sell housing units with a higher probability in the city center, as reservation dividends are lower. Being local price setters, they optimally post higher prices, since they know that they are more likely to meet a searcher that is willing to buy. As in the standard monocentric city model, the underlying factor for equilibrium prices to decrease with distance to the city center is the cost of travel to the city center.[30]

Further remarks. We choose to build on the canonical monocentric city model because it is a well-established framework. Our mechanism does not require a single city center, or any city center whatsoever to function. Our additional empirical analysis with focal ZIP Codes across the United States further illustrates this statement empirically. Whenever there is a location for which homebuyers share a common preference to live nearby, generating spatial patterns in market tightness, our mechanism applies. City centers provide established examples for such focal points, and as such a special case of our mechanism. Note that in practice, the cost of travel to a focal point may sometimes not increase with distance to this focal point due to, for example, rivers or other factors that influence local transportation. In such a case, we would not expect liquidity and prices

[29] As an additional result, in Supplemental Appendix J.1, we show that the variance of time on the market increases with distance to the city center and confirm this result empirically.

[30] In Supplemental Appendix J.2, we show that the model furthermore predicts the price gradient to be steeper than the liquidity gradient due to the dynamic nature of the seller's problem and confirm this result empirically.

to decrease with distance to this focal point.

Next, note that we assume all agents to be identical. In principle, different buyer clienteles in the city center and the outskirts could also generate spatial variation in liquidity and prices. However, first, within-city housing market search tends to be integrated via “broad searchers” (Piazzesi, Schneider, and Stroebel, 2020) who search across many locations. Second, in our empirical analysis, we condition on apartment size and on borough fixed effects for German cities, both of which should capture some dimension of buyer heterogeneity. For U.S. cities, we control for ZIP-Code-level demographic characteristics. It is therefore consistent with the empirical part of the paper to abstract from buyer heterogeneity in the model.

Moreover, we assume that buyers randomly visit housing units and observe their idiosyncratic dividends during these visits. If buyers were more likely to visit properties in the city center, this would also affect the time on the market. The result on “broad searchers” from Piazzesi, Schneider, and Stroebel (2020) partly counteracts also this concern. Moreover, in Carrillo (2012), searchers observe part of their dividends before deciding to visit properties, which, however, is estimated to play a quantitatively negligible role in housing purchase decisions. In any case, more search flowing towards the center would increase the probability of sale, just as our mechanism predicts. Hence, under the alternative mechanism of spatial differences in search intensity, the driving force behind spatial differences in liquidity and prices would equally consist of spatial differences in market tightness.

Furthermore, note that if housing units are more heterogeneous in the outskirts and this causes higher search costs, buyers are also less likely to buy properties in the outskirts. If heterogeneity is increasing gradually with distance to the city center, this could provide a mechanism for the decreasing market tightness. However, such a systematic gradually evolving spatial pattern in the housing stock is unrealistic. Following the urban economics literature, we focus on travel costs as the underlying fundamental that yields the gradual spatial pattern in market tightness.

Lastly, as we show in Supplemental Appendix J.1, lower market tightness in the outskirts also increases the uncertainty about housing liquidity. We assume risk neutrality of agents for tractability. Risk-averse agents would discount uncertainty about liquidity more in the outskirts than in the city center. This would be a complementary mechanism:

spatial price differences would be reinforced.

4.4 Calibration and estimation of model parameters

Now, we turn to our quantitative exercise and first calibrate and estimate the structural parameters of our model. Since our equilibrium conditions gives us a set of non-linear equations, we solve the model numerically to this end.[31] To do so, we discretize the set of distances to the city center: $\mathscr{D}^{\Delta} = \{d_1^{\Delta}, \ldots, d_z^{\Delta}\}$, where $\underline{d} = d_1^{\Delta}$ and $\overline{d} = d_z^{\Delta}$. To obtain the discretized distances $\mathscr{D}^{\Delta}$, we group the distances to the city center from the pooled German and U.S. datasets net of city-time fixed effects and controls into $z = 15$ bins with equal numbers of observations, using the distance bins from the binned scatterplots in Figure 1. We obtain the corresponding travel time estimates as explained in Section 2.3 and convert them into travel cost estimates, assuming that $\tau(d^{\Delta}) = \mu\tilde{\tau}(d^{\Delta})$, where $\tilde{\tau}(d^{\Delta})$ is the travel time to the city center in minutes. This conversion of travel time into travel costs follows established approaches (see, for example, Ahlfeldt et al., 2015). The scaling parameter μ measures the cost in model units of traveling 2 minutes by car, as agents travel from their property to the city center and back every day. We follow the canonical monocentric city model and calibrate the travel cost as a physical cost of travel, but also provide an alternative calculation in Supplemental Appendix J.3 in which we think of the travel cost as an opportunity cost due to lost time and thus foregone wages. We convert between model units and euros or dollars via the average apartment sales price.

Calibrated parameters. We set $\beta = \sqrt[365]{0.95} \approx 0.9999$ such that the annual discount factor is 0.95. For German cities, the housing match persistence is given by $\pi = 1 - (1/(30 \times 122)) \approx 0.9997$, as the average holding period in the data is 122 months. This value is based on observations from January 1990 to 2024 to capture the full length of holding periods as well as possible. For Hamburg, we do not have data on holding periods available, thus the calibrated housing match persistence is based on information from Munich, Cologne, Frankfurt, and Duesseldorf. For the U.S., we use a holding period of 120 months as a broadly suitable value for large cities, based on the Redfin data.

Estimated parameters. We estimate the travel cost scaling parameter μ and the uniform distribution bounds $\underline{\varepsilon}$ and $\overline{\varepsilon}$ with the method of simulated moments. We target only

[31] Supplemental Appendix I describes our numerical model solution method.

a single moment per sample, the average time on the market, using an identity weighting matrix for our three parameters. We obtain 95% confidence intervals by drawing 1,000 bootstrapped replications of data inputs sized 1/3 of the entire sample with replacement, estimating the model for each draw, and using the 0.025 quantiles and 0.975 quantiles of the resulting parameter distributions as confidence bounds. The estimation results are displayed in Table 6. By construction, we match the average time on the market in the pooled German city (13.51 weeks) and the pooled U.S. city (7.60 weeks). Note that the estimated lower bound of the housing dividend distribution is negative for Germany, but positive for the United States. This stems from the level difference in time on the market between the two countries, as the U.S. housing market is substantially more liquid than the German housing market.

Table 6: *Estimated parameters, pooled German and U.S. cities*

Parameter	Value	Bootstrapped 95% CI
μ^{Germany}	0.00619	[0.00618,0.00630]
$\mu^{\text{U.S.}}$	0.00420	[0.00417,0.00422]
$\underline{\varepsilon}^{\text{Germany}}$	-0.437	[-0.443,-0.427]
$\underline{\varepsilon}^{\text{U.S.}}$	0.290	[0.282,0.290]
$\overline{\varepsilon}^{\text{Germany}}$	0.533	[0.527,0.541]
$\overline{\varepsilon}^{\text{U.S.}}$	0.702	[0.696,0.711]

Untargeted moments. The estimated values of μ imply an average daily travel cost for the German cities of €20.45, which is in the range of average daily car operating costs in Germany of around €15 (see Andor et al., 2020). For the United States, the average daily travel cost in the model is $29.59 which is in the range of daily car operating costs in the U.S. of around $25 (see Moody et al., 2021).[32] The cited empirical travel cost estimates are broad calculations at the country level and likely vary to a considerable degree at the city level. It is furthermore not entire clear that the car operating cost per se captures the full travel costs or is the only suitable measure. Our opportunity travel cost calculation in Supplemental Appendix J.5 provides an alternative measure.

The average sales price is matched by construction, as we convert between model

[32]Most of the average car operating cost consists of fuel costs, depreciation costs, and repair costs which we find plausible to be linear in car travel time. Since empirically we find that public transport travel times are approximately interchangeable with car travel times, we do not repeat this robustness analysis here for the model.

units and euros or dollars via the average apartment sales price. Then, with averages matched, we can focus on the spatial gradients of the time on the market and sales prices – which we do not target whatsoever in our calibration. The obtained spatial variation is, therefore, our first key quantitative model result.

4.5 Model results

Figure 3: *Spatial distributions of liquidity and prices: model vs. data*

(a) *Germany*

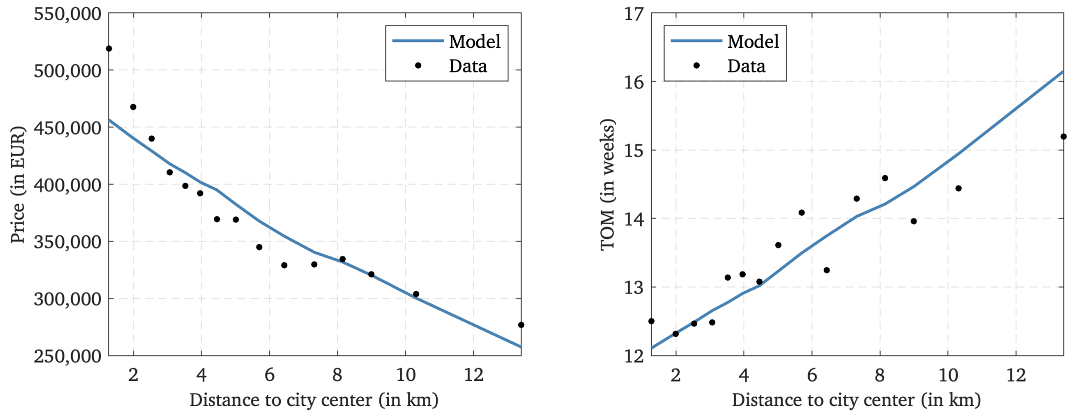

(b) *United States*

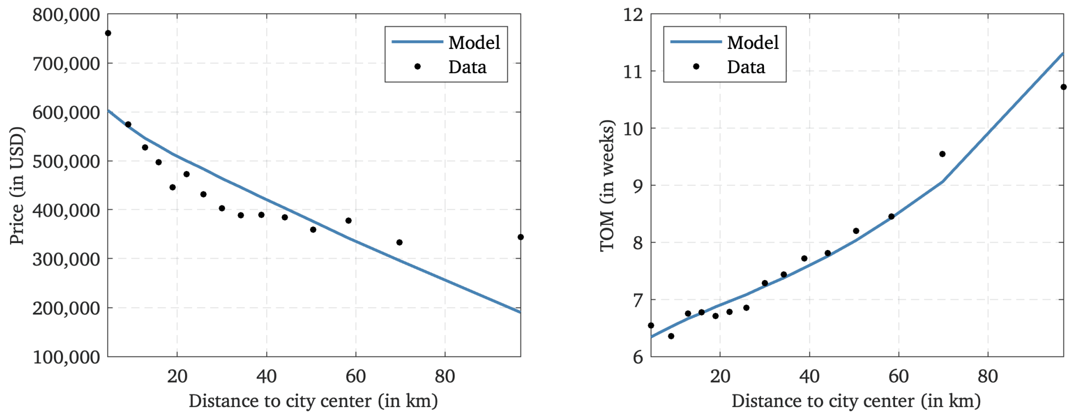

Notes: "TOM" refers to the (expected) time on the market. The data points are calculated using Regression (1) *with city-time fixed effects and all controls, as displayed in Figure 1. The binned scatter plots are produced following Cattaneo et al. (2024), using 15 equally-sized distance bins.*

Even though we do not target the spatial gradients of time on the market and sales prices, our results exhibit spatial variation that closely aligns with the data, as displayed in Figure 3. Supplemental Appendix J.3 provides the spatial distributions of the remaining endogenous variables. The model requires the spatial distribution of travel time to the city center as the only spatial input and, using additional city-wide average values, produces accurate spatial liquidity and price distributions for both German and U.S. cities. As such, we argue for the cost of travel to the city center to be a quantitatively strong fundamental that generates within-city spatial variation in both housing liquidity and housing prices. Nevertheless, the model fails to capture the steep price gradients near the city center, and, for the U.S., the flat price gradient in the outskirts. This leaves explanatory room for factors other than the cost of travel to the city center to systematically drive the within-city variation in apartment prices. Possible factors are, for example, housing supply elasticity (Baum-Snow and Han, 2024) or residential amenities (Garcia-López and Viladecans-Marsal, 2024). Without further analysis, which goes beyond the scope of this paper, we cannot shed light on this issue.

5 Housing liquidity, welfare, and spatial asset pricing

In the previous sections, we have established that spatial variation in travel costs leads to spatial variation in market tightness, which in turn creates spatial gradients in housing liquidity and prices. This result holds both qualitatively and quantitatively: empirical variation in travel costs generates spatial gradients in liquidity and prices close to those that we observe in the data. However, we also know from the literature on search markets that asset liquidity affects welfare and prices. Therefore, we now investigate to which extent housing liquidity affects welfare and housing prices across space.

In our model, illiquidity arises from search frictions, and these frictions can affect welfare and prices through two main channels. First, search frictions impose search costs on buyers. Since buyers need to search more in the outskirts, search costs are higher in those areas, which is reflected in a lower market tightness. Second, sellers adjust their posted prices by internalizing spatial differences in market tightness. In particular, in the city center where the market is tighter, sellers have more pricing power and can charge relatively higher prices. These mechanisms are analogous to frictional search in over-the-counter (OTC) markets, where welfare and prices are shaped by search costs and the bargaining power of dealers (see Duffie, Gârleanu, and Pedersen, 2005). Disentangling the two channels allows us to offer a detailed perspective on how spatial differences in liquidity affect welfare and prices across space.

To do so, we conduct a structural counterfactual analysis, comparing our baseline model with two alternatives: a frictionless model without search, referred to as the *efficient model*, and a model with constrained search, the *constrained-efficient model*.[33] A reduced-form estimation would likely suffer from endogeneity issues, as prices and liquidity are jointly determined by the same underlying factors.

Constrained-efficient model. First, following Krainer and LeRoy (2002), we consider a counterfactual constrained-efficient version of our model which is characterized by optimal buyer search behavior given physical search constraints, but no strategic internalization of this search behavior in the price posting of sellers. To implement this allocation, we calculate reservation dividends $\varepsilon^{\mathrm{CE}}(d^{\Delta})$ that maximize welfare $\mathbb{W}(d^{\Delta})$ at every distance $d^{\Delta} \in \mathscr{D}^{\Delta}$ defined as the expected value of being matched, such that

$$\mathbb{W}(d^{\Delta}) = m(d^{\Delta}) \left(\mathbb{E}_{\varepsilon} \left[\varepsilon \mid \varepsilon \geq \varepsilon^{\mathrm{CE}}(d^{\Delta}) \right] - \tau(d^{\Delta}) \right), \tag{21}$$

where $m(d^{\Delta})$ denotes the probability of being matched and introduces physical constraints into the maximization problem. Without this factor, the optimal reservation dividend would be the maximum dividend $\overline{\varepsilon}$. However, search implies a tradeoff: if the reservation dividend is high, the probability of being matched is low. Correspondingly, the optimal constrained-efficient reservation dividends imply an optimal level of time on the market and hence illiquidity larger than zero, given physical constraints. This is analogous to a natural unemployment rate. Note that the counterpart of $m(d^{\Delta})$ is the steady-state vacancy rate $1 - m(d^{\Delta})$.[34]

Within the welfare definition, the expected idiosyncratic dividend at distance d^{Δ} is $(\varepsilon^{\mathrm{CE}}(d^{\Delta}) + \overline{\varepsilon})/2$ with uniformly distributed idiosyncratic dividends, while the travel cost $\tau(d^{\Delta}) = \mu \tilde{\tau}(d^{\Delta})$ is fixed.[35] Moreover, agents transition from being unmatched to being matched with probability $(\overline{\varepsilon} - \varepsilon^{\mathrm{CE}}(d^{\Delta}))/(\overline{\varepsilon} - \underline{\varepsilon})$ and keep a housing unit with probability π. The transition probability from being unmatched to being matched is a flow probability.

[33] Note that in our counterfactual analysis, we use the estimated structural parameters from the baseline model. By doing so, we assume that our baseline model, which matches the data on liquidity and prices with high precision, represents reality reasonably well and hence provides us with the starting point. Then, when building a counterfactual model with a different market structure and using the estimated structural parameters (which refer to buyer preferences and travel costs) from our baseline model, we pose the question what would happen if the market structure changes while buyer preferences and travel costs remain the same.

[34] Our baseline model correctly predicts the level as well as the spatial variation in the vacancy rate, both of which we did not target in our calibration. We plot these spatial distributions as part of our additional model results in Supplemental Appendix J.3.

[35] Note that we do not differentiate in notation between the German sample and the U.S. sample here and in the rest of this section to avoid unnecessary notation.

The steady-state probability of being matched, a stock probability, is therefore

$$m(d^{\Delta}) = \pi\, m(d^{\Delta}) + \pi\big(1 - m(d^{\Delta})\big)\frac{\overline{\varepsilon} - \varepsilon^{\text{CE}}(d^{\Delta})}{\overline{\varepsilon} - \underline{\varepsilon}}, \tag{22}$$

which allows us to calculate welfare in the constrained-efficient model version as

$$\max_{\varepsilon^{\text{CE}}(d^{\Delta})} \left(\frac{\pi \frac{\overline{\varepsilon} - \varepsilon^{\text{CE}}(d^{\Delta})}{\overline{\varepsilon} - \underline{\varepsilon}}}{1 - \pi + \pi \frac{\overline{\varepsilon} - \varepsilon^{\text{CE}}(d^{\Delta})}{\overline{\varepsilon} - \underline{\varepsilon}}} \right) \left(\frac{\varepsilon^{\text{CE}}(d^{\Delta}) + \overline{\varepsilon}}{2} - \mu\, \tilde{\tau}(d^{\Delta}) \right). \tag{23}$$

Efficient model. In a fully efficient version of the model, agents do not face search frictions. Matches happen instantaneously and the time on the market is zero everywhere. This translates to $m(d^{\Delta}) = 1$ at every distance to the city center, such that there are no vacancies. Similarly, every agent can move directly into the housing unit they prefer best. Hence, with the definition from (21), welfare in the efficient model version at distance d^{Δ} is given by $\overline{\varepsilon} - \mu\, \tilde{\tau}(d^{\Delta})$.

Figure 4: *Spatial welfare loss distributions*

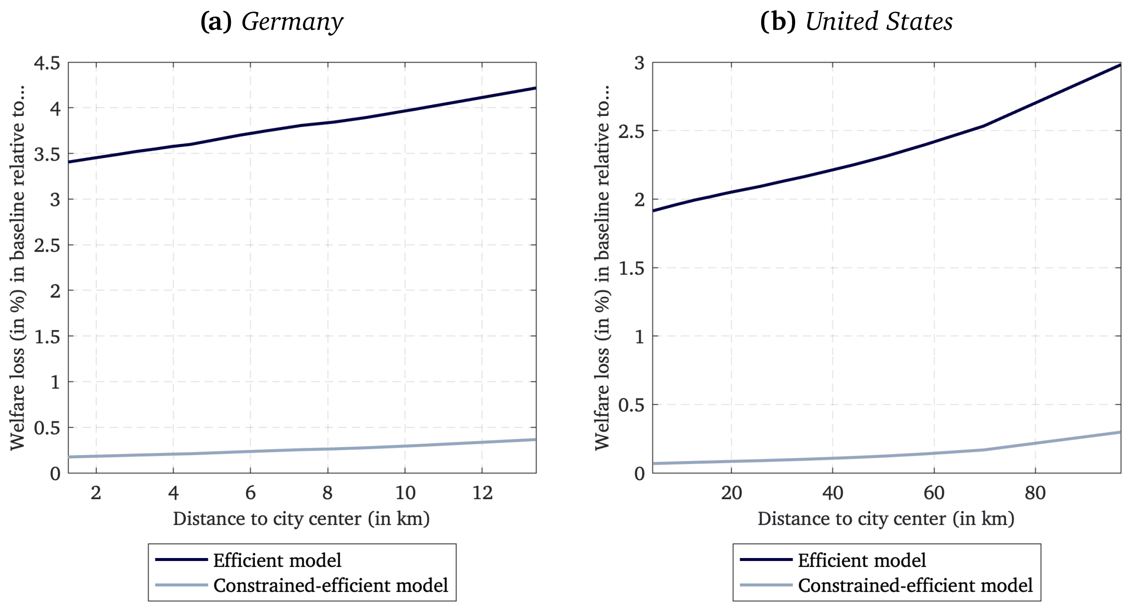

Notes: Welfare is calculated as defined in (21). *The percentages refer to the loss in welfare in the baseline model relative to a counterfactual at every distance to the city center.*

Welfare analysis. We calculate the spatial distributions of welfare, as defined in (21), in the two counterfactual model versions and compare them to the one in the baseline model in Figure 4. First, we notice that search frictions cause large welfare losses. Compared to the efficient model which abstracts from search frictions entirely, welfare losses in the baseline model are on average 3.7% in Germany and 2.2% in the United States.[36] The smaller average welfare loss in the U.S. arises due the fact that the U.S. housing market is more liquid, which means that there is less room for welfare gains when eliminating search frictions. On average in both countries, welfare losses amount to 3%.[37] These results are well within the range of estimated welfare losses due to frictional illiquidity in other search markets, such as municipal bond markets (see Hugonnier, Lester, and Weill, 2019).

The welfare loss in the baseline model relative to the constrained-efficient model is rather small, reaching up to 0.4% in Germany and 0.3% in the United States. The difference in the constrained-efficient model compared to the baseline model lies in the pricing power of sellers. Hence, according to our findings, the interaction of pricing power and search frictions in the housing market causes small welfare losses.

Figure 5: *Spatial welfare loss distributions: decomposition*

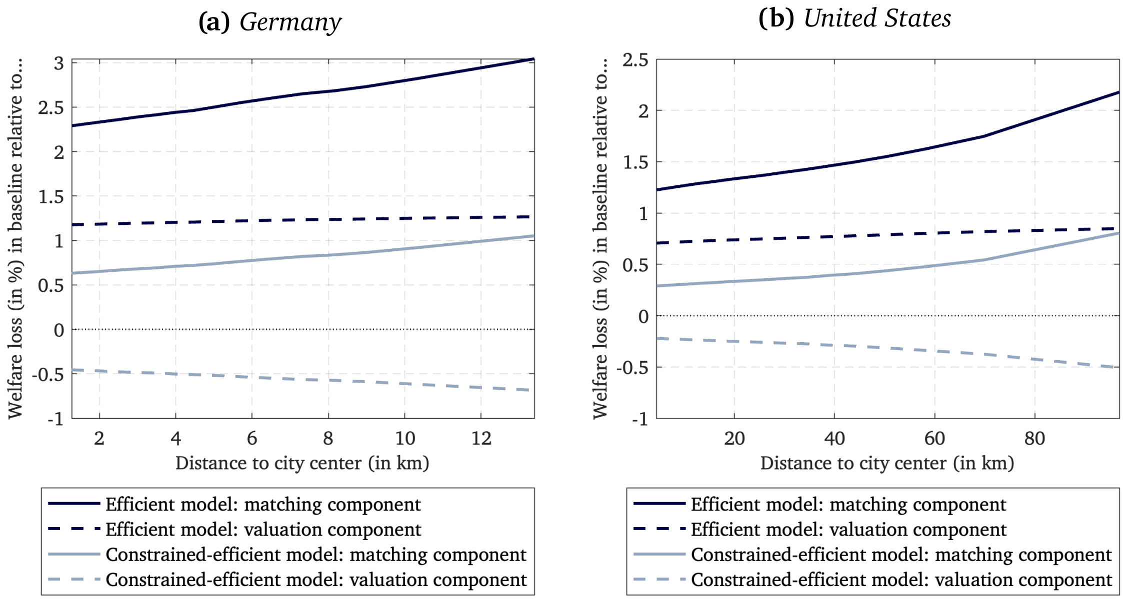

Notes: Welfare is calculated as defined in (21) *and decomposed into the percentage change in the first factor* $m(d^{\Delta})$ *("matching component") and the second factor* $\mathbb{E}_{\varepsilon}\left[\varepsilon \mid \varepsilon \geq \varepsilon^{CE}(d^{\Delta})\right] - \tau(d^{\Delta})$ *("valuation component"). The percentages refer to the loss in welfare in the baseline model relative to a counterfactual at every distance to the city center.*

[36] In Supplemental Appendix J.3, we document that the average welfare loss measured relative to housing prices amounts to 2% in Germany and to 1% in the United States. Hence, on average, welfare losses amount to 1.5% relative to housing prices.

[37] A possible objection to our welfare calculations is the omission of a rental market in our model. For the U.S., owner-occupied housing is prevalent and owner-occupied and rental housing markets are highly segmented, so this is not a particular concern. For Germany, this is not the case, hence it might be an issue – however, our empirical results from Table 5 show negative liquidity and price gradients for German rental markets, therefore, the same mechanism and the corresponding welfare effects should be present when including a rental market.

To understand the welfare differences, we further decompose welfare losses to assess how much is due to a lower probability of being matched (the "matching component") and how much is due to lower average dividends (the "valuation component"). This decomposition is shown in Figure 5. We distill two key findings. First, the matching component is the dominant component for welfare losses relative to both counterfactuals.[38] The matching probability decreases with search frictions. In other words, at any given point in time, a larger fraction of the housing stock remains vacant, which has large welfare costs.

Next, we examine spatial patterns in welfare losses due to frictional illiquidity. As shown in Figure 4, welfare losses increase with distance to the city center. In Germany, agents in the outskirts lose 4.2% welfare in the baseline model relative to the efficient model, whereas agents in the city center lose 3.4%. The difference between these welfare losses amounts to one-fifth of the average welfare loss at 3.7%. In the United States, spatial differences in welfare losses are even larger (1.9% in the center and 3.0% in the outskirts) and amount to half of the average welfare loss at 2.2%. As a population-weighted average, the difference in welfare losses between city center and outskirts amounts to *one-third* of the average welfare loss. Hence, a welfare calculation which does not take into account these spatial differences would miss a fundamental and large component of variation in welfare losses. Spatial differences in welfare losses stem almost entirely from the matching component: matches are particularly infrequent and vacancies are particularly high in the outskirts in the baseline model. In contrast, welfare losses due to the valuation component are relatively stable across space.[39] Overall, we find that the matching component is key for both the aggregate welfare loss levels and and for the spatial variation.

Furthermore, we provide a sensitivity analysis in Supplemental Appendix J.4. We find

[38] In fact, even though the total welfare loss relative to the constrained-efficient model is small, the isolated welfare loss from the matching component is considerable: in the baseline model, agents search more than in the constrained-efficient model and end up with a lower probability of being matched, which lowers welfare. However, this welfare loss gets canceled out by a welfare *gain* in the valuation component. Reservation dividends in the baseline model are higher than in the constrained-efficient model, such that matched agents have a higher valuation on average. Why? In the constrained-efficient model, agents have to trade off a higher matching frequency with a higher valuation. If agents want to match more often, they need to lower their reservation dividends. It turns out that, with our model calibration, these two factors approximately cancel out, except in the outskirts.

[39] For the constrained-efficient model, the negative welfare loss, that is, the welfare gain, becomes mildly more negative with distance to the city center: there is less scope for pricing power to distort reservation dividends in the outskirts where markets are less tight.

that, first, bootstrapped 95% confidence intervals for welfare losses are quite narrow and second, the welfare loss estimates are robust to alternative choices for the housing match persistence and the discount factor. As we would expect, when we decrease the match persistence, welfare losses become somewhat larger, since agents have to search more often. The choice of the discount factor has close to no effect on the welfare loss estimates.

In summary, we have found that welfare losses in the baseline model relative to more efficient model versions, in particular relative to the efficient model version without search frictions, accrue mostly in the outskirts and mostly due to the matching component of welfare. Due to relatively high reservation dividends in the outskirts, the market equilibrium yields a relatively low probability of sale (that is, market tightness) and therefore relatively high time on the market (that is, liquidity). This should imply larger relative price differences between the city center and the outskirts in the baseline model compared to the efficient model.

Spatial price gradient comparison. Our efficient counterfactual model describes a frictionless housing market very close to the canonical monocentric city model, in which the spatial price gradient is determined solely by the exogenously given travel cost gradient (see, for example, Duranton and Puga, 2015). We have to make an additional assumption about time to translate between our model and the monocentric city model. Our model has a notion of time, whereas the monocentric city model does not. We scale up the daily travel cost $\tau(d^{\Delta}) = \mu\tilde{\tau}(d^{\Delta})$ to an expected lifetime travel cost (where "lifetime" refers to the lifetime of a match) with factor $\beta/(1-\pi\beta)$, assuming that when an agent becomes unmatched, they immediately find a new match. Then, we have that for the i-th distance to the city center with $i \geq 2$,

$$p^{\mathrm{E}}(d_i^{\Delta}) - p^{\mathrm{E}}(d_{i-1}^{\Delta}) = -\frac{\beta}{1-\pi\beta}\left(\mu\tilde{\tau}(d_i^{\Delta}) - \mu\tilde{\tau}(d_{i-1}^{\Delta})\right), \tag{24}$$

where $p^{\mathrm{E}}(d^{\Delta})$ is the price in the efficient model at distance d^{Δ}. This equation only considers spatial price differences. To obtain a straightforward comparison to the baseline model prices, we set the price in the city center to 1 and scale the spatial differences in (24) by the price in the distance bin closest to the city center from the baseline model.

We plot the resulting spatial price gradients in Figure 6. Recall that spatial differences in welfare losses are more relevant for the U.S. than for Germany. Consistently, the relative price distortion in the baseline model compared to the efficient model is larger in the U.S. In the baseline model, U.S. housing prices in the outskirts are 32% of those in the city center, while in the efficient model, this amounts to 77%.[40] Prices therefore decrease by 0.7% per kilometer in the baseline model, but only by 0.2% per kilometer in the efficient model. For Germany, prices decrease by 3.3% per kilometer in the baseline model, but only by 1.1% per kilometer in the efficient model. Spatial price distortions due to inefficient illiquidity are therefore sizable. For both Germany and the United States, our model implies that the spatial gradient becomes about 3 times as steep due to search frictions.

Figure 6: *Spatial price gradients*

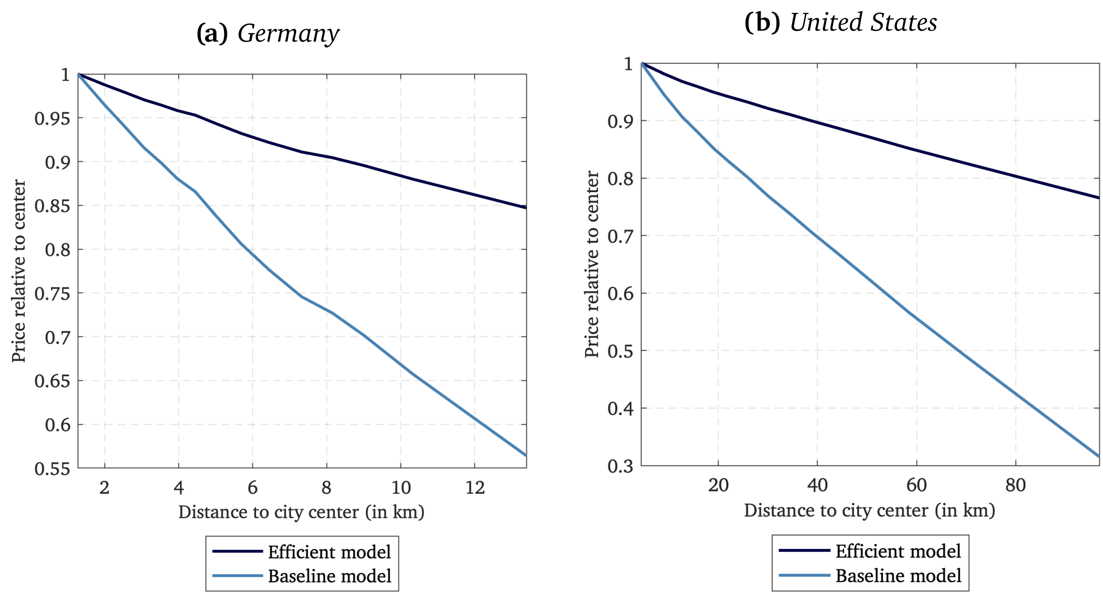

Notes: For the baseline model, all prices are normalized by the price in the first distance bin. For the efficient model, the price in the first distance bin is set to 1 and the spatial differences in prices thereafter, as defined in (24)*, are normalized by the price in the first distance bin from the baseline model.*

6 Conclusion

In this paper, we use novel spatial datasets from Germany and the United States to demonstrate that housing market liquidity declines with distance to the city center. We

[40] Note that, as discussed in the analysis of Figure 3, the model has difficulties in matching the flatter parts of the spatial price distribution in U.S. outskirts. In the U.S. data, prices in the outskirts are 45% of those in the center. Moreover, the model has difficulties in matching the high prices very close to the city center. In the spatial price gradient analysis done here, higher prices in the city center would shrink all relative prices equally, as we normalize by prices in the city center, so this is not an issue.

develop a spatial search model of the housing market and show that higher travel costs to the city center lead to lower market tightness, which in turn reduces liquidity and depresses sales prices. Moreover, we structurally estimate the extent to which search frictions – operating through search costs and seller pricing power – shape the spatial distribution of welfare and housing prices. We conclude that accounting for search frictions and their impact on housing prices is essential for a more realistic perspective on housing markets. Our findings can also inform research on the link between liquidity and the valuation of real assets. In particular, given the recent "great rotation" (Koijen, Shah, and Van Nieuwerburgh, 2025) toward infrequently traded, heterogeneous private and real assets, our results can help future research identify systematic variation in the pricing of such assets.

References

Ahlfeldt, Gabriel M., Stephen J. Redding, Daniel M. Sturm, and Nikolaus Wolf (2015). "The economics of density: Evidence from the Berlin Wall". In: *Econometrica* 83(6), pp. 2127–2189.

Albouy, David, Gabriel Ehrlich, and Minchul Shin (2018). "Metropolitan land values". In: *Review of Economics and Statistics* 100(3), pp. 454–466.

Alonso, William (1964). *Location and land use: Toward a general theory of land rent*. Harvard University Press.

Amaral, Francisco, Martin Dohmen, Moritz Schularick, and Jonas Zdrzalek (2023). "German Real Estate Index (GREIX)". ECONtribute Discussion Paper No. 231.

Andor, Mark A., Andreas Gerster, Kenneth T. Gillingham, and Marco Horvath (2020). "Running a car costs much more than people think: Stalling the uptake of green travel". In: *Nature* 580, pp. 453–455.

Baum-Snow, Nathaniel and Lu Han (2024). "The microgeography of housing supply". In: *Journal of Political Economy* 132(6), pp. 1897–1946.

Biljanovska, Nina and Giovanni Dell'Ariccia (2023). "Flattening the curve and the flight of the rich: Pandemic-induced shifts in US and European housing markets". IMF Working Paper No. 2023/266.

Carrillo, Paul E. (2012). “An empirical stationary equilibrium search model of the housing market”. In: *International Economic Review* 53(1), pp. 203–234.

Cattaneo, Matias D., Richard K. Crump, Max H. Farrell, and Yingjie Feng (2024). “On binscatter”. In: *American Economic Review* 114(5), pp. 1488–1514.

Chetty, Raj, John N. Friedman, Nathaniel Hendren, Maggie R. Jones, and Sonya R. Porter (2025). “The Opportunity Atlas: Mapping the childhood roots of social mobility”. Working paper.

Delventhal, Matthew J. and Andrii Parkhomenko (2024). “Spatial implications of telecommuting”. Working paper.

Dijkstra, Lewis, Hugo Poelman, and Paolo Veneri (2019). “The EU-OECD definition of a functional urban area”. OECD Regional Development Working Paper No. 2019/11.

Duffie, Darrell, Nicolae Gârleanu, and Lasse H. Pedersen (2005). “Over-the-counter markets”. In: *Econometrica* 73(6), pp. 1815–1847.

Duranton, Gilles and Diego Puga (2015). “Chapter 8 - Urban land use”. In: *Handbook of Regional and Urban Economics*. Ed. by Gilles Duranton, J. Vernon Henderson, and William C. Strange. Vol. 5. Elsevier, pp. 467–560.

Favilukis, Jack, Pierre Mabille, and Stijn Van Nieuwerburgh (2023). “Affordable housing and city welfare”. In: *The Review of Economic Studies* 90(1), pp. 293–330.

Garcia-López, Miquel-Àngel and Elisabet Viladecans-Marsal (2024). “The role of historic amenities in shaping cities”. In: *Regional Science and Urban Economics* 109:104042.

Garriga, Carlos and Aaron Hedlund (2020). “Mortgage debt, consumption, and illiquid housing markets in the Great Recession”. In: *American Economic Review* 110(6), pp. 1603–1634.

Gerardi, Kristopher, Franklin Qian, and David Zhang (2025). “Mortgage lock-in, lifecycle migration, and the welfare effects of housing market liquidity”. Working paper.

Glaeser, Edward L. and Joseph Gyourko (2008). “Arbitrage in housing markets”. Harvard Institute of Economic Research Discussion Paper No. 2151.

Gupta, Arpit, Vrinda Mittal, Jonas Peeters, and Stijn Van Nieuwerburgh (2022). “Flattening the curve: Pandemic-induced revaluation of urban real estate”. In: *Journal of Financial Economics* 146(2), pp. 594–636.

Guren, Adam M. (2018). “House price momentum and strategic complementarity”. In: *Journal of Political Economy* 126(3), pp. 1172–1218.

Guren, Adam M. and Timothy J. McQuade (2020). “How do foreclosures exacerbate housing downturns?” In: *The Review of Economic Studies* 87(3), pp. 1331–1364.

Han, Lu and William C. Strange (2015). “Chapter 13 - The microstructure of housing markets: Search, bargaining, and brokerage”. In: *Handbook of Regional and Urban Economics*. Ed. by Gilles Duranton, J. Vernon Henderson, and William C. Strange. Vol. 5. Elsevier, pp. 813–886.

Harris, Nathaniel (2024). “Measuring aggregate land values using individual city land value gradients”. In: *Regional Science and Urban Economics* 106:103995.

Head, Allen, Huw Lloyd-Ellis, and Hongfei Sun (2014). “Search, liquidity, and the dynamics of house prices and construction”. In: *American Economic Review* 104(4), pp. 1172–1210.

Hugonnier, Julien, Benjamin Lester, and Pierre-Olivier Weill (2019). “Frictional intermediation in over-the-counter markets”. In: *The Review of Economic Studies* 87(3), pp. 1432–1469.

Jiang, Erica Xuewei, Nadia Kotova, and Anthony Lee Zhang (2024). “Liquidity in residential real estate markets”. Working paper.

Koijen, Ralph, Neel Shah, and Stijn Van Nieuwerburgh (2025). “The commercial real estate ecosystem”. CEPR Discussion Paper No. 20053.

Krainer, John (2001). “A theory of liquidity in residential real estate markets”. In: *Journal of Urban Economics* 49(1), pp. 32–53.

Krainer, John and Stephen F. LeRoy (2002). “Equilibrium valuation of illiquid assets”. In: *Economic Theory* 19(2), pp. 223–242.

Lagos, Ricardo and Guillaume Rocheteau (2009). “Liquidity in asset markets with search frictions”. In: *Econometrica* 77(2), pp. 403–426.

Liotta, Charlotte, Vincent Viguié, and Quentin Lepetit (2022). “Testing the monocentric standard urban model in a global sample of cities”. In: *Regional Science and Urban Economics* 97:103832.

Mills, Edwin S. (1967). “An aggregative model of resource allocation in a metropolitan area”. In: *The American Economic Review* 57(2), pp. 197–210.

Moody, Joanna, Elizabeth Farr, Marisa Papagelis, and David R. Keith (2021). “The value of car ownership and use in the United States”. In: *Nature Sustainability* 4, pp. 769–774.

Moreno-Monroy, Ana I., Marcello Schiavina, and Paolo Veneri (2021). “Metropolitan areas in the world. Delineation and population trends”. In: *Journal of Urban Economics* 125:103242.

Muth, Richard F. (1969). *Cities and housing – The spatial pattern of urban residential land use*. University of Chicago Press.

Nechyba, Thomas J. and Randall P. Walsh (2004). “Urban sprawl”. In: *Journal of Economic Perspectives* 18(4), pp. 177–200.

Ngai, L. Rachel and Silvana Tenreyro (2014). “Hot and cold seasons in the housing market”. In: *American Economic Review* 104(12), pp. 3991–4026.

Piazzesi, Monika, Martin Schneider, and Johannes Stroebel (2020). “Segmented housing search”. In: *American Economic Review* 110(3), pp. 720–759.

Rogerson, Richard, Robert Shimer, and Randall Wright (2005). “Search-theoretic models of the labor market: A survey”. In: *Journal of Economic Literature* 43(4), pp. 959–988.

RWI - Leibniz-Institut für Wirtschaftsforschung and ImmobilienScout24 (2024). “RWI Real Estate Data - Hauskauf - SUF”. RWI-GEO-RED.

U.S. Census Bureau (2012–2023a). “Median income in the past 12 months”. 2012–2023 American Community Survey 5-year estimates.

U.S. Census Bureau (2012–2023b). “Physical housing characteristics for occupied housing units”. 2012–2023 American Community Survey 5-year estimates.

U.S. Census Bureau (2012–2023c). “Selected housing characteristics”. 2012–2023 American Community Survey 5-year estimates.

Vanhapelto, Tuuli and Thierry Magnac (2024). *Housing search and liquidity in spatial equilibrium*. TSE Working Paper No. 24-1596.

Supplemental Appendix for
"Spatial distribution of housing liquidity"

Francisco Amaral, Mark Toth, and Jonas Zdrzalek

A Data sources and cleaning procedures

In this section, we present in detail the steps that we took to prepare the data for the empirical analysis.

A.1 German data

Matching algorithm. We start the algorithm by matching each transaction to potential ads based on location. This gives us a pool of potential matching ads for each transaction. We then follow a series of steps to eliminate those ads that are unrealistic matches. First, we exclude advertisements that were published after the contract date and ads that were removed more than one year before the contract date. The algorithm proceeds by matching observations with complete addresses, that is, addresses which include street names and house numbers. However, for apartments, having information on solely the street name and the house number is insufficient for a successful match, as there may be multiple apartment transactions related to the same building. If that is the case, the algorithm excludes ads based on property characteristics in the following order:

1. The living area differs by more than 10%.
2. The floor number differs by more than 2.
3. The building year differs by more than 5 years.

We choose these property characteristics since they have the lowest number of missing values from the set of variables that are covered by both datasets and select numeric values for the criteria that give us reasonable buffers for measurement errors due to incorrect user inputs. If, after this process, we still have more than one potential listing for a particular transaction, we continue to eliminate listings in the following sequential steps until we have only one listing for a particular transaction:

1. We keep the ad(s) that minimize(s) the distance to the transaction in terms of living area.
2. We keep the ad(s) that minimize(s) the distance in terms of floor number.
3. We keep the ad(s) that minimize(s) the spread between the listing price and the sales price.
4. We eliminate listings that were taken out more than three months prior to the actual transaction.

If we still have multiple matches after these steps, we drop them because we have no way of identifying the correct match.

Next, we check if we have assigned an ad to multiple transactions. If this is the case, we keep only the most likely match following the steps described above. When we match based on the building's exact address, we do not exclude matches with different building years. Matching by address is sufficient to identify a building, and typically the building year is the same for all flats within a building. When this is not the case, we attribute the different building years to measurement error, that is, incorrect user-specified information on the advertisement websites. We match the transactions which do not have entries with complete addresses via the same process as for those with complete addresses, but condition sequentially on the following geographical objects: street name, ZIP Code, and neighborhood (*Stadtteil*), until we have a unique match. If there is no unique match, we drop the observation.

On average, we match about 30% of the transactions across cities. The relatively low proportion of transactions that are matched is largely due to overmatching, that is, the fact that in many cases we end up with more than one potential advertisement for a given transaction after the algorithm has applied all criteria. In Table A1, we provide further information on the matched observations by city.

Table A1: *Summary statistics: matched dataset*

City	# Transactions	# Ads	# Matched	Avg. sales price (€)	Avg. asking price (€)
Hamburg	80,157	78,342	20,418	356,541	358,604
Munich	57,629	112,135	25,966	493,312	495,710
Cologne	41,338	46,349	14,273	237,462	254,164
Frankfurt	35,493	39,083	12,035	388,445	405,843
Duesseldorf	35,581	34,669	11,611	288,863	303,802

Notes: This table reports summary statistics about the matched transaction and advertisement data for the period 2012–2024.

We show that the matched sample is not biased along several important characteristics of the transacted properties in Figure A1. We plot the distributions from the matched sample and the universe of transactions, with all cities pooled together, of the variables living area, building year, distance to the city center, and sales price. For each of these variables, the two distributions mostly overlap, which indicates that the matched sample is representative of the universe of transactions.

Figure A1: *Matched sample and universe of transactions, all German cities pooled*

(a) *Living area in square meters*

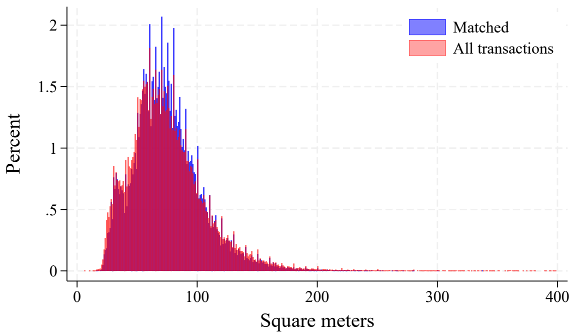

(b) *Building year*

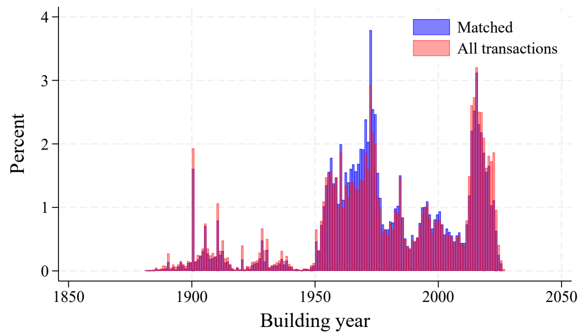

(c) *Distance to the city center*

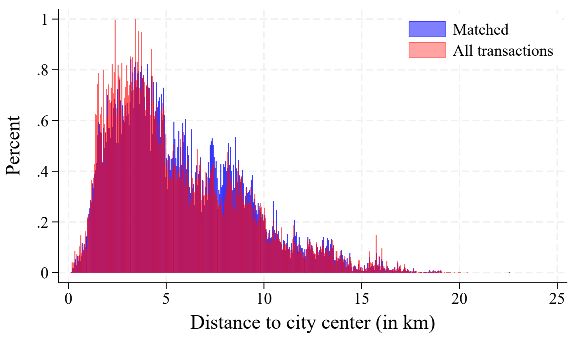

(d) *Sales price*

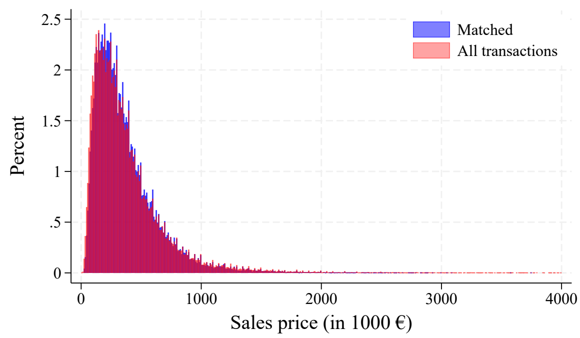

Notes: These plots show histograms of different variables in the matched sample and the universe of transactions. The y-axis measures the frequency in percent of a given value on the x-axis in the respective sample.

Data preparation. We transform several variables to prepare them for regression analysis. We control for the following variables: living area in m^2, living area squared, number of rooms, year of construction, "Altbau" or not, "Neubau" or not, physical condition of the building, whether the apartment is in the upper floor of the house or not, whether the apartment is rented out or not, type of heating, source of heating, whether the apartment has a fitted kitchen or not, whether the apartment has an open kitchen or not, whether the bathroom has a shower, whether the bathroom has a bathtub, whether the apartment has a terrace or balcony, whether the apartment has a basement, whether the apartment has a garden, and the number of parking spaces. These control variables are identical for the regressions with rental housing.

We control for the age of the properties by creating a categorical variable that divides the observations into different construction periods. We follow the commonly used categories introduced by the official German appraisers. In particular, we construct the following categories: pre-1950, 1950–1977, 1978–1990, 1990–2005, and post-2005. We use a categorical variable rather than a continuous variable for the building year of the property because the relationship between age and price or liquidity is highly non-linear in the case of the German housing market, as shown in Amaral et al. (2023). In addition, we also include a category for properties that are being occupied for the first time and another category that identifies properties where construction is not yet complete. We divide the heating type of each home into four different categories. We define "brown" dwellings as those that consume energy produced by oil or coal, or use space heating and tile stove heating. We define "standard" dwellings as those that consume energy produced by gas and use central heating. We define "green" properties as those where the energy comes from solar, heat pumps or pellets, or use district heating or CHP. We also use an "other" category, taken directly from the dataset, which includes other energy sources. We use a categorical variable to consider the quality of the furnishings and interiors of the property and a categorical variable to categorize the quality of the construction of the building, both of which are provided directly in the dataset. We create a categorical variable to control for the number of rooms in the property. The variable has four categories: 1 room, 2 rooms, 3 rooms, and 4 or more rooms. We also control for the number of floors on which the apartment is located and the total number of floors in the building where the apartment is located.

A.2 U.S. data

Redfin is both a real estate brokerage and an online platform. Redfin typically has direct access to data from local multiple listing services (MLS) and adds those listings to the platform. However, unlike the well-known Zillow platform (which we cannot use due to a lack of data availability for liquidity variables at the ZIP-Code level), Redfin has a low coverage of for-sale-by-owner (FSBO) listings because Redfin does not allow sellers to post listings themselves. Since FSBOs account for only about 6% of all home sales in the U.S. (see: National Association of Realtors), by including the majority of MLS listings, Redfin covers most of the market. We clean the data by dropping all ZIP Codes for which the time on the market estimates are, on average, based on less than 10 observations and there is one month with less than 5 observations. For a robustness analysis, we collect data on time on the market from another online platform, Realtor.com, which covers most local MLS in the United States, and compare these results to our baseline results. We estimate the time on the market gradient using both datasets. Because the Realtor.com platform only provides data for an "all residential" category, we cannot perform the comparison for different segments separately. Moreover, the dataset from Realtor.com only starts in 2016, so we limit our analysis to the period between 2016 and 2023. In Table A2, we provide outputs for regressions of time on the market on distance to the city center using both the Redfin and Realtor.com data, with very similar results.

For our U.S. control variables on housing characteristics and demographic composition, we use yearly data from the American Survey 5-year estimates at the ZIP-Code level from 2012 to 2023. The variables are listed in Section 3.1. Lastly, for the measure of U.S. neighborhood quality, we use data from Chetty et al. (2025). We calculate ZIP-Code-level averages of the fraction of children born between 1978 and 1983 who were incarcerated on April 1st, 2010 (*jail_pooled_pooled_mean*).

Table A2: *Time on the market and distance to the city center in the U.S. (2016–2023)*

	(1)	(2)	(3)	(4)
	Redfin	Realtor.com	Redfin	Realtor.com
Distance to center (in km)	0.01^{**}	0.02^{***}	0.02^{***}	0.02^{***}
	(0.006)	(0.002)	(0.005)	(0.002)
Median income			-0.93^{***}	-0.86^{***}
			(0.051)	(0.039)
MSA × Year-Month FE	✓	✓	✓	✓
State FE	✓	✓	✓	✓
Property characteristics			✓	✓
N	507,490	507,490	507,490	507,490
ZIP Codes	5,673	5,673	5,673	5,673
Adj. R^2	0.20	0.34	0.24	0.40
Mean(TOM)	6.45	7.34	6.45	7.34

Notes: This table shows results for regressions of time on the market on the distance to the city center as specified in Regression (1). *Time on the market is measured in weeks. Standard errors (in parentheses) are clustered at the MSA-year level. Median income and property characteristics are control variables. The underlying data bundles all residential housing types into one category.* $*: p < 0.1$; $**: p < 0.05$; $***: p < 0.01$.

B Summary statistics

B.1 German cities

Table A3: *Summary statistics: time on the market and prices in German cities (2012–2024)*

	Time on the market in weeks				Sales price in €1,000				
City	Mean	SD	P25	P75	Mean	SD	P25	P75	N
Hamburg	15.13	17.59	3.10	20.40	357	267	188	437	20,418
Munich	12.34	15.53	2.30	16.30	493	308	285	611	25,966
Cologne	12.42	16.19	2.30	16.20	237	153	130	300	14,273
Frankfurt	15.04	18.23	2.60	20.20	388	253	210	499	12,035
Duesseldorf	12.99	16.28	2.30	17.00	289	225	137	365	11,611

Notes: This table reports summary statistics of time on the market and sales prices by city for the period 2012–2024. All estimates are based on the matched dataset. N is the total number of transactions in the respective matched dataset.

B.2 U.S. cities

Table A4: *Summary statistics: time on the market and prices in U.S. cities (2012–2023)*

	Time on the market in weeks				Sales price in $1,000					
MSA	Mean	SD	P25	P75	Mean	SD	P25	P75	Nr. ZIP Codes	N
Atlanta-Sandy Springs-Alpharetta, GA	6.70	5.06	3.71	8.57	274	188	150	348	190	26,992
Austin-Round Rock-Georgetown, TX	5.93	4.75	2.93	7.71	413	263	238	502	73	10,509
Baltimore-Columbia-Towson, MD	7.33	5.96	3.64	9.43	406	178	281	497	121	17,477
Boston-Cambridge-Newton, MA-NH	7.49	6.64	2.64	11.36	577	369	350	668	247	24,295
Charlotte-Concord-Gastonia, NC-SC	10.87	7.42	6.43	13.29	256	175	148	315	105	13,508
Chicago-Naperville-Elgin, IL-IN-WI	8.30	5.49	5.00	10.29	288	230	158	348	342	25,102
Cincinnati, OH-KY-IN	10.87	9.51	6.71	13.71	188	105	118	236	123	17,681
Dallas-Fort Worth-Arlington, TX	5.83	3.77	3.43	7.07	285	200	165	348	245	18,665
Denver-Aurora-Lakewood, CO	4.08	6.15	1.21	4.71	455	198	315	561	108	15,480
Detroit-Warren-Dearborn, MI	5.04	4.30	2.50	6.50	210	130	118	285	201	16,703
Houston-The Woodlands-Sugar Land, TX	6.17	4.42	3.14	8.00	266	201	156	302	204	29,363
Las Vegas-Henderson-Paradise, NV	9.44	7.12	6.00	11.21	296	145	200	366	62	8,858
Los Angeles-Long Beach-Anaheim, CA	5.98	4.86	3.93	7.07	934	738	512	1,066	337	30,265
Miami-Fort Lauderdale-Pompano Beach, FL	9.93	5.48	6.79	11.29	533	638	275	560	174	7,709
Minneapolis-St. Paul-Bloomington, MN-WI	6.77	7.31	3.07	8.36	307	146	210	373	196	27,638
New York-Newark-Jersey City, NY-NJ-PA	11.12	9.67	5.43	14.14	627	810	353	698	739	23,776
Orlando-Kissimmee-Sanford, FL	7.81	7.96	3.21	10.57	279	143	179	350	85	11,945
Philadelphia-Camden-Wilmington, PA-NJ-DE-MD	7.96	5.97	4.00	10.36	320	184	193	398	270	11,026
Phoenix-Mesa-Chandler, AZ	7.01	3.61	4.86	8.14	338	241	200	410	142	20,050
Pittsburgh, PA	13.62	7.18	8.57	16.57	176	111	102	221	149	21,432
Portland-Vancouver-Hillsboro, OR-WA	4.95	5.23	1.57	6.29	426	185	294	525	110	15,046
Riverside-San Bernardino-Ontario, CA	7.20	4.72	4.43	8.71	375	205	233	478	125	17,534
Sacramento-Roseville-Folsom, CA	4.21	4.07	1.86	5.14	424	208	288	519	85	12,198
San Antonio-New Braunfels, TX	8.11	5.58	4.79	9.86	238	125	151	304	93	13,386
San Diego-Chula Vista-Carlsbad, CA	4.51	4.42	2.14	5.29	788	531	479	895	84	12,239
San Francisco-Oakland-Berkeley, CA	2.77	1.65	1.86	3.14	1,218	857	680	1,504	130	8,610
Seattle-Tacoma-Bellevue, WA	3.27	3.39	1.07	4.43	599	441	330	722	140	11,693
St. Louis, MO-IL	11.85	27.78	5.29	12.86	182	137	94	230	213	25,043
Tampa-St. Petersburg-Clearwater, FL	7.57	5.83	3.14	10.64	281	191	164	345	126	18,144
Washington-Arlington-Alexandria, DC-VA-MD-WV	6.23	5.16	3.14	7.79	541	295	340	658	248	23,122

Notes: This table reports summary statistics of time on the market and sales prices by MSA for the period 2012–2023. N is the number of ZIP-Code-year-month observations in the respective subset of data.

C Additional empirical results

C.1 Time series of housing liquidity and prices in the U.S.

As we mention in the main text, our documented within-city spatial variation in housing liquidity and prices is comparable to the variation over time. Figure A2 displays Redfin time series of U.S.-level quarterly log median sales prices and time on the market, decomposed via a Hodrick–Prescott filter with standard penalty parameter $\lambda = 1{,}600$. The cyclical variation is obtained by isolating the cyclical component of a seasonally adjusted time series (provided by Redfin via X-13ARIMA-SEATS) from the Hodrick–Prescott filter. The seasonal variation is obtained by isolating the cyclical component of the unadjusted time series from the Hodrick–Prescott filter and subtracting the cyclical time series.

As becomes evident from the figure, the seasonal variation in prices amounts to about 10%, while the variation over the business cycle amounts to 10-15%. This is comparable to a spatial price difference in the U.S. over 20-30km (with prices changing by 0.5% per kilometer, see Table A19). For the time on the market, the seasonal variation amounts to about 2 weeks, while the the variation over the business cycle amounts to 2-3 weeks. This is comparable to a spatial price difference in the U.S. over 40-60km (with the time on the market changing by 0.05 weeks per kilometer, see Table A18).

Figure A2: *Variation in U.S. housing market variables around long-run trends*

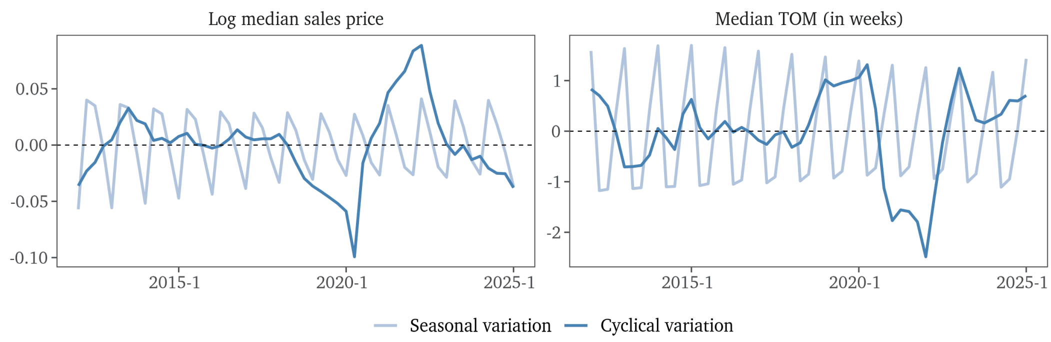

Notes: These plots display decomposed time series of U.S.-level quarterly log median sales prices and time on the market (TOM).

C.2 Spatial distribution of time on the market in German cities

Figure A3: *Time on the market across space, Germany (2012–2024)*

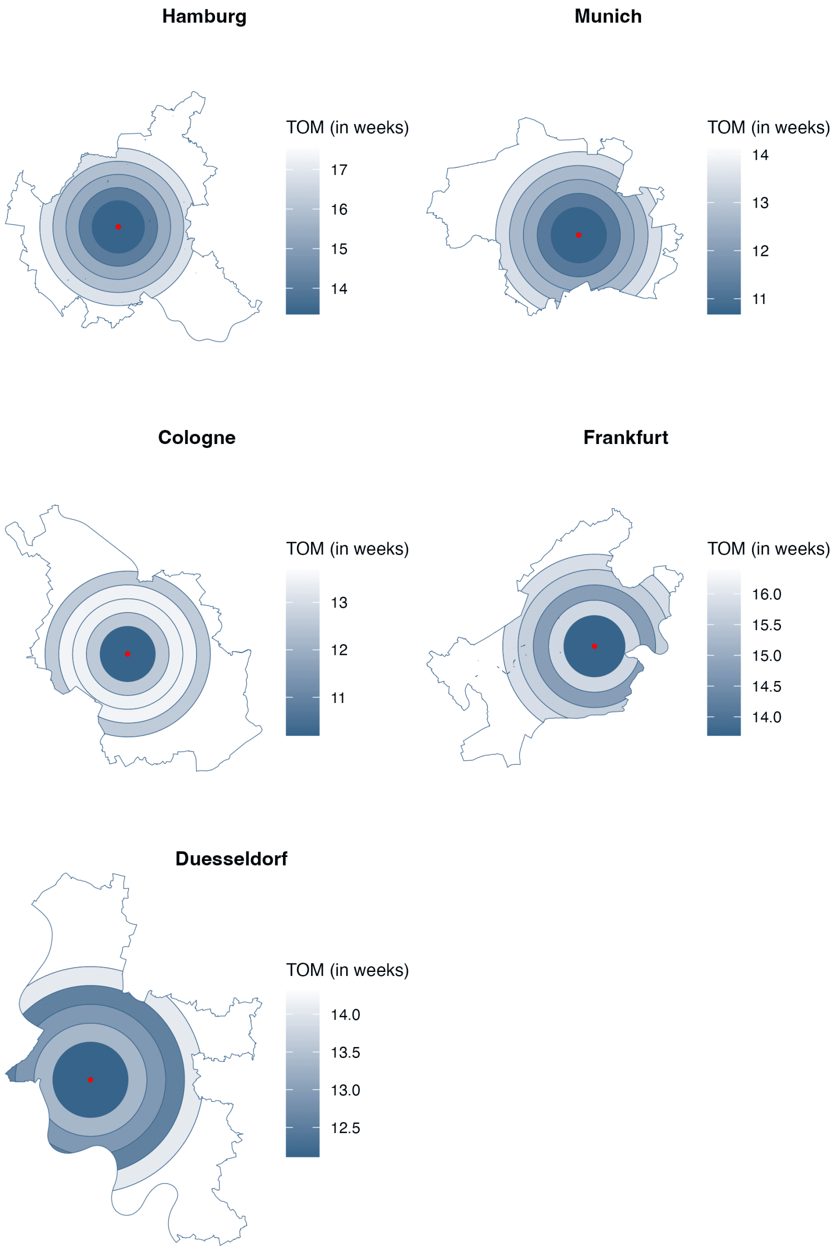

Notes: These maps display the spatial distribution of time on the market (TOM) by city from our matched German dataset, averaged within rings around city centers. Shapefile data sources:
Hamburg: `https://suche.transparenz.hamburg.de/dataset/stadtteil-profile-hamburg10`.
Munich: `https://opendata.muenchen.de/dataset/vablock_stadtbezirke_opendata`.
Cologne: `https://offenedaten-koeln.de/dataset/stadtbezirke-köln`.
Frankfurt: `https://geowebdienste.frankfurt.de/WFS_Stadtgebietsgliederung`.
Duesseldorf: `https://opendata.duesseldorf.de/dataset/stadtteilgrenzen-düsseldorf-2025`.

C.3 Spatial distribution of sales prices in German cities

Figure A4: *Sales prices across space, Germany (2012–2024)*

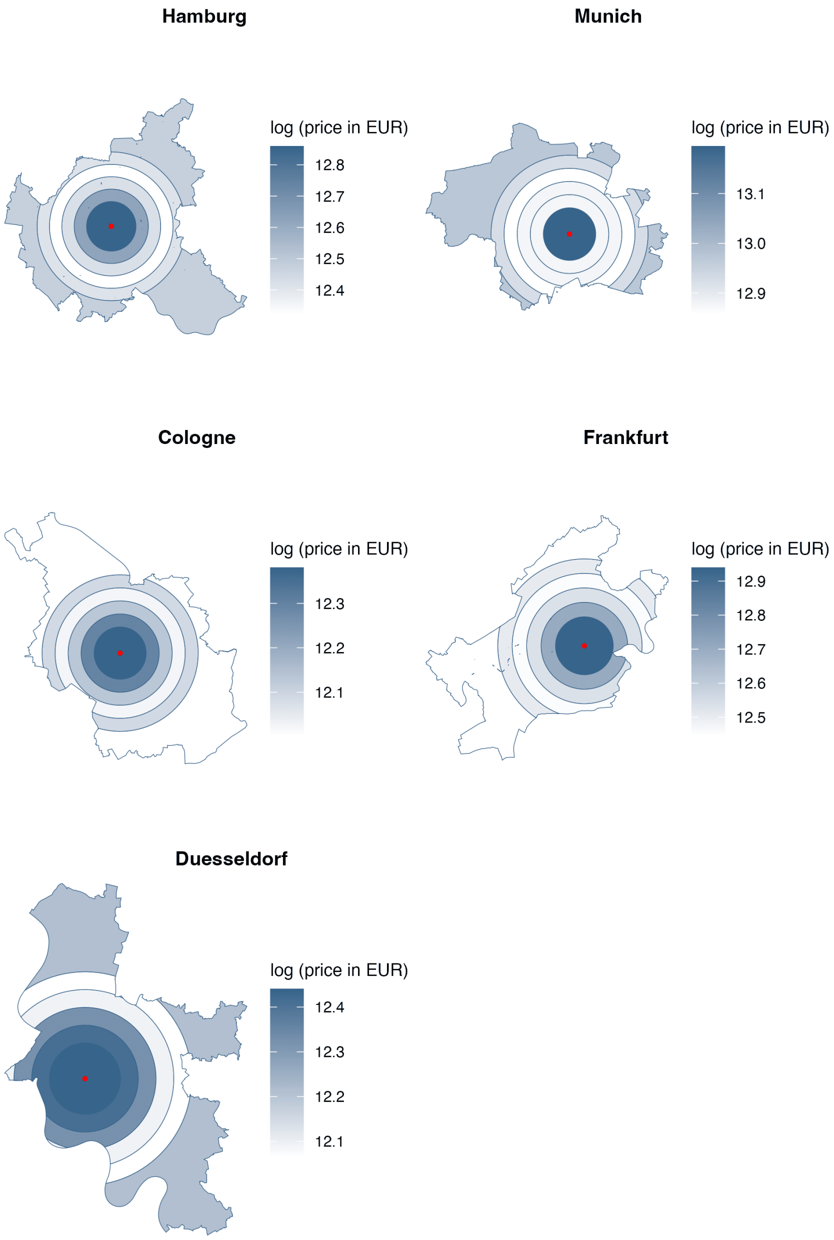

Notes: These maps display the spatial distribution of sales prices by city from our matched German dataset, averaged within rings around city centers. Shapefile data sources:
Hamburg: `https://suche.transparenz.hamburg.de/dataset/stadtteil-profile-hamburg10`.
Munich: `https://opendata.muenchen.de/dataset/vablock_stadtbezirke_opendata`.
Cologne: `https://offenedaten-koeln.de/dataset/stadtbezirke-köln`.
Frankfurt: `https://geowebdienste.frankfurt.de/WFS_Stadtgebietsgliederung`.
Duesseldorf: `https://opendata.duesseldorf.de/dataset/stadtteilgrenzen-düsseldorf-2025`.

Table A5: *Log sales prices and distance to the city center, Germany (2012–2024)*

	(1)	(2)	(3)	(4)	(5)	(6)
	Price	Price	Price	Price	Price	Price
Distance to center (in km)	-0.04***	-0.05***	-0.04***			
	(0.00)	(0.00)	(0.00)			
Travel time to center (in min)				-0.02***	-0.02***	-0.02***
				(0.00)	(0.00)	(0.00)
City $\times$ Year-quarter FE	✓	✓	✓	✓	✓	✓
Property characteristics		✓	✓		✓	✓
Borough FE			✓			✓
N	84,292	84,292	84,292	84,292	84,292	84,292
Adj. R^2	0.31	0.86	0.88	0.31	0.86	0.88
Mean(log(price))	12.60	12.60	12.60	12.60	12.60	12.60

Notes: This table shows results for regressions of the log sales price on the distance to the city center as specified in the regression specification (1). *"Price" refers to the sales price in log euros. Standard errors (in parentheses) are clustered at the city-year level. The list of property characteristics controls is available in Supplemental Appendix A.1.* $*: p < 0.1; **: p < 0.05; ***: p < 0.01$.

C.4 Additional determinants of housing liquidity in German cities

In our main analysis, we focus on how liquidity varies across space. Nevertheless, houses differ in other dimensions which might also impact their liquidity. In particular, the size and age of properties might be strong determinants of liquidity, as typically the market is also segmented along these dimensions. Although our focus in this paper is not on these additional dimensions, we also provide evidence that location has a stronger effect on liquidity than these other factors. In Figure A5, we plot the standardized coefficients for the living area in square meters, the age of the building, and the distance to the city center. The coefficients are derived from Regression (1). All coefficients are positive and significant, suggesting that these dimensions have a significant impact on liquidity as measured by time on the market. As is also evident from the plot, the distance to the city center has the strongest impact on liquidity.

C.5 Alternative travel times

In our main analysis, we use car travel times from openrouteservice. Here, we also present our regression results using travel times obtained from Google Maps. We retrieve

Figure A5: *Determinants of time on the market, (2012–2024)*

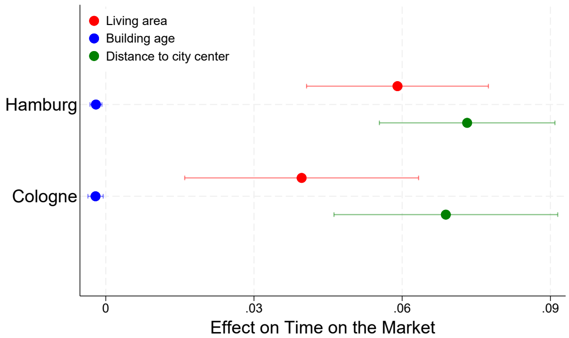

Notes: This plots shows OLS regression coefficients by city, as well as their respective 99% confidence intervals. Distance to the city center is measured as the kilometer distance. The coefficients are standardized across the displayed determinants using the respective sample standard deviation.

car travel times and public transport travel times to the city center. In Tables A6 and A7, we present the results for Germany, using Google car travel times and public transport times, respectively. The results are both quantitatively and qualitatively similar to those in our baseline analysis.

We then perform the same analysis for the United States. The results are shown in Tables A8 and A9. For car travel times, we find that the results remain unchanged compared to the baseline. For public transport, however, we find that both time on the market and price gradients are considerably smaller. This is probably due to the fact that only a small part of the population uses public transport to commute in some U.S. cities, meaning that it serves as a poor proxy for actual commuting costs. In the United States, only about 5% of the population uses public transport to commute to work daily (Burrows, Burd, and McKenzie, 2021).

Table A6: *Liquidity and price gradients with Google car travel times, Germany (2012–2024)*

	(1) TOM	(2) TOM	(3) TOM	(4) Price	(5) Price	(6) Price
Google travel time (in min)	0.15***	0.10***	0.08***	-0.02***	-0.02***	-0.02***
	(0.02)	(0.01)	(0.02)	(0.00)	(0.00)	(0.00)
City × Year-quarter FE	✓	✓	✓	✓	✓	✓
Property characteristics		✓	✓		✓	✓
Borough FE			✓			✓
N	84,292	84,292	84,292	84,292	84,292	84,292
Adj. R^2	0.04	0.13	0.13	0.30	0.86	0.88
Mean(dependent variable)	13.51	13.51	13.51	12.60	12.60	12.60

Notes: This table displays the output of Regression (1) on time on the market (TOM), measured in weeks, and log sales prices using Google car travel times to measure commuting time to the city center. The list of property characteristics controls is available in Supplemental Appendix A.1. The regressions are based on data for apartments for the five cities in our sample in the period between 2012–2024. Standard errors (in parentheses) are clustered at the city-year level. $*: p < 0.1; **: p < 0.05; ***: p < 0.01$.

Table A7: *Liquidity and price gradients with public transport travel times, Germany (2012–2024)*

	(1) TOM	(2) TOM	(3) TOM	(4) Price	(5) Price	(6) Price
Public transport travel time (in min)	0.09***	0.06***	0.04***	-0.01***	-0.01***	-0.01***
	(0.01)	(0.01)	(0.01)	(0.00)	(0.00)	(0.00)
City × Year-quarter FE	✓	✓	✓	✓	✓	✓
Property characteristics		✓	✓		✓	✓
Borough FE			✓			✓
N	84,292	84,292	84,292	84,292	84,292	84,292
Adj. R^2	0.04	0.13	0.13	0.29	0.85	0.87
Mean(dependent variable)	13.51	13.51	13.51	12.60	12.60	12.60

Notes: This table displays the output of Regression (1) on time on the market (TOM), measured in weeks, and log sales prices using Google public transport travel times to measure commuting time to the city center. The list of property characteristics controls is available in Supplemental Appendix A.1. The regressions are based on data for apartments for the five cities in our sample in the period between 2012–2024. Standard errors (in parentheses) are clustered at the city-year level. $*: p < 0.1; **: p < 0.05; ***: p < 0.01$.

Table A8: *Liquidity and price gradients with Google car travel times, U.S. (2012–2023)*

	(1) TOM	(2) TOM	(3) TOM	(4) Price	(5) Price	(6) Price
Google car travel time (in min)	0.052***	0.045***	0.070***	-0.004***	-0.003***	-0.004***
	(0.0079)	(0.0074)	(0.0061)	(0.0005)	(0.0005)	(0.0003)
MSA × Year-month FE	✓	✓	✓	✓	✓	✓
State FE	✓	✓	✓	✓	✓	✓
Property characteristics			✓			✓
Demographic controls			✓			✓
N	682,100	682,100	682,100	682,100	682,100	682,100
ZIP Codes	4,943	4,943	4,943	4,943	4,943	4,943
Adj. R^2	0.29	0.29	0.32	0.56	0.62	0.85
Mean(dependent variable)	7.60	7.60	7.60	12.69	12.69	12.69

Notes: This table displays the output of Regression (1) *on time on the market (TOM), measured in weeks, and log sales prices using Google car transport travel times to measure commuting time to the city center. The regressions are based on data for single-family houses for the 30 largest MSAs in the U.S. in the period between 2012–2023. Standard errors (in parentheses) are clustered at the MSA-year level.* $*: p < 0.1; **: p < 0.05; ***: p < 0.01$.

Table A9: *Liquidity and price gradients with public transport travel times, U.S. (2012–2023)*

	(1) TOM	(2) TOM	(3) TOM	(4) Price	(5) Price	(6) Price
Public transport travel time (in min)	-0.000	-0.001	0.007***	-0.001***	-0.001***	-0.001***
	(0.0022)	(0.0020)	(0.0010)	(0.0002)	(0.0002)	(0.0001)
MSA × Year-month FE	✓	✓	✓	✓	✓	✓
State FE	✓	✓	✓	✓	✓	✓
Property characteristics			✓			✓
Demographic controls			✓			✓
N	479,116	479,116	479,116	479,116	479,116	479,116
ZIP Codes	3,485	3,485	3,485	3,485	3,485	3,485
Adj. R^2	0.41	0.42	0.46	0.57	0.65	0.87
Mean(dependent variable)	7.03	7.03	7.03	12.78	12.78	12.78

Notes: This table displays the output of Regression (1) *on time on the market (TOM), measured in weeks, and log sales prices using Google public transport travel times to measure commuting time to the city center. The regressions are based on data for single-family houses for the 30 largest MSAs in the U.S. in the period between 2012–2023. Standard errors (in parentheses) are clustered at the MSA-year level.* $*: p < 0.1; **: p < 0.05; ***: p < 0.01$.

C.6 Asking price discount

In Figure A6, we plot a histogram of the asking price discount for our matched German sample by city. The majority of transactions exhibit a negative discount, that is, properties typically sell below their asking prices. The distribution resembles a normal distribution but has a more positive skew and thinner tails. On average, a property is transacted at a sales price below its asking price. There is a clear bunching at an asking price discount of 0%. This finding has been documented for other countries and reflects that the asking price is a relevant anchor for the bargaining process in housing markets, as it is a partial commitment for the seller (Han and Strange, 2016). In Table A10, we present results for regressions of the asking price discount on distance to the city center. For all specifications, there is a negative and highly significant coefficient on the distance to the city center.

Figure A6: *Histograms of asking price discount (2012–2024)*

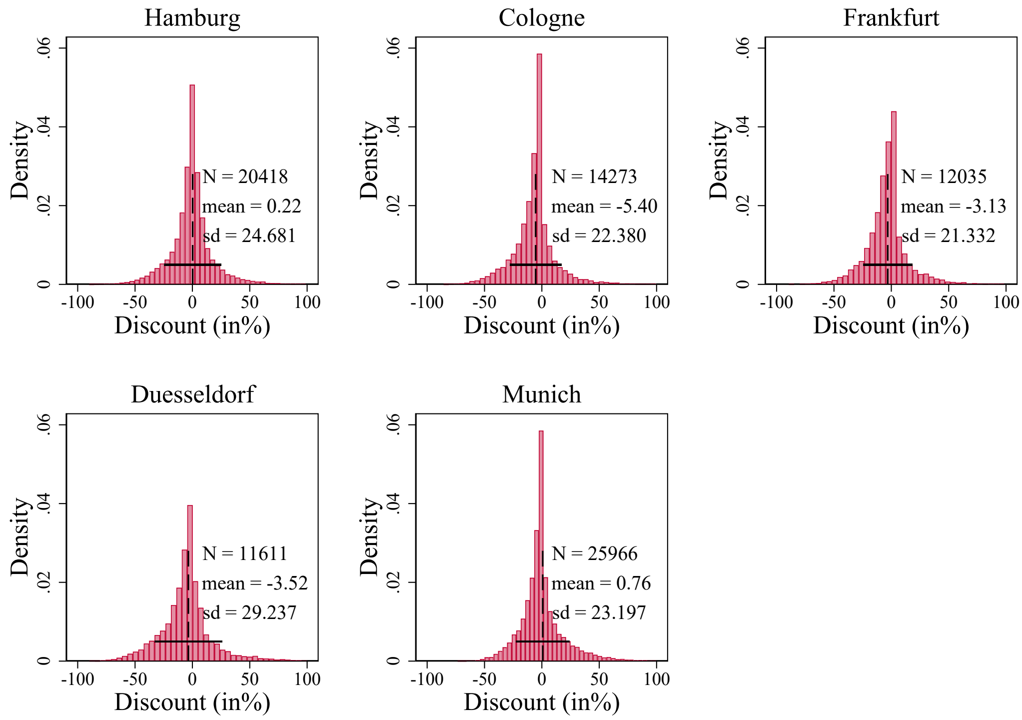

Notes: These plots show histograms for the asking price discount in our matched data set.

Table A10: *Asking price discount and distance to the city center, Germany (2012–2024)*

	(1) APD	(2) APD	(3) APD	(4) APD	(5) APD	(6) APD
Distance to center (in km)	-0.15***	-0.16***	-0.11**			
	(0.04)	(0.03)	(0.05)			
Travel time to center (in min)				-0.07***	-0.07***	-0.03
				(0.02)	(0.01)	(0.03)
City × Year-quarter FE	✓	✓	✓	✓	✓	✓
Property characteristics		✓	✓		✓	✓
Borough FE			✓			✓
N	84,292	84,292	84,292	84,292	84,292	84,292
Adj. R^2	0.02	0.05	0.05	0.02	0.05	0.05
Mean(APD)	-1.56	-1.56	-1.56	-1.56	-1.56	-1.56

Notes: This table shows results for regressions of the asking price discount on the distance to the city center as specified in Regression (1). *"APD" refers to the asking price discount in percent. Standard errors (in parentheses) are clustered at the city-year level. The list of property characteristics controls is available in Supplemental Appendix A.1.* $*: p < 0.1$; $**: p < 0.05$; $***: p < 0.01$.

Table A11: *Asking price discount and distance to the city center, U.S. (2012–2023)*

	(1)	(2)	(3)	(4)	(5)	(6)
	APD	APD	APD	APD	APD	APD
Distance to center (in km)	-0.02***	-0.01***	-0.03***			
	(0.002)	(0.002)	(0.001)			
Travel time to center (in min)				-0.02***	-0.02***	-0.03***
				(0.002)	(0.002)	(0.002)
Median income		0.28***	0.28***		0.28***	0.26***
		(0.041)	(0.034)		(0.041)	(0.032)
MSA × Year-month FE	✓	✓	✓	✓	✓	✓
State FE	✓	✓	✓	✓	✓	✓
Property characteristics			✓			✓
Demographic controls			✓			✓
N	682,034	682,034	682,034	682,034	682,034	682,034
ZIP Codes	4,943	4,943	4,943	4,943	4,943	4,943
Adj. R^2	0.49	0.49	0.51	0.49	0.49	0.52
Mean(APD)	-1.49	-1.49	-1.49	-1.49	-1.49	-1.49

Notes: This table displays the output of Regression (1) *on asking price discount (APD), measured in percent of the asking price. The regressions are based on data for single-family houses for the 30 largest MSAs in the U.S. in the period between 2012–2023. Standard errors (in parentheses) are clustered at the MSA-year level.* $*: p < 0.1; **: p < 0.05; ***: p < 0.01$.

C.7 Market tightness in German cities

Next, we present results for regressions of contact clicks per ad on distance to the city center. The data is from RWI - Leibniz-Institut für Wirtschaftsforschung and ImmobilienScout24 (2024). Since in this dataset we do not have the exact location of each apartment, but only the ZIP Code, we calculate distances to the city center using the centroids of ZIP Code areas. For the same reason, we cannot present results with ZIP Code fixed effects. In addition to year-quarter- and city fixed effects, we control for the following property characteristics: size in square meters, number of rooms, bathrooms, kitchens, and balconies, floor number of the apartment, building year category, type of heating system, whether the building is a landmark, and whether the apartment is owner-occupied or rented. The results are documented in Table A12. The number of contact clicks per ad decreases significantly with distance to the city center, confirming the results from the binned scatterplot in the main text.

Moreover, as mentioned in the main text, these results on market tightness are unlikely to be driven by an increasing supply of housing with distance to the city center. In Figure A7, we plot the amount of residential built-up volume by distance to the city center in the German cities from our sample and the 5 largest U.S. cities, retrieved via the Global Human Settlement Layer Database (Pesaresi and Politis, 2023; Pesaresi et al., 2024). We observe that the amount of residential built-up volume in fact decreases with distance to the city center, generally speaking.

To get these measures, we first subtract the non-residential layer of built-up volume (*GHS-BUILT-V-NRES*) from the total layer of built-up volume (*GHS-BUILT-V-RES+NRES*) to obtain residential built-up volume across 100m × 100m grid cells. We select all grid cells within the respective city boundary and calculate the distance to the city center for each grid cell (using the city centers defined in Section 2.3). Then, we create 100 distance bins for these grid cells and sum up the residential built-up volume by distance bin. We select the year 2015 to show results for the definition year of functional urban areas for U.S. cities (see Moreno-Monroy, Marcello Schiavina, and Veneri, 2021), also retrieved via the GHSL database (*GHS-FUA*), which define cities based on commuting flows, following the EU-OECD definition from Dijkstra, Poelman, and Veneri (2019). For consistency, we also show built-up volume in 2015 for German cities, even though here we use administrative boundaries, as in the main empirical exercise.

Table A12: *Contact clicks and distance to the city center, Germany (2012–2024)*

	(1)	(2)
	Clicks	Clicks
Distance to center (in km)	-0.49***	-0.46***
	(0.11)	(0.11)
City × Year-quarter FE	✓	✓
Property characteristics		✓
N	192,512	192,512
Adj. R^2	0.20	0.20
Mean(clicks)	20.72	20.72

Notes: This table shows results for regressions of contact clicks per advertisement on the distance to the city center as specified in Regression (1). "Clicks" refers to the contact clicks per ad as defined in the text. Standard errors (in parentheses) are clustered at the city-year level. The list of property characteristics controls is available in Supplemental Appendix A.1. $*: p < 0.1$; $**: p < 0.05$; $***: p < 0.01$.

Figure A7: *Residential built-up volume by distance to city center (2015)*

Notes: These plots display the amount of residential built-up volume by distance to the city center in the German cities from our sample and the 5 largest U.S. cities.

D Robustness analysis

D.1 Results for individual cities

Germany. We run Regression (1) for each city separately and report the coefficients with the corresponding 95% confidence intervals by city bundled in Figure A8. For all cities, the coefficients for both kilometer distance and car travel time are positive and highly significant. The coefficient magnitudes are similar across cities, especially after including controls.

Figure A8: *Time on the market and distance to city center by city (2012–2024)*

(a) *Distance to city center (in km)* **(b)** *Travel time to city center (in min)*

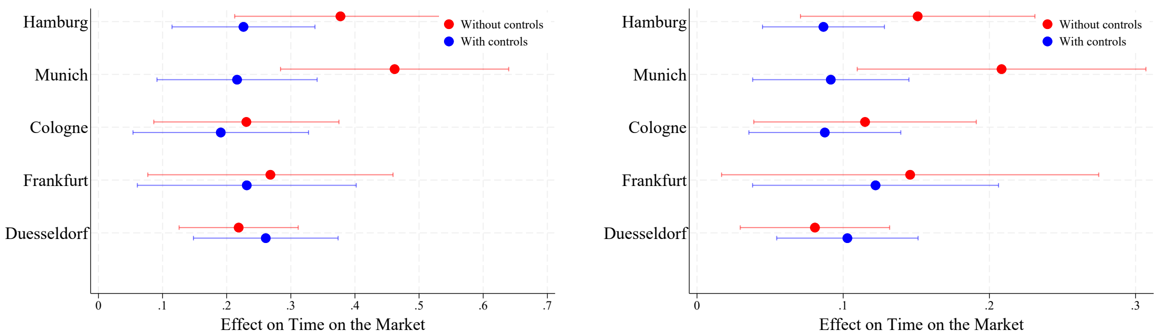

Notes: These plots show the OLS regression coefficients of distance to the city center as specified in (1) *with 95% confidence intervals with the standard errors clustered at the year level. All regressions include year-quarter fixed effects. See Supplemental Appendix A.1 for a full list of property characteristics controls.*

United States. We also test whether we can find the time on the market gradient for individual MSAs. For all cities, we find a positive time on the market gradient, with the exception of San Francisco-Oakland-Berkeley, CA. For San Francisco-Oakland-Berkeley, CA, the Realtor.com data show a larger inventory than the Redfin data, suggesting that the latter do not provide good coverage. In fact, with the Realtor.com data, we find a positive slope for San Francisco.

Table A13: *TOM and price gradient by MSA, 2012–2023*

MSA	TOM gradient	Price gradient	P-value TOM	P-value Price	N
Atlanta-Sandy Springs-Alpharetta, GA	0.075	-0.009	0.00	0.00	27,202
Austin-Round Rock-Georgetown, TX	0.131	-0.016	0.00	0.00	10,509
Baltimore-Columbia-Towson, MD	0.113	-0.002	0.00	0.00	17,413
Boston-Cambridge-Newton, MA-NH	0.065	-0.010	0.00	0.00	35,411
Charlotte-Concord-Gastonia, NC-SC	0.109	-0.011	0.00	0.00	13,508
Chicago-Naperville-Elgin, IL-IN-WI	0.048	-0.012	0.00	0.00	49,092
Cincinnati, OH-KY-IN	0.058	-0.006	0.00	0.00	17,681
Dallas-Fort Worth-Arlington, TX	0.045	-0.004	0.00	0.00	34,548
Denver-Aurora-Lakewood, CO	0.170	-0.002	0.00	0.00	15,480
Detroit-Warren-Dearborn, MI	0.027	-0.001	0.01	0.01	28,146
Houston-The Woodlands-Sugar Land, TX	0.061	-0.003	0.00	0.00	29,363
Las Vegas-Henderson-Paradise, NV	0.063	-0.002	0.00	0.00	8,782
Los Angeles-Long Beach-Anaheim, CA	0.033	-0.001	0.01	0.06	48,366
Miami-Fort Lauderdale-Pompano Beach, FL	0.026	-0.000	0.00	0.13	23,083
Minneapolis-St. Paul-Bloomington, MN-WI	0.116	-0.007	0.00	0.00	28,208
New York-Newark-Jersey City, NY-NJ-PA	0.016	-0.004	0.01	0.00	86,390
Orlando-Kissimmee-Sanford, FL	0.103	-0.005	0.00	0.00	12,230
Philadelphia-Camden-Wilmington, PA-NJ-DE-MD	0.062	-0.005	0.00	0.00	38,705
Phoenix-Mesa-Chandler, AZ	0.056	-0.004	0.00	0.00	20,294
Pittsburgh, PA	0.078	-0.007	0.00	0.00	21,432
Portland-Vancouver-Hillsboro, OR-WA	0.147	-0.009	0.00	0.00	15,542
Riverside-San Bernardino-Ontario, CA	0.036	-0.005	0.00	0.00	17,818
Sacramento-Roseville-Folsom, CA	0.042	0.003	0.00	0.00	12,091
San Antonio-New Braunfels, TX	0.079	0.006	0.00	0.00	13,386
San Diego-Chula Vista-Carlsbad, CA	0.080	-0.000	0.00	0.69	12,095
San Francisco-Oakland-Berkeley, CA	-0.015	-0.011	0.00	0.00	18,716
Seattle-Tacoma-Bellevue, WA	0.063	-0.015	0.00	0.00	20,158
St. Louis, MO-IL	0.264	-0.006	0.00	0.00	25,000
Tampa-St. Petersburg-Clearwater, FL	0.115	-0.007	0.00	0.00	18,144
Washington-Arlington-Alexandria, DC-VA-MD-WV	0.069	-0.009	0.00	0.00	35,537

Notes: This table reports the output of regressions of time on the market in weeks on distance to the city center, median income, property characteristics, and year-quarter fixed effects by MSA. The underlying data is for single-family houses from Redfin. See the text for information on the data sources. Standard errors are clustered at the year level. N stands for the number of ZIP-Code-year-month observations.

D.2 COVID

This section of the supplemental appendix examines how the liquidity gradient shifted in Germany and the U.S. following the onset of COVID-19 and the widespread adoption of remote work. Tables A14 and A15 report the baseline regression results for the periods before and after 2020. In both countries, the liquidity gradient became significantly flatter, consistently with the increase in working from home. Figures A9a and A9b show how the coefficient on distance to the city center evolved between 2018 and 2023. In both Germany and the U.S., the liquidity gradient nearly disappeared in 2021 and 2022, but began to rise again afterward.

Table A14: *TOM gradients before and after COVID, Germany (2012–2024)*

	(1) Full sample	(2) Pre-2020	(3) Post-2020
Distance to center (in km)	0.24***	0.26***	0.13***
	(0.03)	(0.03)	(0.04)
City × Year-quarter FE	✓	✓	✓
Property characteristics	✓	✓	✓
N	84,292	60,377	23,914
Adj. R^2	0.13	0.14	0.29
Mean(TOM)	13.51	13.46	13.61

Notes: This table displays the output of Regression (1) *on time on the market (TOM), measured in weeks. The list of property characteristics controls is available in Supplemental Appendix A.1. Regressions are based on the matched sample for all cities covering the period between 2012 and 2024. Standard errors (in parentheses) are clustered at the city-year level.* $*: p < 0.1; **: p < 0.05; ***: p < 0.01$.

Table A15: *TOM gradients before and after COVID, U.S. (2012–2023)*

	(1) Full sample	(2) Pre-2020	(3) Post-2020
Distance to center (in km)	0.05***	0.06***	0.02***
	(0.004)	(0.005)	(0.005)
Median income	-0.16*	-0.23*	-0.71***
	(0.091)	(0.138)	(0.099)
MSA × Year-month FE	✓	✓	✓
State FE	✓	✓	✓
Property characteristics	✓	✓	✓
Demographic controls	✓	✓	✓
N	754,331	494,322	260,009
ZIP Codes	5,453	5,453	5,446
Adj. R^2	0.29	0.29	0.21
Mean(TOM)	7.63	8.86	5.28

Notes: This table displays the output of Regression (1) *on time on the market (TOM), measured in weeks. Regressions are based on data for the 30 largest MSAs covering the period between 2012 and 2023. Standard errors (in parentheses) are clustered at the city-year level.* $*: p < 0.1; **: p < 0.05; ***: p < 0.01$.

Figure A9: *Variation over time in the TOM gradient, U.S. and Germany (2018–2023)*

(a) *U.S.* **(b)** *Germany*

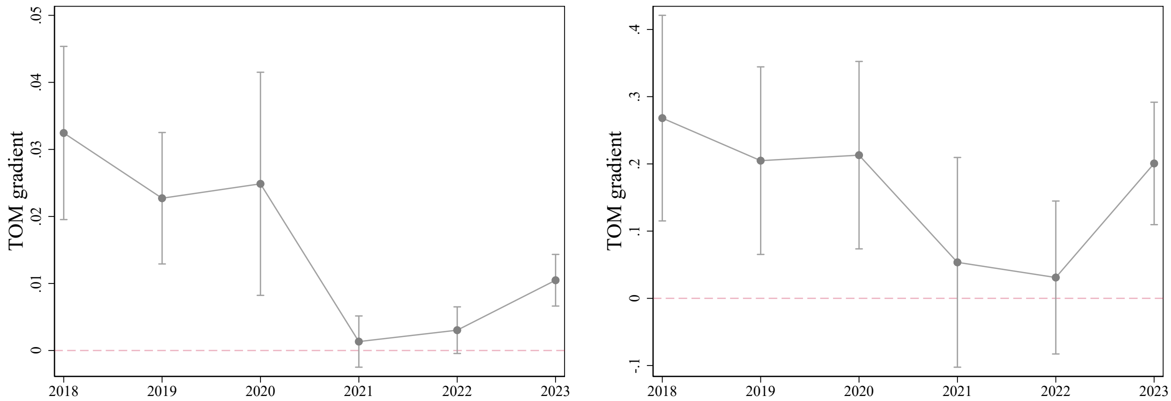

Notes: These plots display outputs by year of Regression (1) *on time on the market (TOM), measured in weeks. Regressions are based on data for the 30 largest MSAs for the U.S. and for the 5 German cities covered by our sample. 90% Confidence bands are constructed using standard errors clustered at the city-year level.*

D.3 Different housing types

This section of the supplemental appendix presents the results for the liquidity gradient across different housing types. Table A16 reports the coefficient on distance to the city center from Regression (1), using time on the market as the dependent variable for our sample of five German cities. Columns 2 to 4 show the results after splitting the sample into different quartiles of the apartment size distribution within cities. Tables A17, A18, and A19 present the results for the 30 largest MSAs in the U.S. Table A17 reports the results for the pooled sample, which includes data on single-family houses, condos, townhouses, and multi-family houses. Table A18 reports the results for time on the market separately by housing type, and Table A19 does so for prices.

Table A16: *Time on the market and distance to the city center by property size, Germany (2012–2024)*

	(1) Full sample	(2) <25th	(3) 25th to 75th	(4) >75th
Distance to center (in km)	0.24***	0.23***	0.29***	0.18***
	(0.03)	(0.06)	(0.03)	(0.06)
Year-quarter-city FEs	✓	✓	✓	✓
Property characteristics	✓	✓	✓	✓
N	84,303	21,425	42,063	20,814
Adj. R^2	0.13	0.10	0.13	0.13
Mean(TOM)	13.51	11.36	13.33	16.08

Notes: This table displays the output of Regression (1) on time on the market (TOM), measured in weeks, for the full sample and for different quartiles of the apartment size distribution within cities. The list of property characteristics controls is available in Supplemental Appendix A.1. Regressions are based on the matched sample for all cities covering the period between 2012 and 2024. Standard errors (in parentheses) are clustered at the city-year level. $*: p < 0.1; **: p < 0.05; ***: p < 0.01$.

Table A17: *Time on the market and distance to city center, U.S.: all housing types (2012–2023)*

	(1) TOM	(2) TOM	(3) TOM	(4) TOM	(5) TOM	(6) TOM
Distance to center (in km)	0.02***	0.02***	0.04***			
	(0.005)	(0.005)	(0.004)			
Travel time to center (in min)				0.02***	0.02***	0.05***
				(0.007)	(0.007)	(0.005)
Median income		-0.53***	-0.20**		-0.53***	-0.17**
		(0.090)	(0.081)		(0.085)	(0.078)
MSA × Year-month FE	✓	✓	✓	✓	✓	✓
Property type FE	✓	✓	✓	✓	✓	✓
State FE	✓	✓	✓	✓	✓	✓
Property characteristics			✓			✓
Demographic controls			✓			✓
N	1,342,681	1,342,681	1,341,818	1,342,681	1,342,681	1,341,818
ZIP Codes	5,128	5,128	5,115	5,128	5,128	5,115
Adj. R^2	0.26	0.26	0.28	0.26	0.26	0.28
Mean(TOM)	7.64	7.64	7.64	7.64	7.64	7.64

Notes: This table displays the output of Regression (1) on time on the market (TOM), measured in weeks. The first three columns show the results for distance to the city center measured in kilometers, while the last three columns show the results for the car travel time to the city center measured in minutes. Regressions are based on data for the 30 largest MSAs covering the period between 2012 and 2023. Standard errors (in parentheses) are clustered at the MSA-year level. $*: p < 0.1; **: p < 0.05; ***: p < 0.01$.

Table A18: *Time on the market and distance to the city center by property type, U.S. (2012–2023)*

	(1) Single-family	(2) Condos	(3) Multi-family	(4) Townhouse
Distance to center (in km)	0.05***	0.02***	0.05***	0.03***
	(0.004)	(0.005)	(0.010)	(0.003)
Median income	-0.14	-0.28*	-0.94***	-0.13
	(0.088)	(0.147)	(0.321)	(0.104)
MSA × Year-month FE	✓	✓	✓	✓
State FE	✓	✓	✓	✓
Property characteristics	✓	✓	✓	✓
Demographic controls	✓	✓	✓	✓
N	682,100	321,653	93,061	244,860
ZIP Codes	4,943	2,422	918	1,837
Adj. R^2	0.32	0.35	0.15	0.30
Mean(TOM)	7.60	7.84	9.52	6.75

Notes: This table displays the output of Regression (1) *on time on the market (TOM), measured in weeks. The four columns show the results for distance to the city center measured in kilometers. Regressions are based on data for each property type separately for the 30 largest MSAs covering the period between 2012 and 2023. Standard errors (in parentheses) are clustered at the MSA-year level.* $*: p < 0.1; **: p < 0.05; ***: p < 0.01$.

Table A19: *Log sales prices and distance to the city center by property type, U.S. (2012–2023)*

	(1) Single-family	(2) Condos	(3) Multi-family	(4) Townhouse
Distance to center (in km)	-0.005***	-0.003***	-0.005***	-0.004***
	(0.000)	(0.000)	(0.001)	(0.001)
Median income	0.110***	0.198***	0.214***	0.313***
	(0.010)	(0.014)	(0.027)	(0.018)
MSA × Year-month FE	✓	✓	✓	✓
State FE	✓	✓	✓	✓
Property characteristics	✓	✓	✓	✓
Demographic controls	✓	✓	✓	✓
N	682,641	321,867	93,061	244,968
ZIP Codes	4,955	2,428	918	1,840
Adj. R^2	0.74	0.69	0.83	0.72
Mean(log(price))	12.69	12.34	12.80	12.49

Notes: This table displays the output of Regression (1) *on log sales prices. The four columns show the results for distance to the city center measured in kilometers. Regressions are based on data for each property type separately for the 30 largest MSAs covering the period between 2012 and 2023. Standard errors (in parentheses) are clustered at the MSA-year level.* $*: p < 0.1; **: p < 0.05; ***: p < 0.01$.

D.4 Alternative city definitions

In this section of the supplemental appendix, we present the results based on the sample of the 30 largest FUAs (functional urban areas) for U.S. cities (see Moreno-Monroy, Marcello Schiavina, and Veneri, 2021), retrieved via the GHSL database (M. Schiavina et al., 2019), which define cities based on commuting flows, following the EU-OECD definition from Dijkstra, Poelman, and Veneri (2019). Columns 1 and 2 of Table A25 show the results using distance to the MSA city center definition, while columns 3 and 4 show the results using distance to the FUA city center definition, which measures the location with the highest residential built-up volume within the FUA.

Table A20: *Price and liquidity gradients for functional urban areas, U.S. (2012–2023)*

	(1) TOM	(2) Price	(3) TOM	(4) Price
Distance to MSA center (in km)	0.020***	-0.004***		
	(0.004)	(0.000)		
Distance to FUA center (in km)			0.026***	-0.007***
			(0.003)	(0.000)
Median income	-0.080	0.208***	-0.061	0.190***
	(0.070)	(0.013)	(0.072)	(0.013)
FUA × Year-month FE	✓	✓	✓	✓
State FE	✓	✓	✓	✓
Property characteristics	✓	✓	✓	✓
Demographic controls	✓	✓	✓	✓
N	656,126	656,126	656,126	656,126
ZIP Codes	4,736	4,736	4,736	4,736
Adj. R^2	0.46	0.75	0.46	0.76
Mean(dependent variable)	7.15	12.74	7.15	12.74

Notes: This table displays the output of Regression (1) *on time on the market (TOM), measured in weeks, and log sales prices. The four columns show the results for distance to the city center measured in kilometers. In the first two columns, the distance is measured to the city hall of the respective MSA, while in the last two columns, the distance is measured to the location with the highest residential built-up volume within the functional urban area (FUA). The regressions are based on data for single-family dwellings in the 30 largest FUAs for the period 2012–2023. Standard errors (in parentheses) are clustered at the FUA-year level.* $*: p < 0.1; **: p < 0.05; ***: p < 0.01$.

D.5 Alternative city centers

In this section of the supplemental appendix, we present the results for the baseline Regression (1) using distance to alternative definitions of the city center. Table A21 shows the results for Germany. Table A25 shows the results for the U.S. in Columns 1 and 2, which we report together with our results on focal locations as multiple alternative city centers.

Table A21: *Price and liquidity gradients using alternative city centers, Germany (2012–2024)*

	(1) TOM	(2) TOM	(3) TOM	(4) Price	(5) Price	(6) Price
Distance to center (in km)	0.31***	0.25***	0.20***	-0.04***	-0.05***	-0.04***
	(0.05)	(0.03)	(0.03)	(0.00)	(0.00)	(0.00)
City × Year-quarter FE	✓	✓	✓	✓	✓	✓
Property characteristics		✓	✓		✓	✓
Borough FE			✓			✓
N	58,326	58,326	58,326	58,326	58,326	58,326
Adj. R^2	0.05	0.13	0.13	0.23	0.84	0.86
Mean(dep. variable)	14.03	14.03	14.03	12.45	12.45	12.45

Notes: This table displays the output of Regression (1) *on time on the market (TOM), measured in weeks, and log sales prices. The six columns show the results for distance to the city center measured in kilometers. The distance is measured to the centroid of the business district with the highest land value (Bodenrichtwert) in the city. The list of property characteristics controls is available in Supplemental Appendix A.1. The regressions are based on data for apartments in Hamburg, Cologne, Frankfurt, and Duesseldorf for the period 2012–2024. Standard errors (in parentheses) are clustered at the city-year level.* $*: p < 0.1; **: p < 0.05; ***: p < 0.01$.

D.6 Properties that do not get sold

We identify listed properties that do not get sold via three steps. First, we match all ads with transactions that occurred within the same neighborhood (*Stadtteil*). Each ad is then associated with a set of potential transactions in the neighborhood. Out of these ads, we identify those as "unsuccessful" that are associated with transactions one year after or before the ad was published. Second, we identify ads as "unsuccessful" that are associated with transactions for which the living area of the matched apartment differs by more than 50%. Third, we identify ads as "unsuccessful" for which the remaining potential matches have a living area and building year that deviate by more than 10% and 10 years.

While this algorithm will identify listings that, with a very high probability, did not end up in a sale, it does not identify all listings that did not end up in a sale. As such, the algorithm presents a lower bound of "unsuccessful" ads. However, we do not have reasons to believe that this lower bound is systematically biased across space, which is the variation we want to explore. We focus only on the three largest cities in our German sample – Hamburg, Munich, and Cologne – because, for the other cities, the number of "unsuccessful" ads is too small to conduct a meaningful statistical analysis.

We first analyze the spatial distribution of unsuccessful ads, measured as the percentage of unsuccessful ads in terms of total ads at the city level, displayed in Figure A10. In all three cities, the relative number of unsuccessful ads is not larger in the city center. If anything, we see that this number slightly increases with distance to the city center.

Figure A10: *Unsuccessful ads and distance to the city center, Germany (2012–2024)*

(a) *Munich* **(b)** *Hamburg* **(c)** *Cologne*

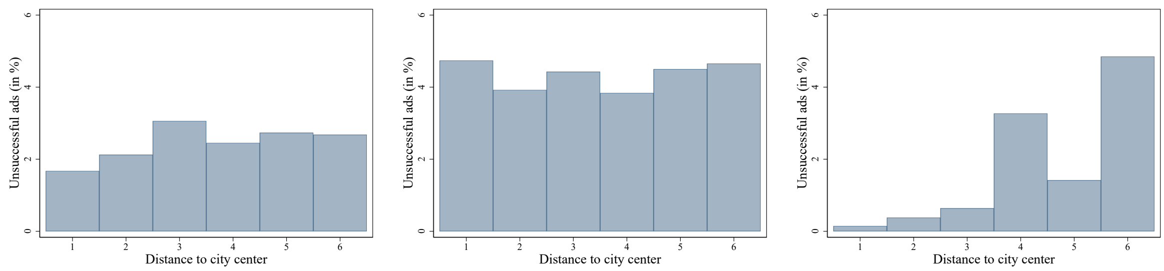

Notes: These plots display the percentage of ads that do not result in a sale by distance to the city center with 6 equally-sized distance bins. The algorithm to identify the "unsuccessful" ads is described in the text.

To conduct a more formal assessment, we run a survival analysis on time on the market. In other words, we test for the relationship between expected time on the market and distance to the city center by estimating the following hazard function for time on the market:

$$h(TOM_{it}) = h_0(TOM) \times \exp\left[\gamma \times \text{distance}_i + \delta \times X_i + f_t + g_c + \varepsilon_{it}\right], \qquad \text{(A1)}$$

where $h_0(TOM)$ is the baseline hazard rate which depends on the assumption on the functional form of the distribution of error terms ε_{it}. The hazard rate $h(TOM_{it})$ denotes the probability of property i being sold at time t, conditional on the seller listing the property in that point in time, the property characteristics are X_i, time fixed effects are f_t, and city fixed effects are g_c. We estimate the hazard rate using various error term distributions and present the results in Table A22. The first row of the table displays the effect of distance to the city center on the hazard rate of time on the market, given by its hazard ratio. Across all specifications, it is significantly larger than one, meaning that a greater distance to the city center is associated with a longer expected time on the market. In other words, an ad has a higher chance of "surviving" in the outskirts than in the city center.

Table A22: *Expected time on the market and distance to city center, Germany (2012–2024)*

	Exponential	Weibull	Cox
Distance to center (in km)	1.013***	1.012***	1.014***
	(0.0032)	(0.0037)	(0.0037)
City × Year FEs	✓	✓	✓
Property characteristics	✓	✓	✓
N	56,279	56,279	56,279

Notes: This table displays the output of Regression (1) *for three different duration models of time on the market, measured in weeks. The first row displays the estimated hazard ratio for the predicted distance to the city center. The regressions are based on data for apartments in Hamburg, Cologne and Munich. The list of property characteristics controls is available in Supplemental Appendix A.1. Standard errors are in parentheses.* $*: p < 0.1; **: p < 0.05; ***: p < 0.01$.

D.7 Information frictions

In this section of the appendix, we present the regression results for the robustness analysis on possible spatial variation in information frictions. Tables A23 and A24 report the estimates from Regression (1) on time on the market (measured in weeks) and asking price discount (measured as a percentage of the asking price) for Germany and the U.S. The first and third columns in both tables are based on the specification with the full set of controls used in our baseline analysis. Columns two and four additionally include controls for the asking price discount and the time on the market, respectively. As shown, the coefficients remain largely unchanged across all specifications for both Germany and the U.S.

Table A23: *Liquidity gradients, Germany (2012–2024)*

	(1) TOM	(2) TOM	(3) APD	(4) APD
Distance to center (in km)	0.241***	0.241***	-0.162***	-0.158***
	(0.0260)	(0.0261)	(0.0279)	(0.0275)
Asking price discount (in %)		-0.006		
		(0.0036)		
Time on the market (in weeks)				-0.014
				(0.0084)
City × Year-quarter FE	✓	✓	✓	✓
Property characteristics	✓	✓	✓	✓
N	84,292	84,292	84,292	84,292
Adj. R^2	0.13	0.13	0.05	0.05
Mean(dependent variable)	13.51	13.51	-1.56	-1.56

Notes: This table presents the results of Regression (1) *on time on the market (TOM), measured in weeks, and asking price discount (APD), measured as a percentage of the asking price. The list of property characteristics controls is available in Supplemental Appendix A.1. The second and fourth columns additionally control for time on the market and the asking price discount, respectively. The regressions are based on the matched sample for all cities, covering the period from 2012 to 2024. Standard errors (in parentheses) are clustered at the city-year level.* $*: p < 0.1; **: p < 0.05; ***: p < 0.01$.

Table A24: *Liquidity gradients, U.S. (2012–2023)*

	(1) TOM	(2) TOM	(3) APD	(4) APD
Distance to center (in km)	0.046***	0.036***	-0.026***	-0.023***
	(0.0039)	(0.0036)	(0.0014)	(0.0013)
Asking price discount (in %)		-0.395***		
		(0.0202)		
Time on the market (in weeks)				-0.059***
				(0.0101)
MSA × Year-month FE	✓	✓	✓	✓
State FE	✓	✓	✓	✓
Property characteristics	✓	✓	✓	✓
Demographic controls	✓	✓	✓	✓
N	682,034	682,034	682,034	682,034
ZIP Codes	4,943	4,943	4,943	4,943
Adj. R^2	0.32	0.34	0.51	0.53
Mean(dependent variable)	7.59	7.59	-1.49	-1.49

Notes: This table presents the results of Regression (1) on time on the market (TOM), measured in weeks, and asking price discount (APD), measured as a percentage of the asking price. The second and fourth columns additionally control for time on the market and the asking price discount, respectively. Regressions are based on data for single-family houses for the 30 largest MSAs covering the period between 2012 and 2023. Standard errors (in parentheses) are clustered at the city-year level. $*: p < 0.1$; $**: p < 0.05$; $***: p < 0.01$.

D.8 Focal ZIP Codes

In this section of the supplemental appendix, we present the results of Regression (1), allowing for multiple city centers within an MSA for the U.S. Columns 1 and 2 of Table A25 show the results when defining a single city center based on the job access index using data from Delventhal and Parkhomenko (2024). To obtain the job access index, we calculate the distance-weighted average of the number of jobs that can be accessed from a ZIP Code and normalize such that 1 represents the maximum available number of jobs across all ZIP Codes. Columns 3 and 4 show the results when defining 3 focal ZIP Codes per MSA as the three ZIP Codes with the highest job access index. Columns 5 and 6 display the results when defining 5 focal ZIP Codes. Our results hold for any definition of focal ZIP Codes.

Table A25: *Time on the market and distance to job centers, U.S. (2012–2023)*

	(1) TOM	(2) TOM	(3) TOM	(4) TOM	(5) TOM	(6) TOM
Distance to largest job center (in km)	0.02***	0.02***				
	(0.005)	(0.003)				
Distance to nearest job center (in km)			0.02***	0.03***		
			(0.006)	(0.003)		
Distance to nearest job center (in km)					0.02***	0.02***
					(0.007)	(0.004)
MSA × Year-month FE	✓	✓	✓	✓	✓	✓
State FE	✓	✓	✓	✓	✓	✓
Property characteristics		✓		✓		✓
Demographic controls		✓		✓		✓
N	595,732	595,732	595,732	595,732	595,732	595,732
ZIP Codes	4,311	4,311	4,311	4,311	4,311	4,311
Adj. R^2	0.39	0.44	0.39	0.44	0.39	0.44
Mean(TOM)	7.27	7.27	7.27	7.27	7.27	7.27

Notes: This table displays the output of Regression (1) *on time on the market (TOM), measured in weeks, using focal points from the job access index instead of the city center. Columns 3 and 4 assume 3 different focal ZIP Codes, while columns 5 and 6 assume 5 different focal ZIP Codes. The regressions are based on data for single-family dwellings in the 30 largest MSAs for the period 2012–2023. Standard errors (in parentheses) are clustered at the MSA-year level.* $*$: $p < 0.1$; $**$: $p < 0.05$; $***$: $p < 0.01$.

E Local maximum in the seller's optimization problem

To save on notation, we show that the first-order condition of the seller's profit maximization problem provides a local maximum via

$$\frac{\partial \Pi}{\partial p(d)|_d} = \gamma(d) + p(d)\frac{\partial \gamma}{\partial p(d)|_d} - \beta \Pi(d)\frac{\partial \gamma}{\partial p(d)|_d} = 0 \tag{A2}$$

rather than the reformulated expression (6) in the main text. The second-order condition for a local maximum is

$$\frac{\partial^2 \Pi}{\partial p^2(d)|_d} = 2\,\frac{\partial \gamma}{\partial p(d)|_d} + \frac{\partial^2 \gamma}{\partial p^2(d)|_d}\big(p(d) - \beta \Pi(d)\big) < 0. \tag{A3}$$

From (12), we know that

$$\frac{\partial \gamma}{\partial p(d)|_d} = -f(\varepsilon^*(d))\,\frac{1-\pi\beta}{\beta} \leq 0 \tag{A4}$$

and therefore

$$\frac{\partial^2 \gamma}{\partial p^2(d)|_d} = -f'(\varepsilon^*(d))\,\frac{1-\pi\beta}{\beta}\,\frac{\partial \varepsilon^*}{\partial p(d)|_d} = -f'(\varepsilon^*(d))\left(\frac{1-\pi\beta}{\beta}\right)^2. \tag{A5}$$

Hence, for (A3) to hold, we need that

$$-2\,f(\varepsilon^*(d))\frac{1-\pi\beta}{\beta} - f'(\varepsilon^*(d))\left(\frac{1-\pi\beta}{\beta}\right)^2\big(p(d) - \beta\Pi(d)\big) < 0 \tag{A6}$$

or

$$f'(\varepsilon^*(d)) > \frac{-2\,f(\varepsilon^*(d))\frac{1-\pi\beta}{\beta}}{\left(\frac{1-\pi\beta}{\beta}\right)^2\big(p(d) - \beta\Pi(d)\big)}, \tag{A7}$$

where $p(d) - \beta\Pi(d) > 0$ follows immediately from (6) and (12). In particular, for $\varepsilon \sim U[\underline{\varepsilon}, \overline{\varepsilon}]$,

$$f'(\varepsilon^*(d)) = 0 > \frac{-2\,\frac{1}{\overline{\varepsilon}-\underline{\varepsilon}}\,\frac{1-\pi\beta}{\beta}}{\left(\frac{1-\pi\beta}{\beta}\right)^2\big(p(d) - \beta\Pi(d)\big)}. \tag{A8}$$

F Analytical results with more general dividend distributions

In this section, we show that the buyer reservation dividend $\varepsilon^*(d)$ increases with distance to the city center d with more general assumptions on the cumulative distribution function of buyer dividends F than with the uniform distribution applied in the main text. As in Section 4.3, we start from the expression for the equilibrium price (A9):

$$p(d) = \frac{-1}{\partial \gamma(d)/\partial p(d)|_d}\left(\gamma(d) + \frac{\beta}{1-\beta}\left(\gamma(d)\right)^2\right),$$

Plugging in the equilibrium relations between probabilities of sale and reservation dividends (8) and (12), we have that

$$p(d) = \frac{\beta}{1-\pi\beta}\frac{1-F(\varepsilon^*(d))}{f(\varepsilon^*(d))} + \frac{\beta^2}{(1-\beta)(1-\pi\beta)}\frac{\left(1-F(\varepsilon^*(d))\right)^2}{f(\varepsilon^*(d))}. \tag{A9}$$

and, via the seller optimality condition (6),

$$\Pi(d) = \frac{\beta}{(1-\beta)(1-\pi\beta)}\frac{\left(1-F(\varepsilon^*(d))\right)^2}{f(\varepsilon^*(d))}. \tag{A10}$$

Plugging these results into the linear expression for buyer dividends (11) yields

$$\begin{aligned}\varepsilon^*(d) = {} & \frac{1-F(\varepsilon^*(d))}{f(\varepsilon^*(d))} + \frac{\beta}{1-\beta}\frac{\left(1-F(\varepsilon^*(d))\right)^2}{f(\varepsilon^*(d))} - \frac{(1-\pi)\beta}{(1-\beta)(1-\pi\beta)}\frac{\left(1-F(\varepsilon^*(d))\right)^2}{f(\varepsilon^*(d))} \\ & + \tau(d) + (\pi - \pi\beta)W. \end{aligned} \tag{A11}$$

Taking the derivative with respect to d gives us

$$\begin{aligned}&\frac{\partial \varepsilon^*}{\partial d}\left(1 + \frac{\left(f(\varepsilon^*(d))\right)^2 + f'(\varepsilon^*(d))\left(1-F(\varepsilon^*(d))\right)}{\left(f(\varepsilon^*(d))\right)^2}\right. \\ &\left. + \frac{2\left(1-F(\varepsilon^*(d))\right)\left(f(\varepsilon^*(d))\right)^2 + f'(\varepsilon^*(d))\left(1-F(\varepsilon^*(d))\right)^2}{\left(f(\varepsilon^*(d))\right)^2}\right) = \frac{\partial \tau}{\partial d} > 0. \end{aligned} \tag{A12}$$

Hence, for $\partial\varepsilon^*/\partial d > 0$, we need

$$f'(\varepsilon^*(d)) > \frac{-\left(f(\varepsilon^*(d))\right)^2\left(2 + 2\left(1-F(\varepsilon^*(d))\right)\right)}{\left(1-F(\varepsilon^*(d))\right) + \left(1-F(\varepsilon^*(d))\right)^2}, \tag{A13}$$

that is, $f'(\varepsilon^*(d))$ may be negative, but not too negative. For the uniform distribution in the main text, this holds immediately with $f'(\varepsilon^*(d)) = 0$. Another distribution commonly used in housing search models is the exponential distribution (see, for example, Guren and McQuade, 2020). With an exponential distribution with rate parameter $\lambda > 0$,

$$f'(\varepsilon^*(d)) = -\lambda^2 \exp(-\lambda \varepsilon^*(d)) \tag{A14}$$

and

$$\frac{-\big(f(\varepsilon^*(d))\big)^2\Big(2+2\big(1-F(\varepsilon^*(d))\big)\Big)}{\big(1-F(\varepsilon^*(d))\big)+\big(1-F(\varepsilon^*(d))\big)^2} = \frac{-2\lambda^2\exp(-2\lambda\varepsilon^*(d)) - 2\lambda^2\exp(-3\lambda\varepsilon^*(d))}{\exp(-\lambda\varepsilon^*(d)) + \exp(-2\lambda\varepsilon^*(d))}. \tag{A15}$$

Hence, noting that

$$\big(1-F(\varepsilon^*(d))\big)+\big(1-F(\varepsilon^*(d))\big)^2 = \exp(-\lambda\varepsilon^*(d)) + \exp(-2\lambda\varepsilon^*(d)) > 0, \tag{A16}$$

we have that

$$\begin{aligned} &f'(\varepsilon^*(d))\Big(\big(1-F(\varepsilon^*(d))\big)+\big(1-F(\varepsilon^*(d))\big)^2\Big) \\ &= -\lambda^2\exp(-2\lambda\varepsilon^*(d)) - \lambda^2\exp(-3\lambda\varepsilon^*(d)) \\ &= -\lambda^2\Big(\exp(-2\lambda\varepsilon^*(d)) + \exp(-3\lambda\varepsilon^*(d))\Big) < 0, \end{aligned} \tag{A17}$$

while in the numerator of (A15),

$$\begin{aligned} &-\big(f(\varepsilon^*(d))\big)^2\Big(2+2\big(1-F(\varepsilon^*(d))\big)\Big) \\ &= -2\lambda^2\Big(\exp(-2\lambda\varepsilon^*(d)) + \exp(-3\lambda\varepsilon^*(d))\Big) < 0. \end{aligned} \tag{A18}$$

Therefore,

$$\begin{aligned} &f'(\varepsilon^*(d))\Big(\big(1-F(\varepsilon^*(d))\big)+\big(1-F(\varepsilon^*(d))\big)^2\Big) \\ &> \big(f(\varepsilon^*(d))\big)^2\Big(2+2\big(1-F(\varepsilon^*(d))\big)\Big) \end{aligned} \tag{A19}$$

as $2 > 1$ and both sides are negative, such that

$$f'(\varepsilon^*(d)) > -\frac{\big(f(\varepsilon^*(d))\big)^2\Big(2+2\big(1-F(\varepsilon^*(d))\big)\Big)}{\big(1-F(\varepsilon^*(d))\big)+\big(1-F(\varepsilon^*(d))\big)^2} \tag{A20}$$

as desired. Even though the exponential distribution's probability density function has a negative slope, it is not too negative, such that our key result that reservation dividends increase with distance to the city center still holds. The results that liquidity and prices decrease with distance to the city center follow from this result, as shown in the main text.

G Extended model with bargaining

We extend our model with a bargaining process, following Carrillo (2012). With this addition, the model features asking prices and sales prices, which allows us to form a model notion of an asking price discount (APD), as in the supplementary empirical results. In this model, the asking price discount will always be weakly negative. In the data, it can reach positive values, however, in most cases, it is indeed weakly negative.

The search process changes as follows. When a buyer visits a housing unit, the buyer and the seller may or may not bargain, which is determined stochastically. With probability θ, the seller does not accept counteroffers, and $p(d)$ is a take-it-or-leave-it offer ("no-counteroffer scenario", subscript n). The buyer accepts or rejects the offer. If the buyer accepts, the seller receives $p(d)$, and the buyer receives their first housing dividend ε and incurs their first commuting cost $\tau(d)$ in the following period. If the buyer rejects, the seller relists the property, and the buyer visits a new housing unit in the following period. With probability $1-\theta$, the buyer can bargain by making a take-it-or-leave-it counteroffer $o(d)$ to the seller ("counteroffer scenario", subscript c). If the buyer makes a counteroffer, the seller accepts or rejects the offer. The outcomes of accepting or rejecting the offer are analogous to those in the no-counteroffer scenario.

Changes in the seller's problem. The seller maximizes their expectd profit $\Pi(d)$ over an asking price $p(d)$ and a reservation value $r(d)$. We assume that buyers have perfect information about sellers' decision problems. Hence, in the counteroffer scenario, the offer $o(d)$ is equal to the seller's reservation value $r(d)$, as this offer corresponds to the lowest price the seller is willing to accept. In the following, we denote by $\gamma_n(d)$ the probability that a buyer is willing to buy in the no-counteroffer scenario. The analogous probability in the counteroffer scenario is $\gamma_c(d)$. The expected profit is

$$\begin{aligned}\Pi(d) = \theta\Big(\gamma_n(d)p(d) + \big(1-\gamma_n(d)\big)\beta\Pi(d)\Big) \\ + \big(1-\theta\big)\Big(\gamma_c(d)\max\big[r(d), \beta\Pi(d)\big] + \big(1-\gamma_c(d)\big)\beta\Pi(d)\Big).\end{aligned} \tag{A21}$$

Changes in the buyer's problem. The buyer's search value is given by

$$W = E_{d,\varepsilon}\big[\theta V_n(d,\varepsilon) + \big(1-\theta\big)V_c(d,\varepsilon)\big]. \tag{A22}$$

The buyer's value in the no-counteroffer scenario is given by

$$V_n(d,\varepsilon) = \max\left[V(d,\varepsilon) - p(d), \beta W\right]. \tag{A23}$$

The buyer's value in the counteroffer scenario is given by

$$V_c(d,\varepsilon) = \max\left[\delta(d)\big(V(d,\varepsilon) - o(d)\big) + \big(1-\delta(d)\big)\big(\beta W\big), \beta W\right], \tag{A24}$$

where $\delta(d)$ denotes the probability that the seller accepts the buyer's counteroffer. The seller always accepts the optimal counteroffer $o(d) = r(d)$. Hence, $\delta(d) = 1$ at all distances to the city center in equilibrium.

G.1 Equilibrium in the extended model

Seller's optimization. Since the counteroffer $o(d) = r(d)$ is the lowest price that the seller is willing to accept, the seller's reservation value $r(d) = \beta\Pi(d)$. The expression for the expected profit (A21) then simplifies to

$$\Pi(d) = \theta\gamma_n(d)p(d) + \big(1-\theta\gamma_n(d)\big)r(d). \tag{A25}$$

Optimizing with regard to the asking price $p(d)$ yields

$$p(d) = r(d) - \frac{\gamma_n(d)}{\partial\gamma_n/\partial p(d)|_d}, \tag{A26}$$

and plugging the condition $r(d) = \beta\Pi(d)$ into (A25) yields

$$r(d) = \frac{\beta\theta\gamma_n(d)p(d)}{1-\beta\big(1-\theta\gamma_n(d)\big)}. \tag{A27}$$

The pair of the optimal asking price and reservation value for a given distance to the city center solves equations (A26) and (A27) simultaneously.

Buyer's optimization. Via the buyer value function in the no-counteroffer scenario (A23), we define a reservation dividend $\varepsilon_n^*(d)$ such that a buyer is indifferent between buying a housing unit and continuing to search:

$$V(d, \varepsilon_n^*(d)) - p(d) = \beta W. \tag{A28}$$

Analogously, via the buyer value function in the counteroffer scenario (A24), we define a reservation dividend $\varepsilon_c^*(d)$ such that

$$V(d, \varepsilon_c^*(d)) - r(d) = \beta W. \tag{A29}$$

Probability of sale. The probability of sale conditional on a bargaining scenario is equal to the probability that the buyer's idiosyncratic dividend is above their respective reservation dividend. Hence, in the no-counteroffer scenario,

$$\gamma_n(d) = 1 - F(\varepsilon_n^*(d)) \tag{A30}$$

and in the counteroffer scenario,

$$\gamma_c(d) = 1 - F(\varepsilon_c^*(d)). \tag{A31}$$

Thus, for the derivative in the seller optimality condition (A26) we have that

$$\frac{\partial \gamma_n}{\partial p(d)|_d} = -f(\varepsilon_n^*(d)) \frac{\partial \varepsilon_n^*}{\partial p(d)|_d}. \tag{A32}$$

By proceeding as in the main text, we get

$$\varepsilon_n^*(d) = \frac{1 - \pi\beta}{\beta} p(d) + \tau(d) - \big(1 - \pi\big)\Pi(d) + \big(\pi - \pi\beta\big)W \tag{A33}$$

and

$$\frac{\partial \gamma_n}{\partial p(d)|_d} = -f(\varepsilon_n^*(d)) \frac{1 - \pi\beta}{\beta}. \tag{A34}$$

Analogous relations hold for the counteroffer scenario.

G.2 Analytical results in the extended model

Again, we start with auxiliary derivations, applying $\varepsilon \sim U[\underline{\varepsilon},\overline{\varepsilon}]$. First, Lemma 1 enables us to simplify expressions that contain reservation dividends and probabilities of sale.

Lemma 1. *The buyer reservation dividends in the counteroffer scenario and the no-counteroffer scenario relate as $\varepsilon_c^*(d) = 2\varepsilon_n^*(d) - \overline{\varepsilon}$. The probabilities of sale in these two scenarios relate as $\gamma_c(d) = 2\gamma_n(d)$.*

Proof. Using the buyer indifference conditions (A28) and (A29) together with the linear expression of the buyer value function (10), we have that

$$\varepsilon_n^*(d) = \frac{1-\pi\beta}{\beta}p(d) + \tau(d) - \big(1-\pi\big)\big(\Pi(d)+W\big) + \big(1-\pi\beta\big)W \tag{A35}$$

and

$$\varepsilon_c^*(d) = \frac{1-\pi\beta}{\beta}r(d) + \tau(d) - \big(1-\pi\big)\big(\Pi(d)+W\big) + \big(1-\pi\beta\big)W. \tag{A36}$$

With the seller optimality condition (A26), the equilibrium relation between probabilities of sale and reservation dividends in the no-counteroffer scenario (A30), and the value of the derivative in (A34), we get

$$\varepsilon_n^*(d) - \varepsilon_c^*(d) = \frac{1-\pi\beta}{\beta}\big(p(d)-r(d)\big) = \frac{1-\pi\beta}{\beta}\left(-\frac{\gamma_n(d)}{\partial\gamma_n/\partial p(d)|_d}\right) \tag{A37}$$

$$= \frac{1-\pi\beta}{\beta}\left(-\frac{\frac{\overline{\varepsilon}-\varepsilon_n^*(d)}{\overline{\varepsilon}-\underline{\varepsilon}}}{-\frac{1-\pi\beta}{\beta}\frac{1}{\overline{\varepsilon}-\underline{\varepsilon}}}\right) \tag{A38}$$

which means that

$$\varepsilon_c^*(d) = 2\varepsilon_n^*(d) - \overline{\varepsilon}. \tag{A39}$$

Translating the reservation dividends back into probabilities of sale, we have that

$$\overline{\varepsilon} - (\overline{\varepsilon}-\underline{\varepsilon})\gamma_c(d) = 2\big(\overline{\varepsilon} - (\overline{\varepsilon}-\underline{\varepsilon})\gamma_n(d)\big) - \overline{\varepsilon} \tag{A40}$$

and hence $\gamma_c(d) = 2\gamma_n(d)$. □

Lemma 2. *The reservation dividends in the no-counteroffer scenario* $\varepsilon_n^*(d)$ *and in the counteroffer scenario* $\varepsilon_c^*(d)$ *increase with distance to the city center* d*.*

Proof. We know from (A33) that

$$\varepsilon_n^*(d) = \frac{1-\pi\beta}{\beta} p(d) + \tau(d) - \left(1-\pi\right)\Pi(d) + \left(\pi - \pi\beta\right)W.$$

Analogously to the main derivations, we reformulate the asking price $p(d)$ and the expected profit from reselling the property $\Pi(d)$ in terms of the reservation dividend $\varepsilon_n^*(d)$. First, we combine the seller optimality conditions (A26) and (A27) and get

$$p(d) = -\frac{\left(1-\beta\right)\gamma_n(d) + \beta\theta\gamma_n^2(d)}{\left(1-\beta\right)\left(\partial\gamma_n/\partial p(d)|_d\right)}. \tag{A41}$$

Expressing the probability of sale $\gamma_n(d)$ and the derivative $\partial\gamma_n/\partial p(d)|_d$ in terms of the reservation dividend $\varepsilon_n^*(d)$ using the equilibrium relations (A30) and (A34), we have that

$$p(d) = \frac{\beta\left(\overline{\varepsilon} - \varepsilon_n^*(d)\right)}{1-\pi\beta} + \frac{\beta^2\theta\left(\overline{\varepsilon} - \varepsilon_n^*(d)\right)^2}{\left(1-\beta\right)\left(1-\pi\beta\right)\left(\overline{\varepsilon} - \underline{\varepsilon}\right)}. \tag{A42}$$

Next, using the seller's conditions (A25) and (A26), we get

$$\Pi(d) = p(d) + \frac{\gamma_n(d) - \theta\gamma_n^2(d)}{\partial\gamma_n/\partial p(d)|_d}, \tag{A43}$$

which, using (A42) and again expressing the probability of sale and the derivative in terms of the reservation dividend via (A30) and (A34), amounts to

$$\Pi(d) = \frac{\beta\theta\left(\overline{\varepsilon} - \varepsilon_n^*(d)\right)^2}{\left(1-\beta\right)\left(1-\pi\beta\right)\left(\overline{\varepsilon} - \underline{\varepsilon}\right)}. \tag{A44}$$

Plugging these results into the linear reservation dividend expression (A33) and taking the derivative with respect to the distance to the city center d on both sides yields

$$\frac{\partial\varepsilon_n^*}{\partial d}\underbrace{\left(2 + 2\frac{\pi\beta\theta}{1-\pi\beta}\frac{\overline{\varepsilon} - \varepsilon_n^*(d)}{\overline{\varepsilon} - \underline{\varepsilon}}\right)}_{>0} = \frac{\partial\tau}{\partial d} > 0 \tag{A45}$$

and therefore $\partial\varepsilon_n^*/\partial d > 0$. Via Lemma 1, also $\partial\varepsilon_c^*/\partial d > 0$. □

Corollary 1. *The expected profit* $\Pi(d)$*, the asking price* $p(d)$*, the seller reservation value* $r(d)$*, and* $\mathbb{E}\left[\textit{Sales price}(d)\right] = \theta p(d) + \left(1-\theta\right) r(d)$ *decrease with distance to the city center* d*.*

Proof. Using (A44), we have that

$$\frac{\partial \Pi}{\partial d} = -\frac{\partial \varepsilon_n^*}{\partial d} \frac{2\beta\theta\left(\overline{\varepsilon} - \varepsilon_n^*(d)\right)}{\left(1-\beta\right)\left(1-\pi\beta\right)\left(\overline{\varepsilon} - \underline{\varepsilon}\right)} < 0, \tag{A46}$$

where $\partial \varepsilon_n^* / \partial d > 0$ via Lemma 2. Next, using (A42), we get

$$\frac{\partial p}{\partial d} = -\frac{\partial \varepsilon_n^*}{\partial d} \left(\frac{\beta}{1-\pi\beta} + \frac{2\beta^2\theta\left(\overline{\varepsilon} - \varepsilon_n^*(d)\right)}{\left(1-\beta\right)\left(1-\pi\beta\right)\left(\overline{\varepsilon} - \underline{\varepsilon}\right)} \right) < 0. \tag{A47}$$

Proceeding as in the proof of Lemma 1, we have that

$$r(d) = p(d) - \frac{\beta\left(\overline{\varepsilon} - \varepsilon_n^*(d)\right)}{1-\pi\beta} = \frac{\beta^2\theta\left(\overline{\varepsilon} - \varepsilon_n^*(d)\right)^2}{\left(1-\beta\right)\left(1-\pi\beta\right)\left(\overline{\varepsilon} - \underline{\varepsilon}\right)}. \tag{A48}$$

Then,

$$\frac{\partial r}{\partial d} = -\frac{\partial \varepsilon_n^*}{\partial d} \frac{2\beta^2\theta\left(\overline{\varepsilon} - \varepsilon_n^*(d)\right)}{\left(1-\pi\beta\right)\left(1-\beta\right)\left(\overline{\varepsilon} - \underline{\varepsilon}\right)} < 0. \tag{A49}$$

$\mathbb{E}\left[\textit{Sales price}(d)\right] = \theta p(d) + \left(1-\theta\right) r(d)$ decreases with distance to the city center, as both the asking price $p(d)$ and the seller reservation value $r(d)$ decrease with distance to the city center. □

Time on the market. The probability $\gamma_{nc}(d)$ that a housing unit sells in a period is given via the probabilities for the two bargaining scenarios and the corresponding probabilities of sale:

$$\gamma_{nc}(d) = \theta\gamma_n(d) + \left(1-\theta\right)\gamma_c(d). \tag{A50}$$

The expected time on the market at a given distance to the city center is

$$\mathbb{E}\left[TOM(d)\right] = \frac{1}{\gamma_{nc}(d)}. \tag{A51}$$

Proposition 1. *The expected time on the market* $\mathbb{E}\left[TOM(d)\right]$ *increases with distance to the* *city center d in the extended model with bargaining.*

Proof. Using Lemma 1 and the equilibrium relations between the reservation dividends and the probabilities of sale (A30) and (A31), we can express the expected time on the market in terms of the reservation dividend in the no-counteroffer scenario:

$$\mathbb{E}\left[TOM(d)\right] = \frac{1}{(2-\theta)\gamma_n(d)} = \frac{\overline{\varepsilon} - \underline{\varepsilon}}{\left(2-\theta\right)\left(\overline{\varepsilon} - \varepsilon_n^*(d)\right)}. \tag{A52}$$

The derivative of the expected time on the market with respect to the distance to the city center amounts to

$$\frac{\partial \mathbb{E}\left[TOM\right]}{\partial d} = \frac{\partial \varepsilon_n^*}{\partial d} \underbrace{\frac{\overline{\varepsilon} - \underline{\varepsilon}}{2-\theta} \left(\overline{\varepsilon} - \varepsilon_n^*(d)\right)^{-2}}_{>0} > 0. \tag{A53}$$

□

Intuition. See main text.

Asking price discount. The expected asking price discount at a given distance to the city center is

$$\mathbb{E}\left[APD(d)\right] = \theta \times APD_n(d) + \left(1-\theta\right) \times APD_c(d) = \left(1-\theta\right) \times APD_c(d), \tag{A54}$$

where the asking price discount in the no-counteroffer scenario $APD_n(d) = 0$. We define the asking price discount in the counteroffer scenario analogously to our empirical measure as

$$APD_c(d) = \frac{r(d) - p(d)}{p(d)}. \tag{A55}$$

Proposition 2. *Given that the probability of no counteroffer $\theta \in (0,1)$, the expected asking price discount $\mathbb{E}\left[APD(d)\right] < 0$ becomes more negative with distance to the city center d.*

Proof. If $\theta = 1$, then the asking price discount is always equal to zero, as the probability of being in the no-counteroffer scenario is equal to one, and hence the asking price is the same as the sales price at all distances to the city center. This corresponds to the setup in the main model. In the following, we consider $\theta < 1$. Using the expression for the optimal reservation value $r(d)$ of a seller (A27), we have that

$$APD_c(d) = \frac{\frac{\beta\theta\gamma_n(d)p(d)}{1-\beta(1-\theta\gamma_n(d))} - p(d)}{p(d)} = \underbrace{\frac{1}{1-\beta+\beta\theta\frac{\overline{\varepsilon}-\varepsilon_n^*(d)}{\overline{\varepsilon}-\underline{\varepsilon}}}}_{>0}\underbrace{(\beta-1)}_{<0} < 0. \tag{A56}$$

Hence, the expected asking price discount $\mathbb{E}\left[APD(d)\right] = \left(1-\theta\right)APD_c(d) < 0$. The derivative of $\mathbb{E}\left[APD(d)\right]$ with respect to the distance to the city center amounts to

$$\frac{\partial\mathbb{E}\left[APD\right]}{\partial d} = \frac{\partial\mathbb{E}\left[APD_c\right]}{\partial d} = \underbrace{\left(1-\beta+\beta\theta\frac{\overline{\varepsilon}-\varepsilon_n^*(d)}{\overline{\varepsilon}-\underline{\varepsilon}}\right)^{-2}\frac{\beta\theta}{\overline{\varepsilon}-\underline{\varepsilon}}\frac{\partial\varepsilon_n^*}{\partial d}}_{>0}\underbrace{(\beta-1)}_{<0} < 0, \tag{A57}$$

provided that $\theta > 0$. □

Intuition. As for the time on the market, the relevant condition for liquidity in the form of the asking price discount to decrease with distance to the city center is that reservation dividends increase with distance to the city center. In principle, both the asking price and the seller reservation value decrease with distance to the city center (see Corollary 1). For the expected asking price discount to become more negative with distance to the city center, we need that the seller reservation value decreases more steeply with distance to the city center than the asking price.[41] Why is this condition fulfilled? Recall from the seller optimization that the reservation value is equal to the discounted profit of the next period in equilibrium, as otherwise, the seller would always reject the buyer's optimal counteroffer. For the asking price discount to become more negative with distance to the city center, we, therefore, need that the expected profit decreases more steeply than the

[41] Formally,

$$\frac{\partial\mathbb{E}\left[APD\right]}{\partial d} = \left(1-\theta\right)\frac{\partial\left(\frac{r-p}{p}\right)}{\partial d} = \left(1-\theta\right)\left(\frac{\partial r}{\partial d}\frac{1}{p(d)} - \frac{\partial p}{\partial d}\frac{r}{\left(p(d)\right)^2}\right), \tag{A58}$$

such that for the expected asking price discount to decrease with distance to the city center, we need

$$\underbrace{\frac{\partial r/\partial d}{r(d)}}_{<0} < \underbrace{\frac{\partial p/\partial d}{p(d)}}_{<0}, \tag{A59}$$

where both sides of the expression are < 0 due to Corollary 1.

asking price.[42] A formal proof of this statement follows shortly. Intuitively, we can express the expected profit in terms of the probability of sale and the asking price. Since both the probability of sale and the asking price decrease with distance to the city center and the expected profit is composed of the two, the expected profit decreases more steeply than the asking price alone. *Proof: the expected profit decreases more steeply with distance to the city center than the asking price.* Via (A25), we can express the expected profit as

$$\Pi(d) = \theta\gamma_n(d)p(d) + \big(1 - \theta\gamma_n(d)\big)\beta\Pi(d),$$

since the seller's reservation value $r(d) = \beta\Pi(d)$ via the optimal counteroffer of the buyer. Then,

$$\Pi(d) = \frac{\theta\gamma_n(d)p(d)}{1 - \beta + \theta\beta\gamma_n(d)} \tag{A61}$$

and

$$\frac{\partial\Pi}{\partial d} = \frac{\big(1-\beta+\theta\beta\gamma_n(d)\big)\Big(\theta\frac{\partial\gamma_n}{\partial d}p(d) + \theta\gamma_n(d)\frac{\partial p}{\partial d}\Big) - \theta^2\beta\frac{\partial\gamma_n}{\partial d}\gamma_n(d)p(d)}{\big(1-\beta+\theta\beta\gamma_n(d)\big)^2}. \tag{A62}$$

The proportional derivative of $\Pi(d)$ with respect to d is then

$$\frac{\partial\Pi/\partial d}{\Pi(d)} = \underbrace{\frac{\partial\gamma_n/\partial d}{\gamma_n(d)}}_{<0} + \underbrace{\frac{\partial p/\partial d}{p(d)}}_{<0} - \underbrace{\frac{(\theta\beta)(\partial\gamma_n/\partial d)}{1-\beta+\theta\beta\gamma_n(d)}}_{<0}. \tag{A63}$$

Statement (A60) says that

$$\frac{\partial\Pi/\partial d}{\Pi(d)} < \frac{\partial p/\partial d}{p(d)}, \tag{A64}$$

for which to hold we need that

$$\frac{\partial\gamma_n/\partial d}{\gamma_n(d)} < \frac{(\theta\beta)(\partial\gamma_n/\partial d)}{1-\beta+\theta\beta\gamma_n(d)}. \tag{A65}$$

---

[42] Formally,

$$\frac{\partial r/\partial d}{r(d)} = \frac{\partial(\beta\Pi)/\partial d}{\beta\Pi(d)} = \frac{\partial\Pi/\partial d}{\Pi(d)} < \frac{\partial p/\partial d}{p(d)}. \tag{A60}$$

As $\partial\gamma_n/\partial d < 0$, this expression simplifies to

$$\frac{1}{\gamma_n(d)} > \frac{\theta\beta}{1-\beta+\theta\beta\gamma_n(d)}, \tag{A66}$$

or equivalently

$$1-\beta > 0, \tag{A67}$$

which is true, since $\beta \in (0,1)$. Therefore, $\frac{\partial\Pi/\partial d}{\Pi(d)} < \frac{\partial p/\partial d}{p(d)}$, as required. □

Relation between time on the market and asking price discount. Via the proofs of Propositions 1 and 2, we can directly derive that housing units that spend more time on the market also sell at more negative discounts. Thus, lower liquidity in one measure corresponds to lower liquidity in the other measure.

Corollary 2. *Given that the probability of no counteroffer $\theta \in (0,1)$, the model correlation between the expected asking price discount $\mathbb{E}\big[APD(d)\big]$ and the expected time on the market $\mathbb{E}\big[TOM(d)\big]$ is negative.*

Proof. We start by expressing the asking price discount in terms of the time on the market. Then, we evaluate the derivative of the asking price discount with respect to the time on the market at a given distance to the city center. First, from the proofs of Propositions 1 and 2 we have that

$$\mathbb{E}\big[APD(d)\big] = \frac{\beta-1}{1-\beta+\frac{\beta\theta}{(2-\theta)\mathbb{E}[TOM(d)].}} \tag{A68}$$

The derivative of the expected time on the market with respect to the expected asking price discount, given a distance to the city center d is then

$$\frac{\partial\mathbb{E}\big[APD\big]}{\partial\mathbb{E}\big[TOM(d)\big]|_d} = \underbrace{\left(1-\beta+\frac{\beta\theta}{(2-\theta)\mathbb{E}[TOM(d)]}\right)^{-2}\frac{\beta\theta}{2-\theta}\Big(\mathbb{E}\big[TOM(d)\big]\Big)^{-2}}_{>0}\underbrace{(\beta-1)}_{<0} < 0, \tag{A69}$$

provided that $\theta \in (0,1)$. A higher time on the market therefore corresponds to a more negative asking price discount. □

H Equilibrium existence and uniqueness

We show existence and uniqueness of an equilibrium in the extended model. The main model is obtained by setting the probability of the no-counteroffer scenario $\theta = 1$.

H.1 Equilibrium existence

First, we show the existence of a solution. Evidently, we find a solution numerically, nevertheless, we prove its existence formally, following Krainer (2001). As in (10), we can express the buyer's value in the extended model as

$$V(d,\varepsilon) = \frac{\beta}{1-\pi\beta}\Big(\varepsilon - \tau(d) + \big(1-\pi\big)\big(\Pi(d)+W\big)\Big). \tag{A70}$$

Hence, $V(d,\varepsilon)$ is linear in ε and there exist reservation dividends as defined in the buyer indifference conditions (A28) and (A29). In what follows, we express the other endogenous variables in terms of the buyer's reservation dividends, the model parameters, and the travel cost function to prove uniqueness of the solution. The fact that reservation dividends exist then implies that a solution also exists, as the remaining objects listed in the previous sentence are exogenous.

H.2 Equilibrium uniqueness

To show uniqueness, we follow Vanhapelto and Magnac (2024), showing that two possible ways of expressing the value of search allow for only one pair of the buyer reservation dividends $\{\varepsilon_n^*(d), \varepsilon_c^*(d)\}$ at every distance to the city center such that both of these expressions hold. The first expression decreases in the buyer reservation dividends, whereas the second expression increases. Hence, given a set of parameters and a travel cost function, the model's solution is unique, as we express all endogenous variables in terms of parameters, the exogenous travel cost, and the endogenous buyer reservation dividends.

Expression 1. We set up the first expression for the value of search in terms of the buyer reservation dividends via the definitions (A22), (A23), and (A24):

$$W = \mathbb{E}_{d,\varepsilon}\big[\theta \max\big[V(d,\varepsilon)-p(d), \beta W\big] + \big(1-\theta\big)\max\big[V(d,\varepsilon)-r(d), \beta W\big]\big], \tag{A71}$$

and hence

$$W = \frac{1}{1-\beta}\mathbb{E}_{d,\varepsilon}\left[\theta \max\left[V(d,\varepsilon) - p(d) - \beta W, 0\right] + \left(1-\theta\right)\max\left[V(d,\varepsilon) - r(d) - \beta W, 0\right]\right]. \tag{A72}$$

Next, we express the relations within the max operators in terms of the buyer reservation dividends. Note that when the buyer indifference conditions (A28) and (A29) hold, we have that

$$\beta W = V(d, \varepsilon_n^*(d)) - p(d) = V(d, \varepsilon_c^*(d)) - r(d). \tag{A73}$$

Inserting the linear buyer value (A70), we get

$$\beta W = \frac{\beta}{1-\pi\beta}\Big(\varepsilon_n^*(d) - \tau(d) + \left(1-\pi\right)\left(\Pi(d) + W\right)\Big) - p(d) \tag{A74}$$

and

$$\beta W = \frac{\beta}{1-\pi\beta}\Big(\varepsilon_c^*(d) - \tau(d) + \left(1-\pi\right)\left(\Pi(d) + W\right)\Big) - r(d). \tag{A75}$$

Hence,

$$\frac{\beta}{1-\pi\beta}\varepsilon_n^*(d) = \frac{\beta}{1-\pi\beta}\tau(d) - \frac{\beta\left(1-\pi\right)}{1-\pi\beta}\Pi(d) + \frac{\pi\beta\left(1-\beta\right)}{1-\pi\beta}W + p(d) \tag{A76}$$

and

$$\frac{\beta}{1-\pi\beta}\varepsilon_c^*(d) = \frac{\beta}{1-\pi\beta}\tau(d) - \frac{\beta\left(1-\pi\right)}{1-\pi\beta}\Pi(d) + \frac{\pi\beta\left(1-\beta\right)}{1-\pi\beta}W + r(d). \tag{A77}$$

Again using (A70), we can express the sum within the first max operator from (A72) as

$$V(d,\varepsilon) - p(d) - \beta W = \frac{\beta}{1-\pi\beta}\varepsilon + -\frac{\beta}{1-\pi\beta}\tau(d) + \frac{\beta\left(1-\pi\right)}{1-\pi\beta}\Pi(d) - p(d) - \frac{\pi\beta\left(1-\beta\right)}{1-\pi\beta}W.$$

Then, via (A76), we get

$$V(d,\varepsilon) - p(d) - \beta W = \frac{\beta}{1-\pi\beta}\varepsilon - \frac{\beta}{1-\pi\beta}\varepsilon_n^*(d) = \frac{\beta}{1-\pi\beta}\left(\varepsilon - \varepsilon_n^*(d)\right). \tag{A78}$$

Analogously, using (A77), we have that

$$V(d,\varepsilon) - r(d) - \beta W = \frac{\beta}{1-\pi\beta}\big(\varepsilon - \varepsilon_c^*(d)\big). \tag{A79}$$

We can then express the value of search from (A72) as

$$W = \frac{1}{1-\beta}\mathbb{E}_{d,\varepsilon}\left[\theta \max\left[\frac{\beta}{1-\pi\beta}\big(\varepsilon - \varepsilon_n^*(d)\big), 0\right] + \big(1-\theta\big)\max\left[\frac{\beta}{1-\pi\beta}\big(\varepsilon - \varepsilon_c^*(d)\big), 0\right]\right] \tag{A80}$$

which decreases in $\varepsilon_n^*(d)$ and $\varepsilon_c^*(d)$.

Expression 2. We set up the second expression via the buyer indifference conditions First, using the linear form of the buyer value (A70), we can express the indifference condition for the no-counteroffer scenario (A28) as

$$W = \frac{1}{\pi - \pi\beta}\Big(\varepsilon_n^*(d) - \tau(d) + \big(1-\pi\big)\Pi(d) - \frac{1-\pi\beta}{\beta}p(d)\Big). \tag{A81}$$

We can express the price and the profit in terms of the reservation dividend in the no-counteroffer scenario via (A42) and (A44), such that

$$W = \frac{1}{\pi - \pi\beta}\left(2\varepsilon_n^*(d) - \overline{\varepsilon} - \tau(d) - \frac{(\pi - \pi\beta)\beta\theta(\overline{\varepsilon} - \varepsilon_n^*(d))^2}{(1-\beta)(1-\pi\beta)(\overline{\varepsilon} - \underline{\varepsilon})}\right). \tag{A82}$$

Hence,

$$\frac{\partial W}{\partial \varepsilon_n^*(d)|_d} = \frac{2}{\pi - \pi\beta} + \frac{2\beta\theta(\overline{\varepsilon} - \varepsilon_n^*(d))}{(1-\beta)(1-\pi\beta)(\overline{\varepsilon} - \underline{\varepsilon})} > 0. \tag{A83}$$

Via Lemma 1, also $\partial W/\partial \varepsilon_c^*(d)|_d > 0$. Since Expression 1 for the value of search decreases in both reservation dividends and Expression 2 increases in both reservation dividends, there can only be a single pair of reservation dividends $\{\varepsilon_n^*(d), \varepsilon_c^*(d)\}$ at a given distance to the city center such that Expression 1 and Expression 2 hold simultaneously. With W being constant across space, it immediately follows that this holds for all distances to the city center.

I Model solution method

We are not able to solve the model in closed form, as we obtain a nonlinear system of equations via the equilibrium conditions. Hence, we solve the model numerically. The equilibrium condition (4), which describes the value of search W as an expectation over distances to the city center and idiosyncratic dividends, and the equilibrium conditions (2), (6), (7), and (8), which have to hold for all distances to the city center $d^{\Delta} \in \mathscr{D}^{\Delta}$, constitute the relevant system of $1 + z \times 4$ equations. Solving the system as it is via standard solvers brings up problems of numerical instability due to the high degree of non-linearity involved. Hence, we instead iterate over the value of search to find a value that is consistent with (2), (6), (7), and (8) at each $d^{\Delta} \in \mathscr{D}^{\Delta}$.

We implement the iteration as follows. First, we initialize an arbitrary guess for the value of search. Given this guess, we solve (2), (6), (7), and (8) for all $d^{\Delta} \in \mathscr{D}^{\Delta}$. We update the guess via

$$\widetilde{W} = \frac{1}{z} \sum_{d^{\Delta} \in \mathscr{D}^{\Delta}} \gamma(d^{\Delta}) \Big(V\big(d^{\Delta}, \tfrac{\varepsilon^*(d^{\Delta}) + \bar{\varepsilon}}{2}\big) - p(d^{\Delta}) \Big) + \big(1 - \gamma(d^{\Delta})\big) \Big(\beta W \Big), \tag{A84}$$

using that a buyer purchases a housing unit at d^{Δ} with probability of sale $\gamma(d^{\Delta})$ and continues to search with probability $1 - \gamma(d^{\Delta})$, which follows the alternative definition of the value of search in Krainer and LeRoy (2002) and is simply a rewritten version of the expectation in (4). This expression only requires information from (2), (6), (7), and (8). The new guess for the value of search is then set to $\widetilde{W}$, and the whole process is repeated until $W = \widetilde{W}$ up to a fixed iteration tolerance. In principle, convergence is not necessarily guaranteed by the standard contraction mapping theorem, even though $(1 - \gamma(d^{\Delta}))\beta < 1$, as the entire right-hand side of (A84) depends on W. In practice, convergence is not a problem and we obtain fast and reliable solutions, which allows us to estimate the model's structural parameters without problems.

J Additional model results

J.1 Variance of time on the market across space

An additional prediction of our model mentioned in Section 4.3 is that the variance of time on the market increases with distance to the city center. To see this, consider the variance of the geometric distribution that results from the multiplication of sale probabilities over time, together with the equilibrium relation (8) between probabilities of sale and reservation dividends:

$$\mathrm{Var}\left[TOM(d)\right] = \frac{1-\gamma(d)}{\left(\gamma(d)\right)^2} = \frac{\frac{\varepsilon^*(d)-\underline{\varepsilon}}{\overline{\varepsilon}-\underline{\varepsilon}}}{\left(\frac{\overline{\varepsilon}-\varepsilon^*(d)}{\overline{\varepsilon}-\underline{\varepsilon}}\right)^2} = (\overline{\varepsilon}-\underline{\varepsilon})\frac{\varepsilon^*(d)-\underline{\varepsilon}}{(\overline{\varepsilon}-\varepsilon^*(d))^2}. \tag{A85}$$

Taking the derivative with respect to the distance to the city center yields

$$\frac{\partial \mathrm{Var}\left[TOM(d)\right]}{\partial d} = \frac{\partial \varepsilon^*}{\partial d}\underbrace{(\overline{\varepsilon}-\underline{\varepsilon})\frac{\left(\overline{\varepsilon}-\varepsilon^*(d)\right)^2+2\left(\overline{\varepsilon}-\varepsilon^*(d)\right)\left(\varepsilon^*(d)-\underline{\varepsilon}\right)}{\left(\overline{\varepsilon}-\varepsilon^*(d)\right)^4}}_{>0} > 0 \tag{A86}$$

with auxiliary result (17) that the reservation dividend $\varepsilon^*(d)$ increases with distance to the city center. Intuitively, with a lower probability of a successful sale in the outskirts, a higher variability in success rates can realize, and therefore also a higher variability in time on the market.

We test this prediction of the model using transaction-level data from Germany. To focus on the relationship between distance to the city center and the variance of time on the market we estimate Regression (1) with time on the market as the dependent variable. We then use the squared residuals as our measure of time on the market variance, having accounted for differences in property characteristics. Finally, in Figure A11, we plot the squared residuals against distance to the city center. The Figure shows that the variance increases with distance to the city center, thereby confirming the model's prediction.

J.2 Steepness of price vs. liquidity gradient

Another prediction of our model mentioned in Section 4.3. is that the price gradient is steeper than the liquidity gradient. For this comparison, we express both gradients in

Figure A11: *Variance of time on the market and distance to the city center, Germany (2012–2024)*

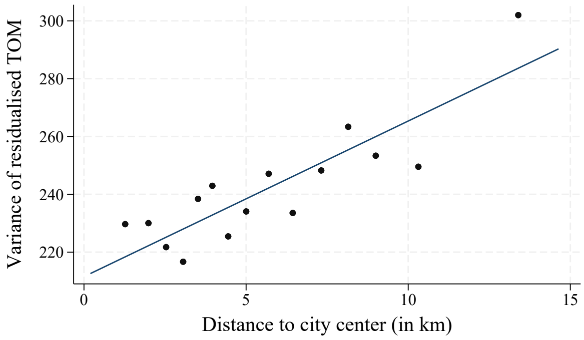

Notes: This binned scatter plot shows the relation between the variance of the residualized time on the market and distance to the city center, using 15 equally-sized distance bins. The binned scatter plot is produced following Cattaneo et al. (2024).

absolute values and in relative terms for immediate comparison. For the expected time on the market, this gradient is

$$\left|\frac{\partial \mathbb{E}[TOM]/\partial d}{\mathbb{E}[TOM(d)]}\right| = \left|\frac{\partial \gamma/\partial d}{\gamma(d)}\right|, \tag{A87}$$

by definition of the time on the market. Using the probability of sale $\gamma(d)$ here instead of the reservation dividend $\varepsilon^*(d)$ simplifies the comparison to the expression for the relative price gradient. Using (12) and (A9), the relative price gradient amounts to

$$\left|\frac{(\partial\gamma/\partial d)\Big(1+2\Big(\beta/(1-\beta)\Big)\gamma(d)\Big)}{\gamma(d)+\Big(\beta/(1-\beta)\Big)(\gamma(d))^2}\right| > \left|\frac{\partial \gamma/\partial d}{\gamma(d)}\right|. \tag{A88}$$

This is due to the factor 2 in front of $(\beta/(1-\beta))$, which results from the expression for expected profit in which the seller obtains a value of selling the property in the next period with probability $(\gamma(d))^2$. This option of selling the property in the future is priced in today. For a given increase in the expected time on the market when going further away from the city center, the corresponding price decreases more. The demand-driven level of liquidity, given a stationary equilibrium, will also determine market conditions in the following period in case the seller is not able to sell their housing unit in this period. With a successful sale in the next period, the seller then obtains the discounted profit.

Table A26: *Standardized TOM and price gradients, Germany and U.S.*

Country	Dataset	TOM gradient	Price gradient
Germany	Condos full sample	0.048	-0.202
U.S.	Single-family FUA (full sample)	0.029	-0.146
U.S.	Single-family MSA (50km radius)	0.048	-0.276
U.S.	Single-family MSA (full sample)	0.134	-0.074

Note: This table presents regression coefficients of time on the market (TOM) and log sales price on property characteristics with time and location fixed effects based on Regression (1). *The coefficients are standardized by the sample standard deviation of the respective variable. For Germany, the fixed effects are at the year-quarter-city level. For the U.S., the fixed effects are at the year-month-MSA or year-month-FUA level. More information on data sources is provided in the main text.*

Table A26 provides empirical comparisons of the steepness of the price and liquidity gradients for Germany and the United States. The theoretical prediction that the price gradient is steeper than the liquidity gradient holds empirically, except in the U.S. at the MSA level across the full sample. This is likely due to the spatial boundaries of some MSAs reaching very far out, which makes the estimates noisier. With functional urban area boundaries, the result holds, as well as when restricting the U.S.-MSA sample to a 50km radius around the MSA center.

J.3 Additional model results

Figure A12: *Spatial distributions of additional variables, Germany*

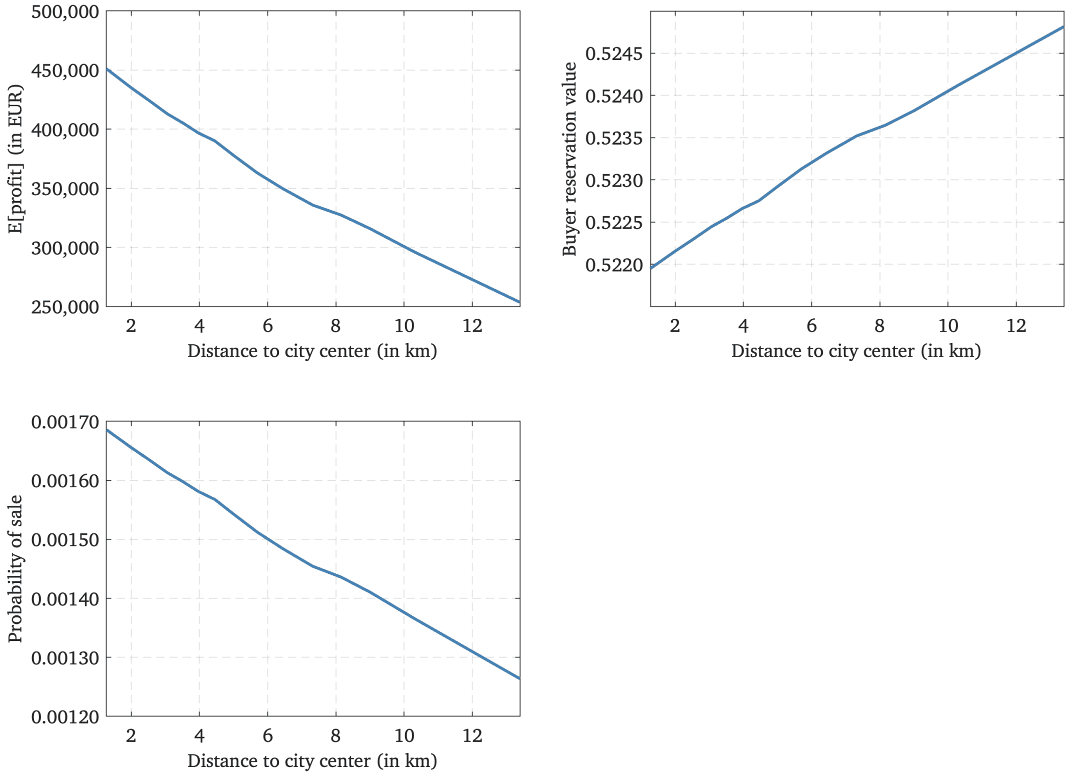

Figure A13: *Spatial distributions of additional variables, United States*

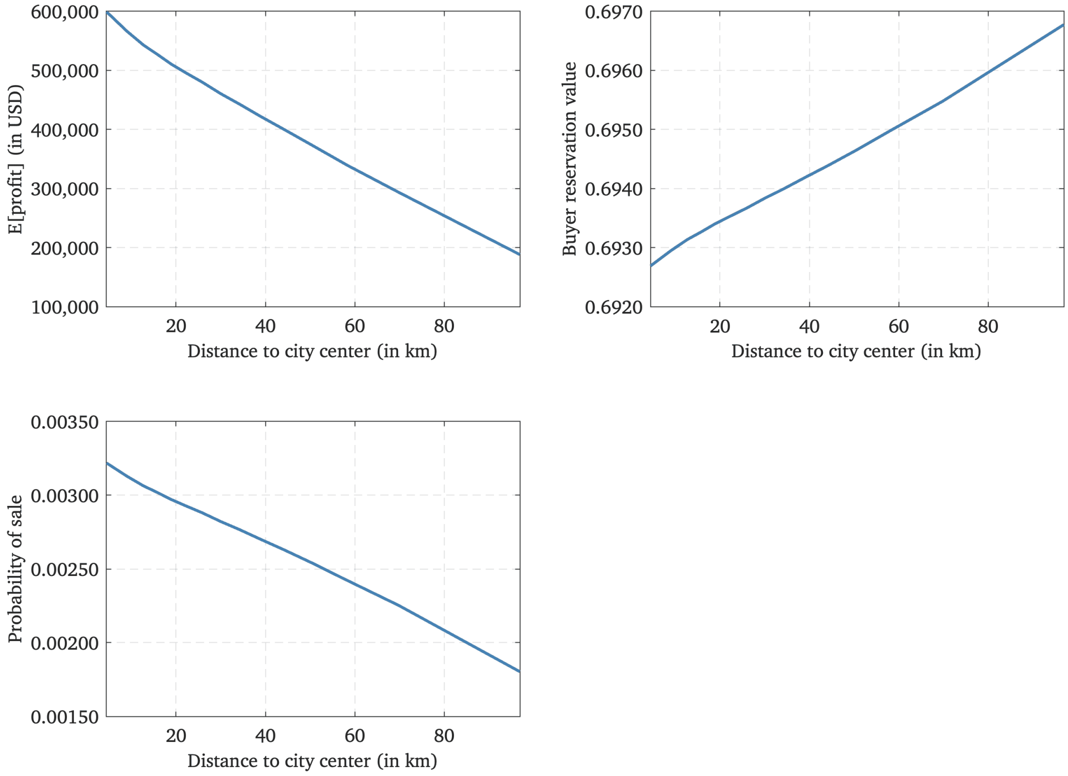

Figure A14: *Spatial welfare loss distributions in terms of housing prices*

(a) *Germany*

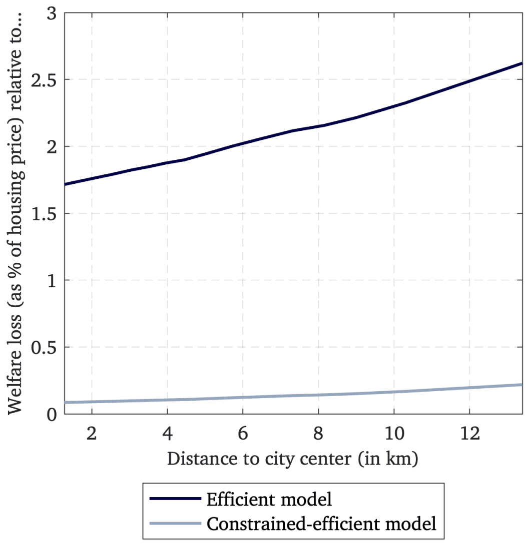

(b) *United States*

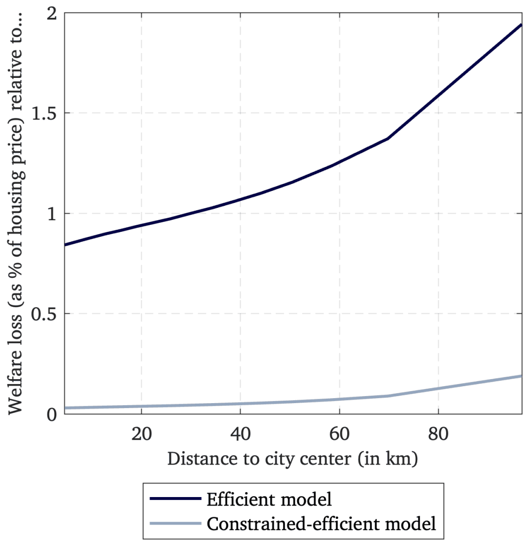

Notes: These plots show the welfare loss in the baseline model compared to the counterfactual model versions by distance to the city center. Welfare is calculated as defined in (21) *and scaled up to an expected lifetime value with factor* $\beta/(1-\pi\beta)$. *The percentages refer to the absolute loss in welfare in the baseline model compared to a counterfactual as a fraction of the housing price at every distance to the city center.*

Figure A15: *Spatial distribution of homeowner vacancy rate, United States*

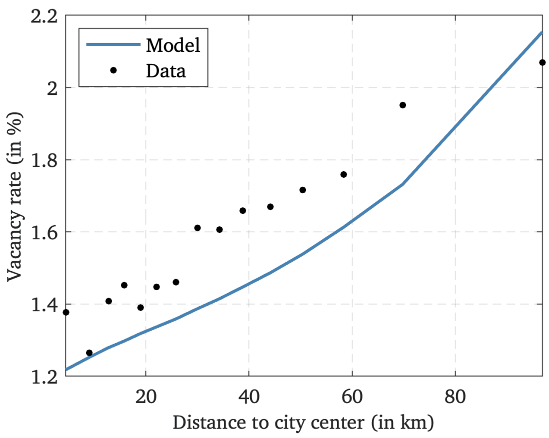

Notes: This plot shows the distribution of the homeowner vacancy rate, that is, the vacancy rate in the owner-occupied housing market, across distances to the city center from our baseline model and from the data. Note that neither the spatial variation nor the level of vacancy rates are targeted in the model calibration. The model vacancy rates are calculated as defined via the probability of being matched, defined in (22). *The data points are calculated using the ZIP-Code level yearly American Community Survey data from 2012–2023 introduced in Supplemental Appendix A.2, using Regression* (1) *with all fixed effects and controls.*

J.4 Model sensitivity analysis

In this subsection, we provide a sensitivity analysis for our welfare estimates. First, in Figure (A16), we plot the welfare loss in the baseline model relative to the efficient model with bootstrapped confidence bounds. As described in the main text, the confidence intervals are narrow, which leaves us confident about our estimates from this side.

Second, in the main calibration, we set the yearly discount factor to 0.95, a standard value. Nevertheless, we check if our illiquidity discount estimates are sensitive to our choice of the discount factor. Moreover, we cannot calculate holding periods for apartments that were transacted before the beginning of our German sample in January 1990, while the holding period for the U.S. is only a rough estimate obtained via Redfin. Hence, we also check if our illiquidity discount estimates change if we use different housing match persistence probabilities. In Figure A17, we plot the welfare loss in the outskirts, varying the yearly discount factor β^{yr} between 0.935 and 0.965 and the yearly housing match persistence π^{yr} between 0.88 and 0.92. Each bar represents a recalibration of the model. As explained in the main text, the choice of the discount factor leaves the welfare loss estimates unaffected, while a lower match persistence increases the welfare loss.

Figure A16: *Bootstrapped welfare loss estimates*

(a) *Germany* **(b)** *United States*

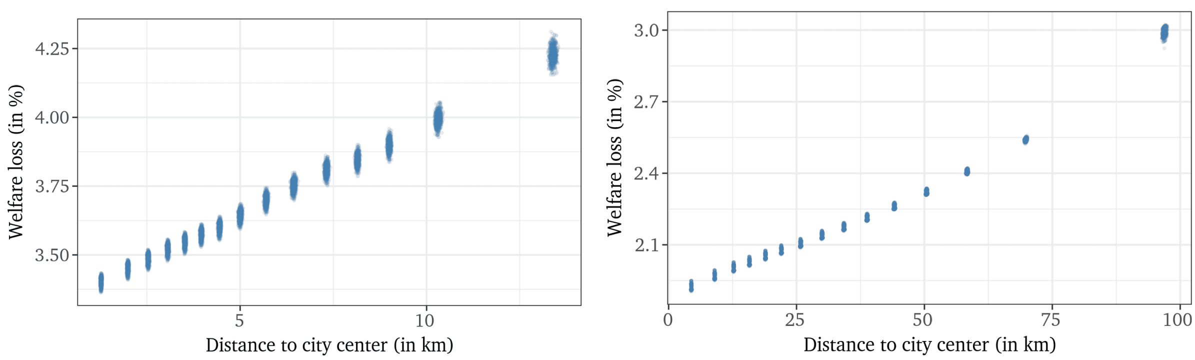

Notes: These plots show the welfare loss in the baseline model compared to the efficient model version by distance to the city center. Welfare is calculated as defined in (21). *The percentages refer to the loss in welfare in the baseline model relative to the efficient model at every individual distance. The individual dots depict the 1,000 bootstrapped replication draws.*

Figure A17: *Sensitivity analysis for outskirt welfare loss*

(a) *By β^{yr}, with $\pi^{yr} = 0.90$, Germany*

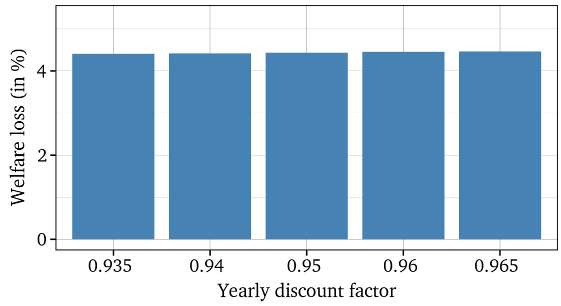

(b) *By π^{yr}, with $\beta^{yr} = 0.95$, Germany*

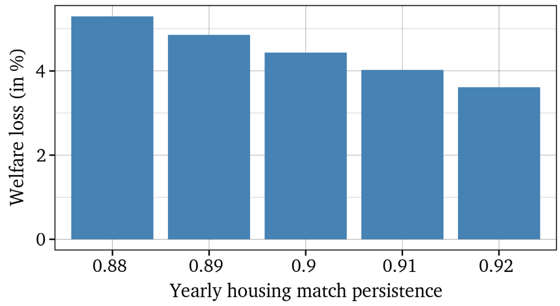

(c) *By β^{yr}, with $\pi^{yr} = 0.90$, United States*

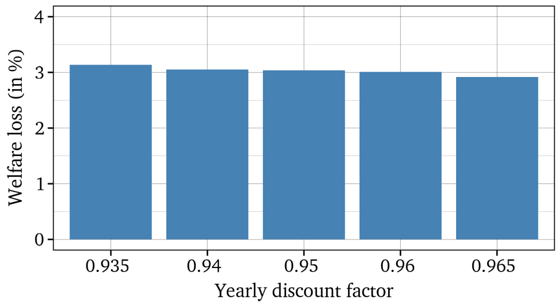

(d) *By π^{yr}, with $\beta^{yr} = 0.95$, United States*

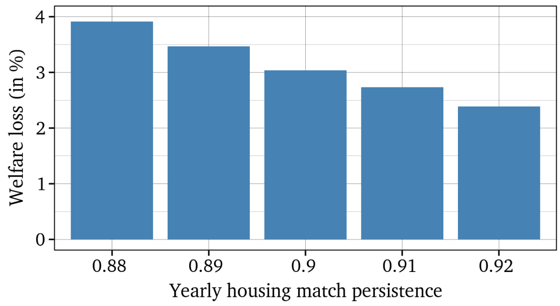

Notes: These plots show the welfare loss in the baseline model compared to the efficient model version at the outmost distance to the city center, with varying yearly discount factors and housing match persistence probabilities. Welfare is calculated as defined in (21). *The percentages refer to the loss in welfare in the baseline model relative to the efficient model at every distance to the city center.*

J.5 Alternative travel cost interpretation

In the main model, we think of a physical cost of car travel when estimating the parameter μ, consistently with the canonical monocentric city model. μ then reflects a conversion of travel time in minutes, fed into the model from our travel time estimates, to the associated travel cost in model units. Alternatively, we can think of the travel cost in the model as an opportunity cost which results from lost time due to traveling to the city center. We also conceptualize this opportunity cost as translating travel time to the city center in minutes linearly into a monetary cost. To do so, we must specify what a minute of travel time is worth to agents in the model. We do this using the average hourly wage in Germany and the United States. For Germany, we retrieve wage statistics via the German Statistical Office (GENESIS database, variable code: 81000-090[43]). For the United States, we retrieve wage statistics via FRED (variable code: CES0500000003,

[43] `https://www.destatis.de/DE/Themen/Wirtschaft/Volkswirtschaftliche-Gesamtrechnungen-Inlandsprodukt/Publikationen/Downloads-Inlandsprodukt/statistischer-bericht-2180120.html`

primary source: U.S. Bureau of Labor Statistics (2025)). We keep the wage rates nominal on purpose for a direct comparison to the nominal travel cost estimates that we use as untargeted moments. We obtain a gross hourly wage in Germany from 2012 to 2024 of €28.33 and in the United States from 2012 to 2023 of $27.49.

Then, we calculate the average travel time in our sample, multiplied by 2, to get a measure of daily travel time. In our model, agents travel to and from the city center for 34 minutes per day on average in Germany and for 84 minutes per day in the United States. Measured in terms of an opportunity cost, if we assume that the value of time lost can be expressed in terms of wages, agents in Germany lose $(34/60) \times$ €$28.33 =$ €16.05 per day, while agents in the United States lose $38.49 per day. The actual losses should be somewhat lower, since these are gross wages, and net wages are typically considerably below gross wages. Moreover, the same words of caution as for the travel cost estimates apply: these calculations are at the country level and likely vary to a considerable degree at the city level, and it is not clear to what extent wages capture the opportunity cost experienced when commuting. Hence, we conclude that, roughly speaking, opportunity costs can serve as an alternative interpretation of travel costs.

J.6 COVID experiment in the model

We test whether our baseline model can replicate the flattening of the price gradient as documented in Gupta et al. (2022) and produce a flattened liquidity gradient as we document in our empirical results. The COVID-19 pandemic induced a shift to working from home. The experiment consists of varying the travel time input, which generates a travel cost curve within the model, such that it reflects the shift in commuting patterns induced by working from home.

Per se, we have no information available on the change in time traveled to the city center across space within cities. Hence, we impose restrictions on the changes that we make by using the results from Gupta et al. (2022). To get the result that prices decrease in the city center and increase in the outskirts compared to before, the travel cost within our model must increase in the city center and decrease in the outskirts compared to before. A straightforward way to implement this is to let the average travel cost stay the same while changing its spatial distribution. Then, we must only specify one number which changes in the experiment. We impose that, keeping the average travel time constant, the slope of the linearly approximated travel time input curve is multiplied by some factor between 0 and 1. We add back the residuals between the original travel time input curve and its linear approximation to the new tilted curve. With a factor of 1/2, we approximately replicate the price decrease of 5-10% in the city center and the price increase of 15-20% in the outskirts estimated for New York City in Gupta et al. (2022) and our flattened liquidity gradients from Supplemental Appendix D.2, see Figure A18.

Figure A18: *Results of COVID experiment in the model*

(a) *Germany*

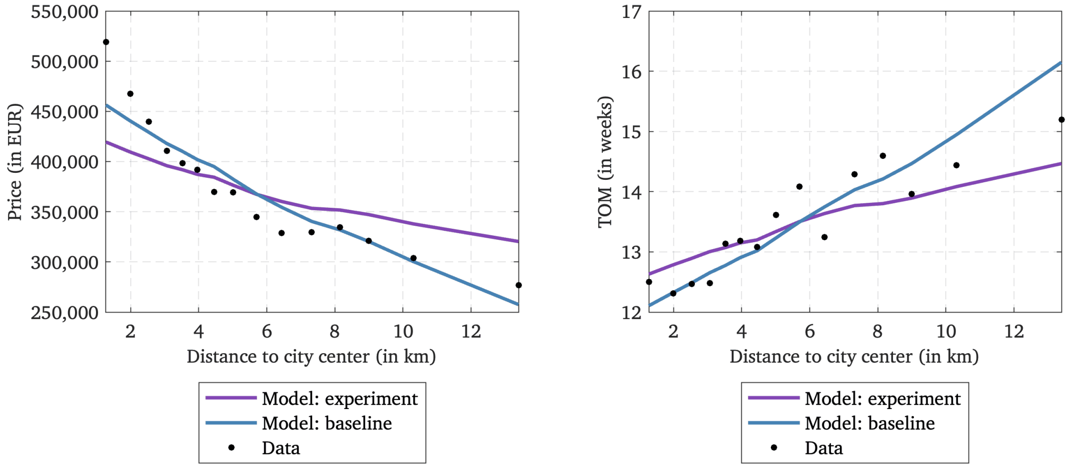

(b) *United States*

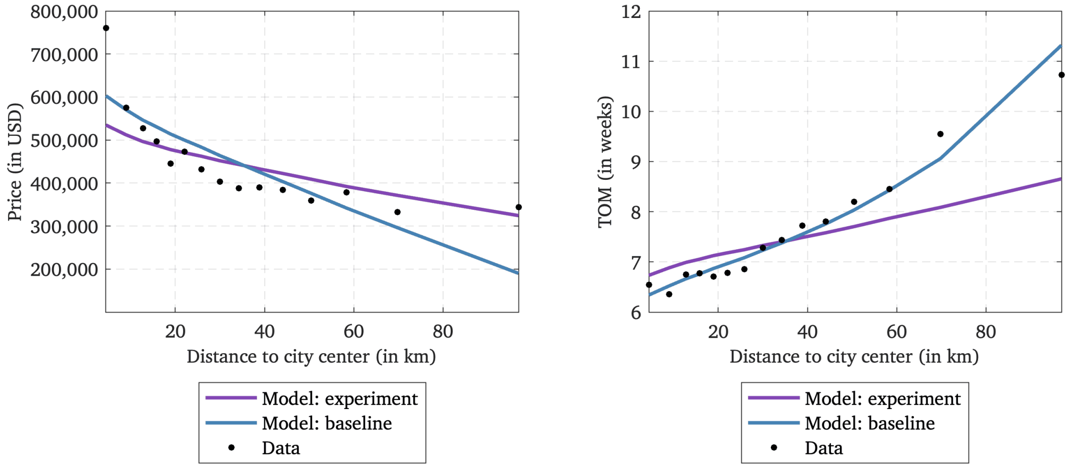

Notes: "TOM" refers to (expected) time on the market. The data points are calculated using Regression (1) *with city-time fixed effects and all controls, as for Figure 1. The binned scatter plots are produced following Cattaneo et al. (2024), using 15 equally-sized distance bins.*

References

Amaral, Francisco, Martin Dohmen, Moritz Schularick, and Jonas Zdrzalek (2023). "German Real Estate Index (GREIX)". ECONtribute Discussion Paper No. 231.

Burrows, Michael, Charlynn Burd, and Brian McKenzie (2021). "Commuting by public transportation in the United States: 2019". American Community Survey Report No. ACS-48.

Carrillo, Paul E. (2012). "An empirical stationary equilibrium search model of the housing market". In: *International Economic Review* 53(1), pp. 203–234.

Cattaneo, Matias D., Richard K. Crump, Max H. Farrell, and Yingjie Feng (2024). "On binscatter". In: *American Economic Review* 114(5), pp. 1488–1514.

Chetty, Raj, John N. Friedman, Nathaniel Hendren, Maggie R. Jones, and Sonya R. Porter (2025). "The Opportunity Atlas: Mapping the childhood roots of social mobility". Working paper.

Delventhal, Matthew J. and Andrii Parkhomenko (2024). "Spatial implications of telecommuting". Working paper.

Dijkstra, Lewis, Hugo Poelman, and Paolo Veneri (2019). "The EU-OECD definition of a functional urban area". OECD Regional Development Working Paper No. 2019/11.

Gupta, Arpit, Vrinda Mittal, Jonas Peeters, and Stijn Van Nieuwerburgh (2022). "Flattening the curve: Pandemic-induced revaluation of urban real estate". In: *Journal of Financial Economics* 146(2), pp. 594–636.

Guren, Adam M. and Timothy J. McQuade (2020). "How do foreclosures exacerbate housing downturns?" In: *The Review of Economic Studies* 87(3), pp. 1331–1364.

Han, Lu and William C. Strange (2016). "What is the role of the asking price for a house?" In: *Journal of Urban Economics* 93, pp. 115–130.

Krainer, John (2001). "A theory of liquidity in residential real estate markets". In: *Journal of Urban Economics* 49(1), pp. 32–53.

Krainer, John and Stephen F. LeRoy (2002). "Equilibrium valuation of illiquid assets". In: *Economic Theory* 19(2), pp. 223–242.

Moreno-Monroy, Ana I., Marcello Schiavina, and Paolo Veneri (2021). "Metropolitan areas in the world. Delineation and population trends". In: *Journal of Urban Economics* 125:103242.

Pesaresi, M. and P. Politis (2023). “GHS-BUILT-V R2023A”. GHS built-up volume grids derived from joint assessment of Sentinel2, Landsat, and global DEM data, multitemporal (1975-2030). European Commission, Joint Research Centre (JRC).

Pesaresi, M. et al. (2024). “Advances on the Global Human Settlement Layer by joint assessment of Earth Observation and population survey data”. In: *International Journal of Digital Earth* 17(1):2390454.

RWI - Leibniz-Institut für Wirtschaftsforschung and ImmobilienScout24 (2024). “RWI Real Estate Data - Hauskauf - SUF”. RWI-GEO-RED.

Schiavina, M., A. Moreno-Monroy, L. Maffenini, and P. Veneri (2019). “GHS-FUA R2019A”. GHS functional urban areas, derived from GHS-UCDB R2019A, (2015), R2019A. European Commission, Joint Research Centre (JRC).

U.S. Bureau of Labor Statistics (2025). “Average hourly earnings of all employees, total private [CES0500000003]”. U.S. Bureau of Labor Statistics. Retrieved from FRED, Federal Reserve Bank of St. Louis.

Vanhapelto, Tuuli and Thierry Magnac (2024). “Housing search and liquidity in the cross-section of market segments”. Working paper.